SUBTASK 2.7 – WET ESP AND AEROSOL TESTING AT COAL CREEK STATION

Final Topical Report

(for the period of July 1, 2020, through November 30, 2021)

Prepared for:

AAD Document Control

National Energy Technology Laboratory
U.S. Department of Energy
626 Cochrans Mill Road
PO Box 10940, MS 921-107
Pittsburgh, PA 15236-0940

Cooperative Agreement No.: DE-FE0024233
DOE Technical Monitor: Katharina (Katy) Daniels

Prepared by:

Joshua R. Strege
John P. Kay
Kyle A. Glazewski
Matthew E. Burton-Kelly
Cody B. Williamson
Janet L. Crossland
Brandon R. Petrick

Energy & Environmental Research Center
University of North Dakota
15 North 23rd Street, Stop 9018
Grand Forks, ND 58202-9018

2021-EERC-11-07 November 2021

EERC DISCLAIMER

LEGAL NOTICE This research report was prepared by the Energy & Environmental Research Center (EERC), an agency of the University of North Dakota, as an account of work sponsored by the U.S. Department of Energy National Energy Technology Laboratory. Because of the research nature of the work performed, neither the EERC nor any of its employees makes any warranty, express or implied, or assumes any legal liability or responsibility for the accuracy, completeness, or usefulness of any information, apparatus, product, or process disclosed or represents that its use would not infringe privately owned rights. Reference herein to any specific commercial product, process, or service by trade name, trademark, manufacturer, or otherwise does not necessarily constitute or imply its endorsement or recommendation by the EERC.

ACKNOWLEDGMENT

This material is based upon work supported by the U.S. Department of Energy National Energy Technology Laboratory under Award No. DE-FE-0024233.

DOE DISCLAIMER

This report was prepared as an account of work sponsored by an agency of the United States Government. Neither the United States Government, nor any agency thereof, nor any of their employees, makes any warranty, express or implied, or assumes any legal liability or responsibility for the accuracy, completeness, or usefulness of any information, apparatus, product, or process disclosed, or represents that its use would not infringe privately owned rights. Reference herein to any specific commercial product, process, or service by trade name, trademark, manufacturer, or otherwise does not necessarily constitute or imply its endorsement, recommendation, or favoring by the United States Government or any agency thereof. The views and opinions of authors expressed herein do not necessarily state or reflect those of the United States Government or any agency thereof.

TABLE OF CONTENTS

Continued . . .

TABLE OF CONTENTS (continued)

LIST OF FIGURES

Continued . . .

LIST OF FIGURES (continued)

Continued . . .

LIST OF FIGURES (continued)

LIST OF TABLES

ABBREVIATIONS AND ACRONYMS

°F	degree Fahrenheit
µm	micrometer
AACE	Advancement of Cost Engineering [International]
acfm	actual cubic foot per minute
AERU	amine emission reduction unit
APEA	Aspen Process Economic Analyzer
Btu	British thermal unit
$CaSO_3$	calcium sulfite
CCS	carbon capture and storage
cm^3	cubic centimeter
CO	carbon monoxide
CO_2	carbon dioxide
COE	cost of electricity
CPVC	chlorinated polyvinyl chloride
DCC	direct contact cooler
DOE	U.S. Department of Energy
EDX	energy-dispersive x-ray [spectroscopy]
EERC	Energy & Environmental Research Center
ELPI	electrical low-pressure impactor
EPA	U.S. Environmental Protection Agency
ESP	electrostatic precipitator
FESEM	field emission scanning electron microscope
FGD	flue gas desulfurization [unit]
ft	foot
FTIR	Fourier transform infrared [spectrometer]
H_2O	water
H_2SO_4	sulfuric acid
HEPA	high-efficiency particulate air
HHV	higher heating value
hr	hour
HSS	heat-stable salt
IC	ion chromatography
ICP	inductively coupled plasma
ICP–MS	inductively coupled plasma–mass spectrometer
ID	induced draft
kV	kilovolt
kW	kilowatt
kW_e	kilowatt electric
kW_t	kilowatt thermal
lb	pound

Continued . . .

ABREVIATIONS AND ACRONYMS (continued)

LLQ	lower limit of quantification
m^3	cubic meter
mA	milliamp
MEA	monoethanolamine
mg	milligram
mg/Nm^3	milligram per normal meter, cubed
MHI	Mitsubishi Heavy Industries
mi	mile
mi^2	square mile
mL	milliliter
MMt	million tonne
MMtpy	million tonne per year
MRYS	Milton R. Young Station
MWh	megawatt hour
nm	nanometer
NO_x	nitrogen oxides
O&M	operating and maintenance [costs]
pc	pulverized coal
PCCC	postcombustion carbon capture
ppb	parts per billion
ppm	parts per million
PSD	particle-size distribution
psig	pounds per square inch gauge
PTC	particulate test combustor
scfm	standard cubic foot per minute
SCR	selective catalytic reduction [unit]
SEM	scanning electron microscopy
SMPS	scanning mobility particle sizer
SO_x	sulfur oxides
SO_2	sulfur dioxide
SO_3	sulfur trioxide
TDS	total dissolved solids
TIC	total inorganic carbon
TOC	total overnight capital [costs]
T&S	transport and storage
UIC	underground injection control
USDW	underground source of drinking water
WESP	wet electrostatic precipitator

SUBTASK 2.7 – WET ESP AND AEROSOL TESTING AT COAL CREEK STATION

EXECUTIVE SUMMARY

Growing concerns over the impact of CO_2 emissions from combustion sources on global climate change have prompted numerous research and development projects aimed at developing cost-effective technologies for CO_2 capture. One family of technologies being demonstrated at pilot and full scale globally is postcombustion carbon capture (PCCC) systems that employ amine-based solvents. The captured CO_2 can be compressed and permanently stored underground or used for enhanced oil recovery. The proximity of North Dakota's lignite-fired fleet of power plants to potential CO_2 storage options creates a unique atmosphere for PCCC within the state. However, the unique components present in lignite flue gas present a challenge for large-scale PCCC at North Dakota power plants by contributing to aerosol formation.

Aerosols can negatively impact the long-term performance of amine-based solvents for CO_2 capture. Amine-based solvents are volatile, and flue gas particulate provides nucleation sites where amine vapors can condense as aerosols. Because aerosols cannot be easily captured at the column outlet using conventional technologies, the amine-laden aerosols escape the system and lead to accelerated solvent losses. Moreover, particulate components can chemically react with amines to form degradation products that can permanently deactivate the amine, cause fouling, and lead to hazardous emissions.

Many of the elements that have been shown to catalyze solvent degradation are present in lignite coals and can exacerbate solvent replacement economics. Understanding this issue is critical to the implementation of solvent-based CO_2 capture systems as applied to lignite-fired generation systems.

The Energy & Environmental Research Center (EERC) designed and carried out this project to fully characterize aerosol behavior with various control technologies installed to better optimize aerosol mitigation technology for CO_2 capture. To meet the goal of this project, the following objectives were identified:

- Determine the effectiveness of a wet electrostatic precipitator (WESP) on mitigating formation of problematic aerosols at Great River Energy's Coal Creek Station, upstream of the PCCC system.

- Determine the effectiveness of the Mitsubishi Heavy Industries (MHI) proprietary amine emission reduction unit (AERU) as a postcapture solvent recovery system for reducing aerosol emissions and extending solvent life downstream of the PCCC system.

- Determine the impact of aerosols on the efficiency and degradation products of both commercial and advanced solvents within the PCCC system.

Work was conducted at Coal Creek Station Unit 1 using a slipstream of flue gas from the outlet of the plant's flue gas desulfurization (FGD) unit. Flue gas was routed through a pilot-scale FGD unit to remove SO_2 to very low levels (~1 ppm) and then through a direct contact cooler (DCC) to further cool the gas and to remove moisture. The gas exiting the DCC was then optionally

routed through a WESP before passing to the CO_2 absorber columns. The MHI solvent was used to scrub CO_2 from the slipstream through a set of two absorber columns. The rich solvent was regenerated in a stripper column by heating to drive off captured CO_2. Flue gas exiting the absorber column was routed to MHI's proprietary AERU to recover entrained solvent. The system operated using a catch-and-release method where the CO_2 was separated to provide data on the process, but the captured CO_2 was released back into the host site stack.

Particulate was measured, collected, and analyzed from multiple locations throughout the pilot-scale system. Unlike the performance observed in prior work, the inlet FGD and DCC did not remove significant particulate matter from the flue gas. This appears to be due to a difference in the nature of the particulate. The DCC seemed to increase particulate size and count, most likely owing to water condensing onto the surfaces of fly ash particles. When the WESP was operated, it achieved >95% particulate capture. Very little particulate matter or indications of solvent were detected at the AERU outlet. When operating with advanced KS-21 solvent, the particulate material at the AERU outlet was even further decreased.

Solvent analysis showed that some species derived from flue gas and ash were slowly concentrating in the solvent over the duration of the test. The levels observed were reported to be within expected ranges and were not of concern to MHI.

A high-level techno-economic assessment of installing CO_2 capture at Coal Creek Station suggested that, when using a standard monoethanolamine (MEA)-based solution with simple heat integration, the energy penalty to net generation would be 34%. The bulk of this was due to steam losses for regenerating solvent, followed by parasitic electrical demand for CO_2 compression and then by increased parasitic load for pushing flue gas through the absorber column. These demands could be decreased with a more advanced solvent that exhibits lower heat of regeneration and lower pressure drop than does a simple MEA solution. Further energy could be saved with more thorough heat integration to recover useful energy from the steam used for solvent regeneration.

Installing a WESP was predicted to increase the cost of electricity by nearly $5/MWh. This would become cost-effective if solvent losses were roughly 10 times the baseline estimate when not using a WESP but could be returned to baseline by installing the WESP.

Piping CO_2 for storage in more favorable geology could help with carbon capture and storage economics. Although storing off-site would necessitate construction of a CO_2 transport pipeline, the cost of this pipeline might be more than offset by reducing the number of wells required, the depths of the wells required, and the electrical demand for the CO_2 compressor. Additional factors that favor off-site storage costs include smaller expected CO_2 plume sizes, which translates to less monitoring and fewer landowner agreements. More detailed assessment of the specific geology in the region under and around Coal Creek Station would be needed to accurately assess the costs and benefits of different storage site options.

This subtask was cofunded through the Energy & Environmental Research Center–U.S. Department of Energy Joint Program on Research and Development for Fossil Energy-Related Resources Cooperative Agreement No. DE-FE0024233. Nonfederal funding was provided by the North Dakota Industrial Commission.

SUBTASK 2.7 – WET ESP AND AEROSOL TESTING AT COAL CREEK STATION

INTRODUCTION AND BACKGROUND

Growing social concerns are creating urgency for fossil fuel-fired power plants to reduce carbon intensity, with carbon capture and storage (CCS) being one of the most feasible near-term options. North Dakota is fortunate to have nearby large-scale sequestration potential in the form of enhanced oil recovery as well as geologic formations favorable to long-term CO_2 storage. However, even with these advantages, establishing a market where coal-powered utilities provide CO_2 to oil producers is still dependent on a cost-effective and proven method for CO_2 capture.

One technical challenge to widespread adoption of CO_2 capture solvent technology that has received significant recent attention is the formation of aerosols. Aerosol formation can negatively impact postcombustion CO_2 capture (PCCC) systems by degrading solvent, exacerbating solvent carryover, and creating undesirable emissions (Benson et al., 2017).

Reactor solvent-based absorbers such as those using amine-based solvents are a leading method to control CO_2 emissions from coal-fired power plants (Wu et al., 2014; Luis, 2016; Le Moullec et al., 2014; Dutcher et al., 2015). During an amine-based PCCC process, pretreated flue gas is contacted with aqueous amine solution in an absorber in a countercurrent fashion to remove CO_2. The CO_2-rich solution is then heated in a stripper/regenerator to release the captured CO_2, and the CO_2-lean solution is cooled and pumped back to the absorber for another cycle. Meanwhile, the treated flue gas is water-washed and discharged.

Common amines used for CO_2 capture include monoethanolamine (MEA), methyldiethanolamine, piperazine, and various blends of these solvents. Most of these amines are volatile and, therefore, small amounts will be emitted to the atmosphere via the treated flue gas stream. Several studies (Kamijo et al., 2013; Brachert et al., 2014; Mertens et al., 2014; Khakharia, 2015; Fulk, 2016) have identified substantial levels of solvent emissions from amine-based CO_2 absorbers. Aerosol-based emissions on the order of grams per normal cubic meter (Nm^3) have been reported, and these emissions are attributed to the presence of particles, such as soot and sulfuric acid aerosol droplets, in the flue gas entering the absorber column. Aerosol-based solvent emission is emerging as a key challenge in the realization of a full-scale absorption–stripping-based PCCC plant.

Aerosol formation can occur as i) a homogeneous process involving spontaneous condensation of vapor-phase species to form fine aerosol particles or ii) a heterogeneous process in which vapors condense on the surfaces of existing particles known as seeds. Homogeneous nucleation occurs when a vapor-phase species becomes rapidly supersaturated. This is likely to occur near the top of the absorber, where rising gas that has been heated by reaction with solvent rapidly cools on contact with cold, lean solvent entering the column from above. Heterogeneous formation occurs when seed particles are present in the inlet gas stream, providing surface area on which supersaturated vapor can more easily condense. As shown in Figure 1, there is a clear correlation of MEA emissions with the change in inlet aerosol (soot and H_2SO_4) concentration, indicating that heterogeneous formation is a major pathway to aerosol formation and solvent losses from a PCCC system.

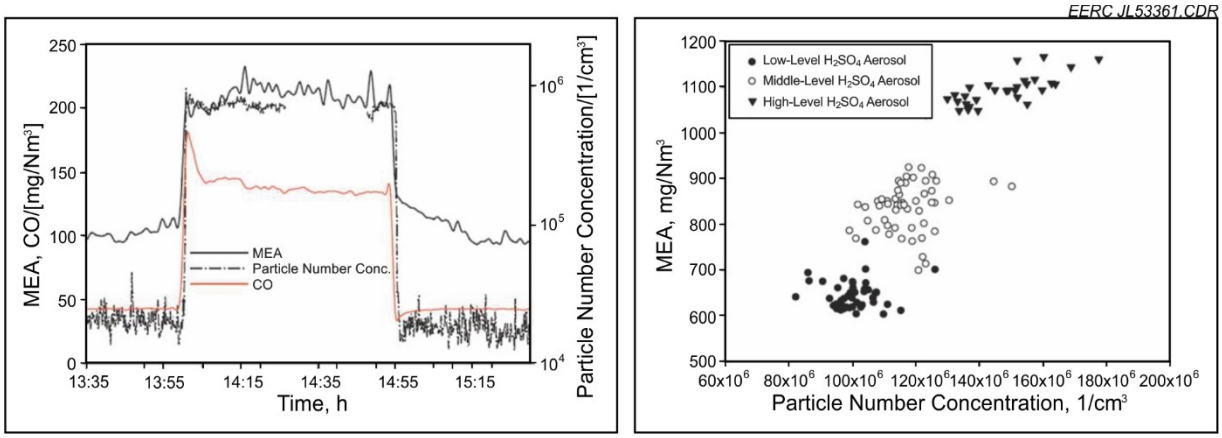

Figure 1. Amine emissions as a function of the number of soot (CO) particles (left), and MEA emissions as a function of the amount of sulfuric acid aerosol particles (right) (Khakharia, 2015).

There are several possible methods to reduce aerosol formation and solvent losses through the absorber. One option is to pretreat the gas entering the absorber column to minimize the presence of flue gas components that can act as seed particles for heterogeneous aerosol formation. Another is to treat gas leaving the absorber column to capture and retain liquids after they escape. A third option is the use of advanced solvents that may exhibit lower volatility and, thus, result in less potential solvent carryover into the treated flue gas stream. Each of these options require further study to demonstrate adequate long-term performance.

In prior work, the Energy & Environmental Research Center (EERC) installed a slipstream CO_2 capture system at Minnkota Power Cooperative's Milton R. Young Station (MRYS) near Center, North Dakota. Initial testing with a wet electrostatic precipitator (WESP), located immediately downstream of the plant's flue gas desulfurization (FGD) unit, led to formation of fine aerosols rich in SO_3. Although the WESP was effective at removing large particulate (>200 nm), it caused an increase in fine particulate (<75 nm) and SO_3. When flue gas was instead passed through a secondary slipstream FGD and direct contact cooling (DCC) spray tower before going to a WESP, much of the particulate matter was removed by the FGD and DCC before reaching the WESP, and there were no indications of sulfur oxidation or aerosol formation through the WESP. With this configuration, the WESP was effective at removing >95% of all particulate matter. Operating without the WESP online led to observable increases in aerosol losses through the absorber column.

Although the results from MRYS were informative, they represent only a snapshot of conditions in a single boiler configuration and a single-solvent technology. Great River Energy's Coal Creek Station near Underwood, North Dakota, presents a different boiler configuration with different flue gas characteristics and different forms of particulate in the flue gas. Advanced solvents may exhibit lower volatility than more conventional amine-based solvents, which might reduce the tendency for aerosol formation and, thus, reduce or eliminate the need for a WESP to reduce particulate count entering the absorber column. The need for a WESP might also be reduced using options for solvent recovery postcapture.

This project—Subtask 2.7 under EERC–U.S. Department of Energy (DOE) Joint Program on Research and Development for Fossil Energy-Related Resources Cooperative Agreement No. DE-FE0024233—was conducted to extend knowledge gained at MRYS on aerosol transformation and composition from lignite-derived flue gas by continuing work at Coal Creek Station. Extensive aerosol sampling was conducted near-simultaneously across multiple pollution control devices when operating with both commercial solvent and with advanced solvent. Gathering samples at multiple points in the process allowed chemical speciation of particulate matter at each step of the pretreatment, CO_2 scrubbing, and postcapture polishing processes.

Subtask 2.7 was performed over a period of 15 months, with a total budget of $3,772,325. The project was funded by DOE's National Energy Technology Laboratory, through the EERC–DOE Cooperative Agreement, and by the North Dakota Industrial Commission.

GOALS AND OBJECTIVES

The goal of Subtask 2.7 was to fully characterize aerosol behavior with various control technologies installed to better optimize aerosol mitigation technology for CO_2 capture. Specific objectives of the work included the following:

- Determine the effectiveness of a WESP on mitigating formation of problematic aerosols at Coal Creek Station, upstream of the PCCC system.

- Determine the effectiveness of the Mitsubishi Heavy Industries (MHI) proprietary amine emission reduction unit (AERU) as a postcapture solvent recovery system for reducing aerosol emissions and extending solvent life downstream of the PCCC system.

- Determine the impact of aerosols on the efficiency and degradation products of both commercial and advanced solvents within the PCCC system.

PROJECT STRUCTURE AND RESEARCH METHODS

To achieve the specific project objectives, work was broken into four activities. Activity 1 involved project management and communication with DOE. This effort ensured that all work proceeded according to schedule and budget and that each component of the project was contributing to the overall success of the project as a whole.

Activity 2 focused on aerosol measurement, control, and modeling when using MHI's commercial KS-1™ solvent. Several trips were made to Coal Creek Station to sample aerosols around each unit operation under different configurations, including with and without a WESP operating. This work provided insight into how effective particulate control strategies might differ at Coal Creek Station from those at MRYS and also helped to assess the effectiveness of MHI's AERU technology on reducing aerosol emissions postcapture. In addition to sampling at Coal Creek Station, Activity 2 also included 1 week of sampling on-site at the EERC, using a standard

MEA capture solution to capture CO_2 in the flue gas from a pilot-scale combustion unit firing North Dakota lignite coal.

Activity 3 was focused on advanced solvent testing using MHI's proprietary KS-21™ solvent. As under Activity 2, aerosol sampling trips were made to Coal Creek Station to assess particulate fate and aerosol formation through each unit operation.

Activity 4 used the results from Activities 2 and 3 to construct techno-economic models of Coal Creek Station with different capture scenarios. Factors considered included the choice of whether to install a WESP and whether to inject captured CO_2 on-site or to pipeline the CO_2 to inject off-site into more favorable geologic formations.

AEROSOL SAMPLING AND CHARACTERIZATION

The EERC's slipstream CO_2 capture system was installed at Coal Creek Station and began operation on MHI's proprietary commercial KS-1 solvent in early October 2020. The system was operated continuously through December 20, 2020, with a break in operation for Thanksgiving. The system was then drained, refilled with MHI's proprietary advanced KS-21 solvent, and operated from December 31, 2020, to January 17, 2021. During operation, the EERC made several discrete trips to conduct particulate sampling around each unit operation in the capture system.

Initial Stack Sampling

During initial stack sampling, October 18–20, 2020, the team collected baseline data on particulate loading and gas composition at various locations inside the plant's stack using an existing scanning mobility particle sizer (SMPS) and Fourier transform infrared (FTIR) spectrometer. These data were used to identify a "typical" location for collecting an overnight Dekati® electrical low-pressure impactor (ELPI) sample. Samples collected on the ELPI substrates were brought back to the EERC for further analysis.

Activity 2 – Commercial KS-1 Solvent Testing

Sampling During KS-1 Operation with WESP Off-Line

During the second sampling trip, November 16–20, 2020, the team sampled at the inlet and outlet of each unit in the process train illustrated in Figure 2 except the WESP, which was bypassed. Conditions at the absorber outlet made direct particulate sampling impossible despite several attempts to modify operations to accommodate particulate sampling equipment needs. The team did not sample this location, but instead treated the combined CO_2 columns and AERU as a single absorber unit operation.

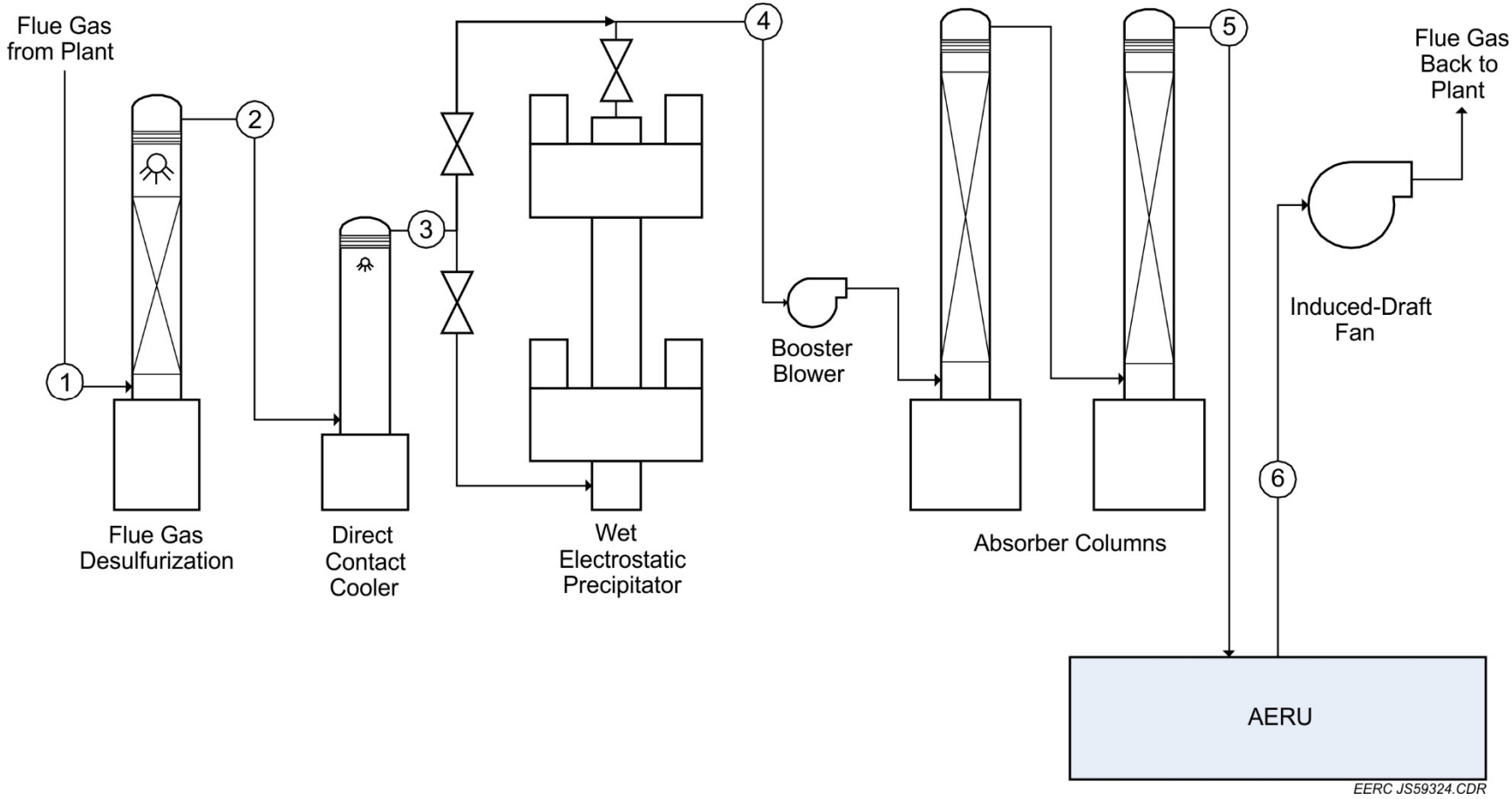

Figure 2. PCCC process train sample locations during operation at Coal Creek Station.

The SMPS that had been used during stack sampling had begun to provide unreliable readings prior to this sampling trip, so the team instead used a NanoScan SMPS for all online aerosol sampling. The NanoScan is a portable unit that can be quickly moved between sample ports, and it was moved repeatedly between inlet and outlet sample ports for each unit operation. This provided data on changes in particulate at the inlet to each unit operation that were occurring while the team was sampling at the outlet. Figure 3 shows an example of how drastically particulate loading could change over the course of 1 hour, with fine particulate (<100 nm) doubling in concentration between 3:42 and 4:39 p.m. on November 18. By repeatedly switching between the inlet and outlet ports to watch for changes in inlet particulate, the team was able to correct for time-based changes in particulate loading to find the true impact of each unit operation on fine particulate and aerosol fate.

Figure 4 shows the average particulate loading at the inlet and outlet to each unit operation during steady-state sample periods. Error bars are included to show standard deviations during the steady-state periods. The particulate loading was reduced by roughly 50% through the FGD and slightly increased through the DCC. This is in stark contrast to previous work done by the EERC at MRYS, where particulate loading dropped by an order of magnitude or more through the combined FGD–DCC process train. In that testing, a high percentage of the particulate in the raw flue gas appeared to be carryover from the plant's FGD unit, which might have made it more readily capturable with aqueous solutions. Analysis of the Dekati substrates collected at Coal Creek Station, which will be discussed later in this report, showed that the particulate was mostly aluminosilicate fly ash. This difference in composition reduced the ability for particulate to be removed in a wet column and also likely led to some aerosol condensation during rapid cooling in the DCC, which resulted in an increase in particulate size and concentration.

Key FTIR results obtained at each sample port are illustrated in Figure 5. As can be seen, the FGD and DCC were effective at reducing moisture and SO_2 at the absorber inlet. The moisture and ammonia then spiked at the absorber outlet as the heated gas exiting the column carried through moisture and solvent. MHI's AERU system recovered some of this material again before the system outlet, but the moisture and amine levels in the final gas remained higher than they had been at the absorber inlet. The extremely high SO_2 at the absorber outlet is artificial. The presence of solvent has been observed to interfere with the signal for SO_2 in past testing using the EERC's FTIR configuration, and this artificially high SO_2 is believed to be the result of this interference. SO_2 readings were measured close to inlet levels at the system outlet, indicating that solvent in the gas had been effectively removed by the AERU.

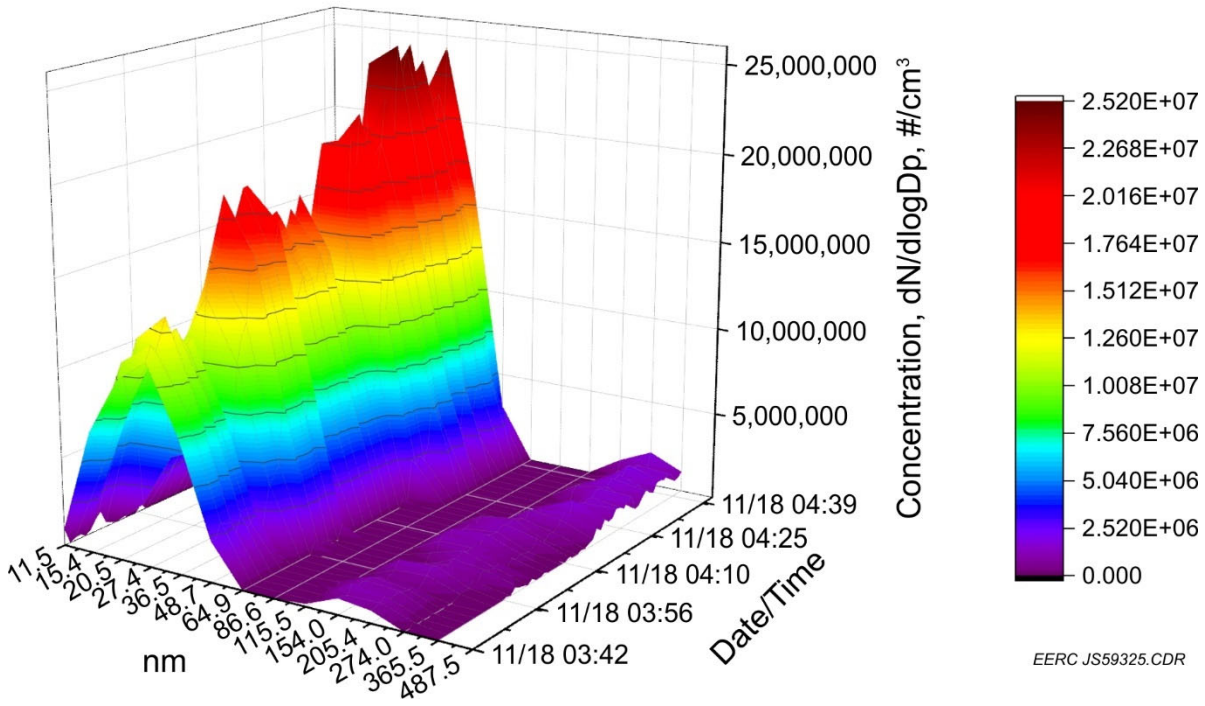

Figure 3. Changes in particulate at the FGD inlet over the course of 1 hour on November 18, 2020.

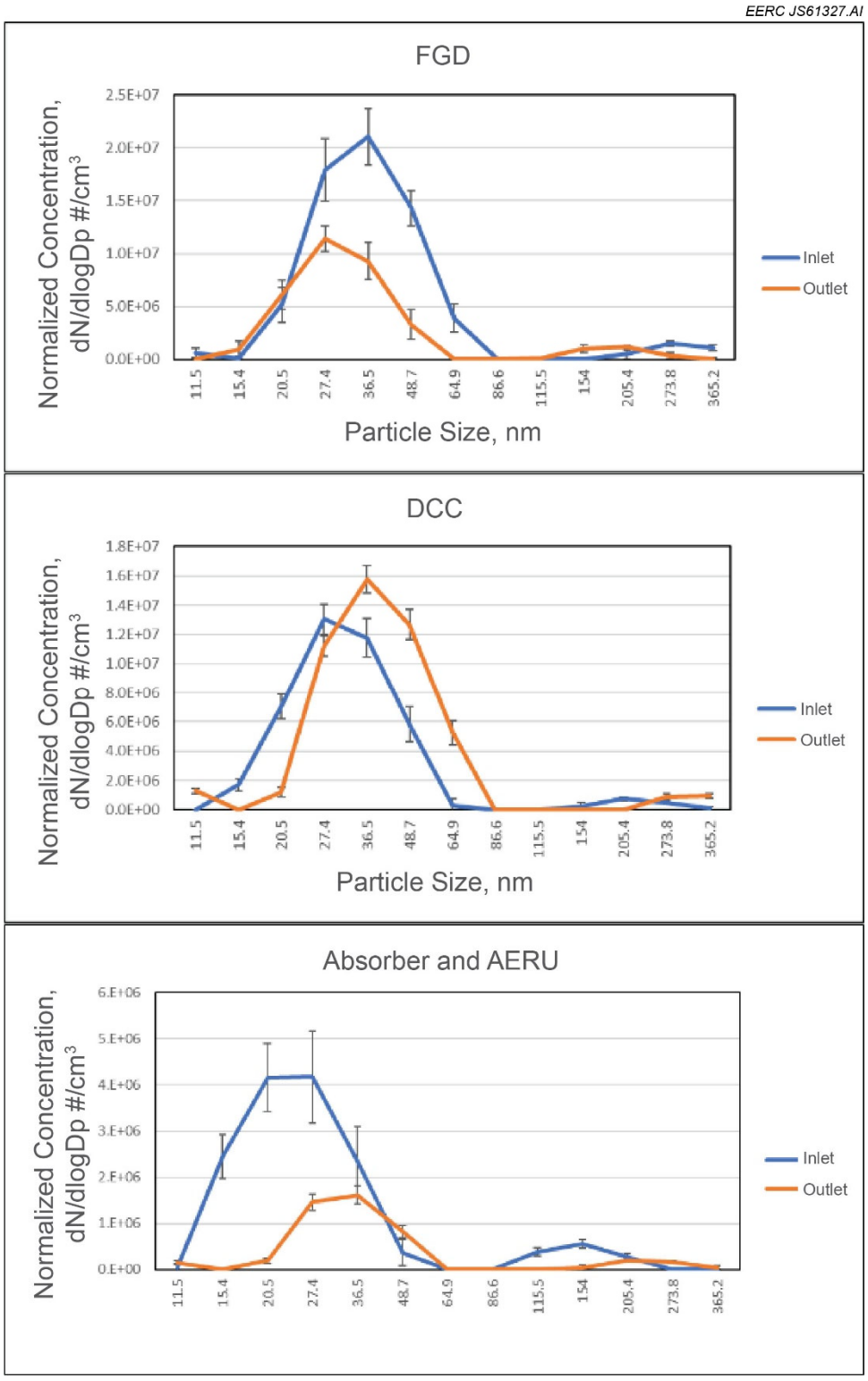

Figure 4. Normalized average particulate loading at the inlet and outlet to each major unit operation during November 16–20, 2020.

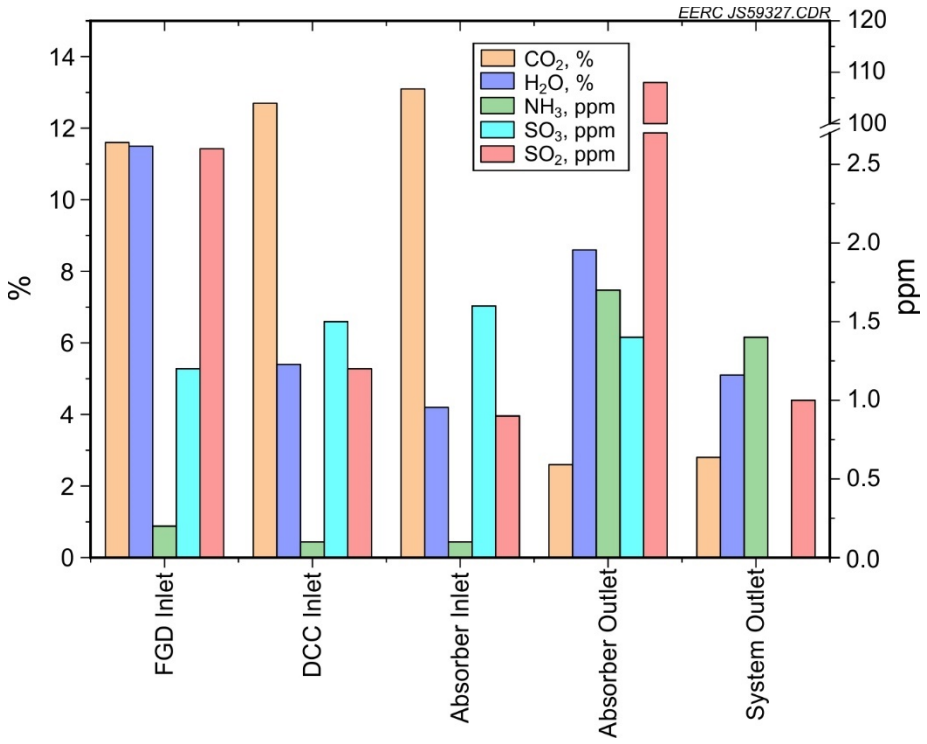

Figure 5. FTIR results from November 21 with the WESP off-line.

Sampling During KS-1 Operation with WESP Online

The fourth sampling trip, December 18–22, 2020, was to sample across each unit operation shown in Figure 2, including the online WESP.

Key FTIR results with the WESP online are shown in Figure 6. The overall trend is similar to what was observed with the WESP off-line, and the FTIR indicated no obvious change in gas composition through the WESP. As before, the SO_2 at the absorber outlet was artificially high because of FTIR interference caused by solvent. This artificial spike in SO_2 largely disappeared at the system outlet after the AERU removed the solvent causing the FTIR interference.

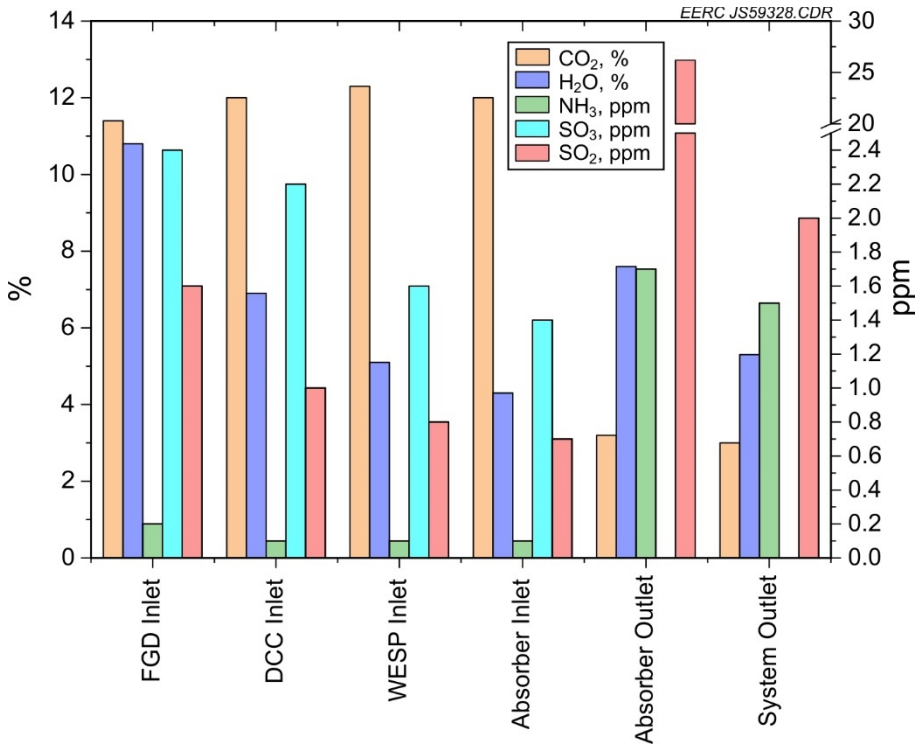

Figure 6. FTIR results from December 18 with the WESP online.

As seen in Figure 7, the trends in particulate loading through the FGD and DCC were similar to those observed previously, with a slight reduction in particulate through the FGD and a slight increase in fine particulate size and concentration through the DCC. The WESP removed well over 95% of the particulate matter upstream of the absorber column, showing similar performance to that previously observed at MRYS. Almost no residual particulate was detected at the AERU outlet. Particulate sampling directly at the absorber column outlet was not possible, so it is impossible to say how much of the residual particulate escaping the WESP was removed by the absorber and how much was removed by the AERU system.

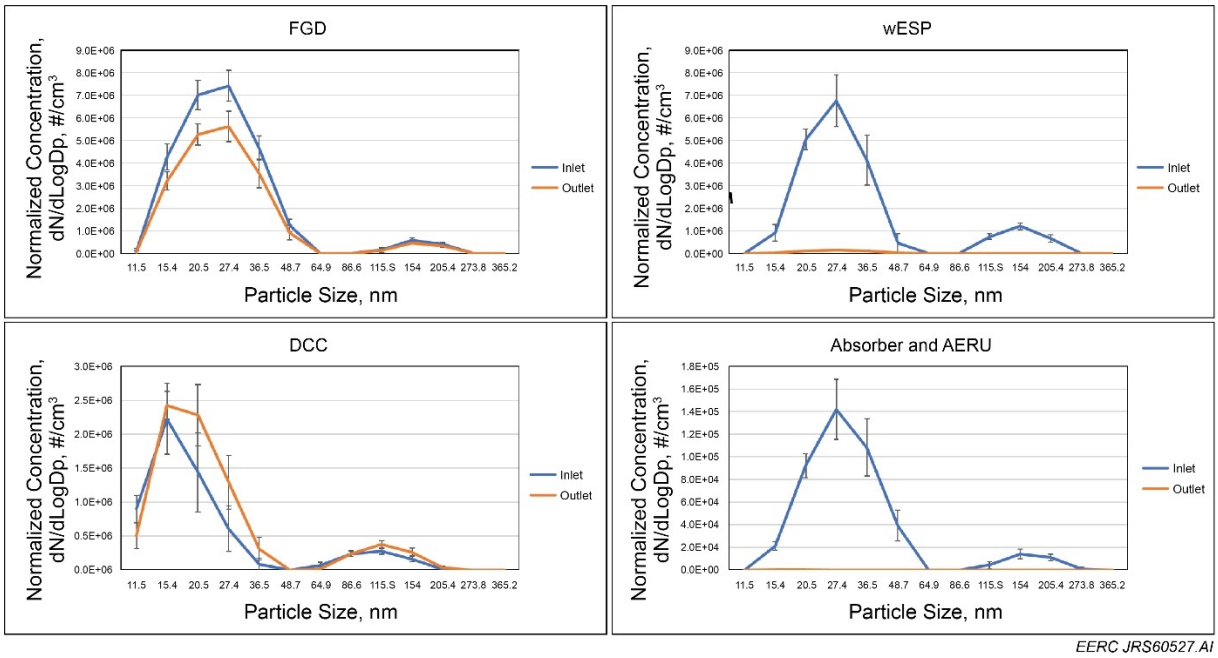

Figure 7. Normalized average particulate loading at the inlet and outlet to each major unit operation during December 18–22, 2020.

It is noteworthy that the scales between each unit are somewhat different, with a peak of around 6.0×10^6 particles/cm³ at the FGD outlet and WESP inlet, but a peak of only 2.5×10^6 particles/cm³ at the DCC, which is between the two units. This difference occurs because of changes in the baseline particulate loading throughout each sampling period. Some of the later FGD samples were several times lower in particle count, and some of the WESP samples were several times higher. The specific charts presented here were chosen because they show periods of steady-state particulate loading through each unit operation. Large changes in baseline particulate loading throughout the course of a day have been observed in previous particulate sampling at other power plants, illustrating the need for near-simultaneous sampling at the inlet and outlet to each unit operation to truly understand particulate fate. In this case, although the absolute scale is different at each unit, the inlet and outlet samples were taken at the same time and provide useful information on what is occurring through each unit regardless of changes in baseline particulate entering the system.

KS-1 Solvent Analyses

During operation of the capture system, samples of the solvent were taken every 2 weeks for analysis of select analytes. Samples of the KS-1 solvent encompass roughly 78 days of continuous operation, and for KS-21, operation spans roughly 16 days. Solvent samples were analyzed for a variety of analytes using ion chromatography (IC), inductively coupled plasma (ICP), and ICP coupled with mass spectrometry (ICP–MS).

Results for KS-1 solvent are presented in Figures 8–11. Major cations that would give strong indication of dissolution of fly ash into the solvent included silicon, sodium, potassium, calcium,

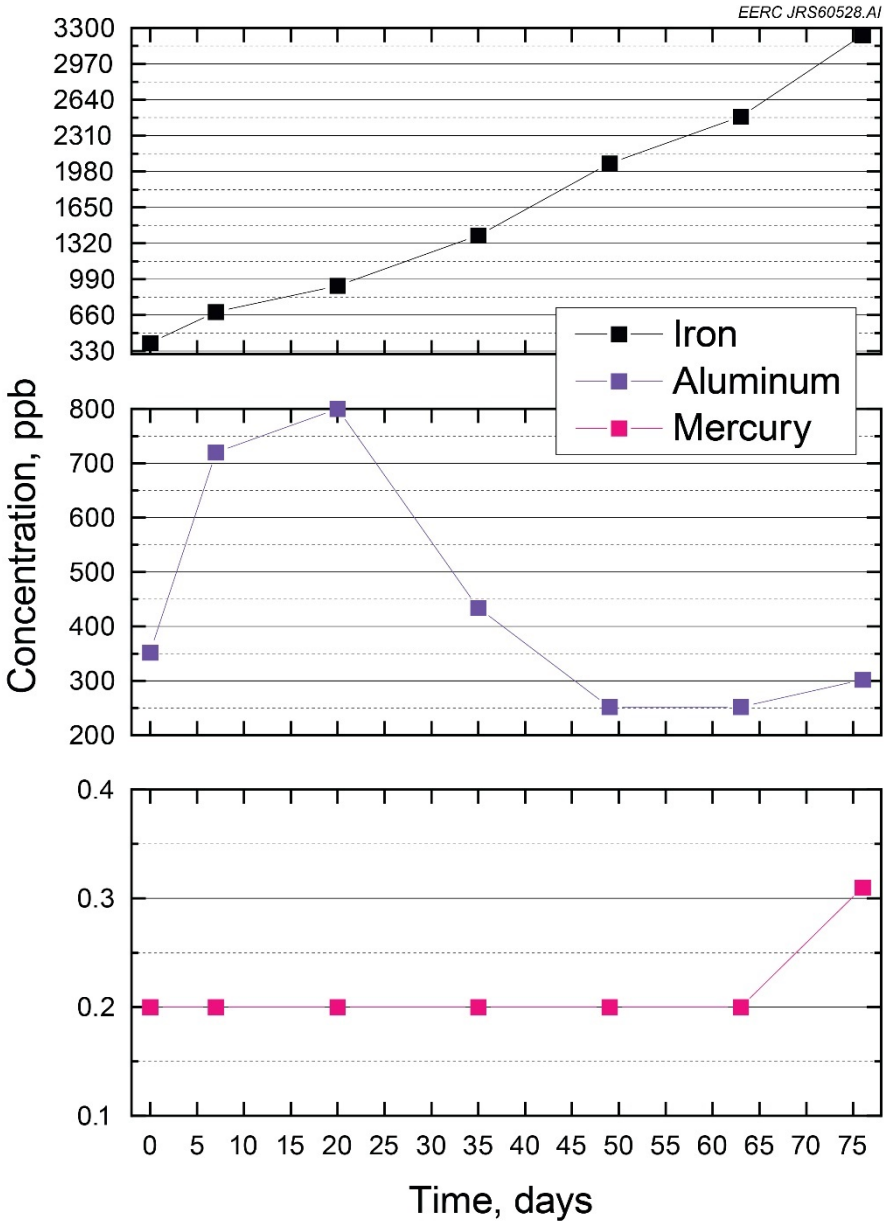

Figure 8. Concentrations of iron, aluminum, and mercury for KS-1. The lower limit of quantification (LLQ) for mercury is 0.2 parts per billion (ppb).

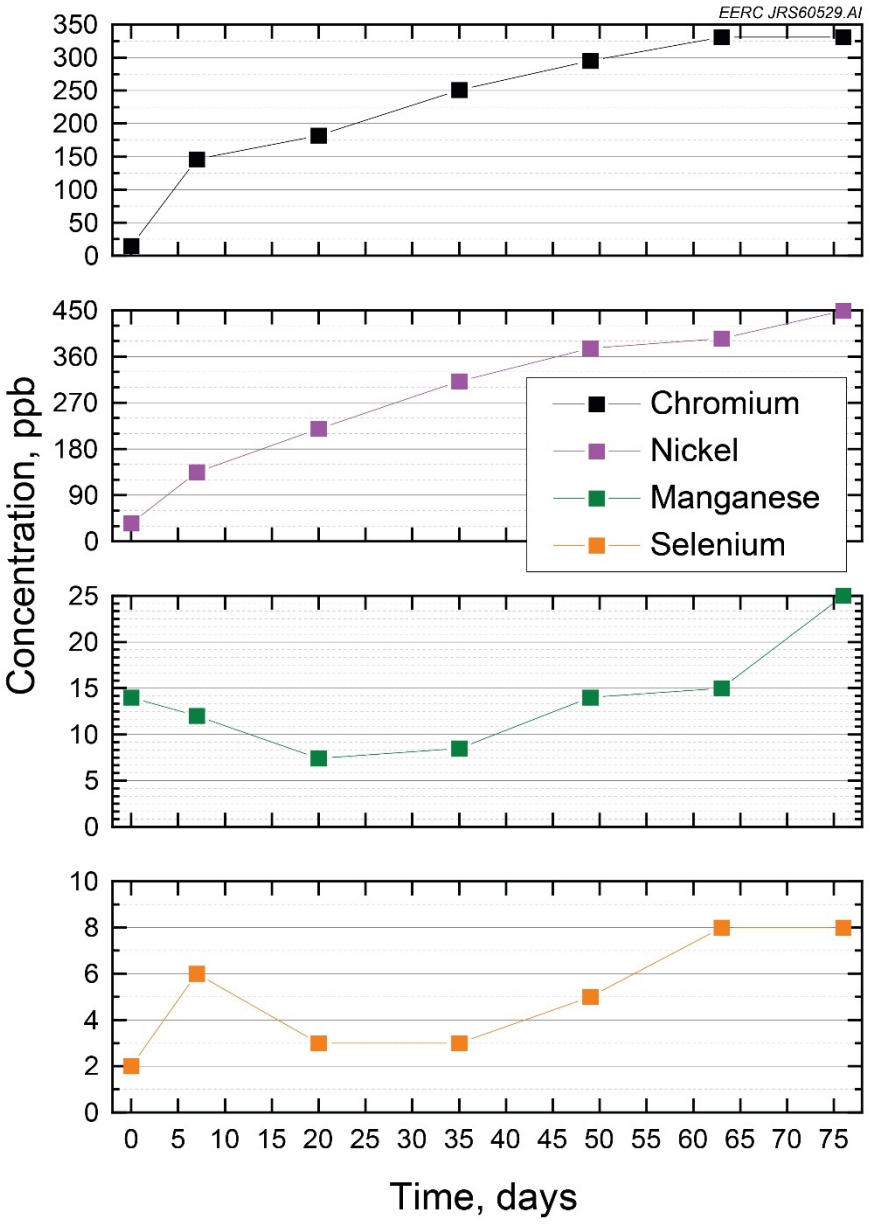

Figure 9. Concentrations of chromium, nickel, manganese, and selenium for KS-1.

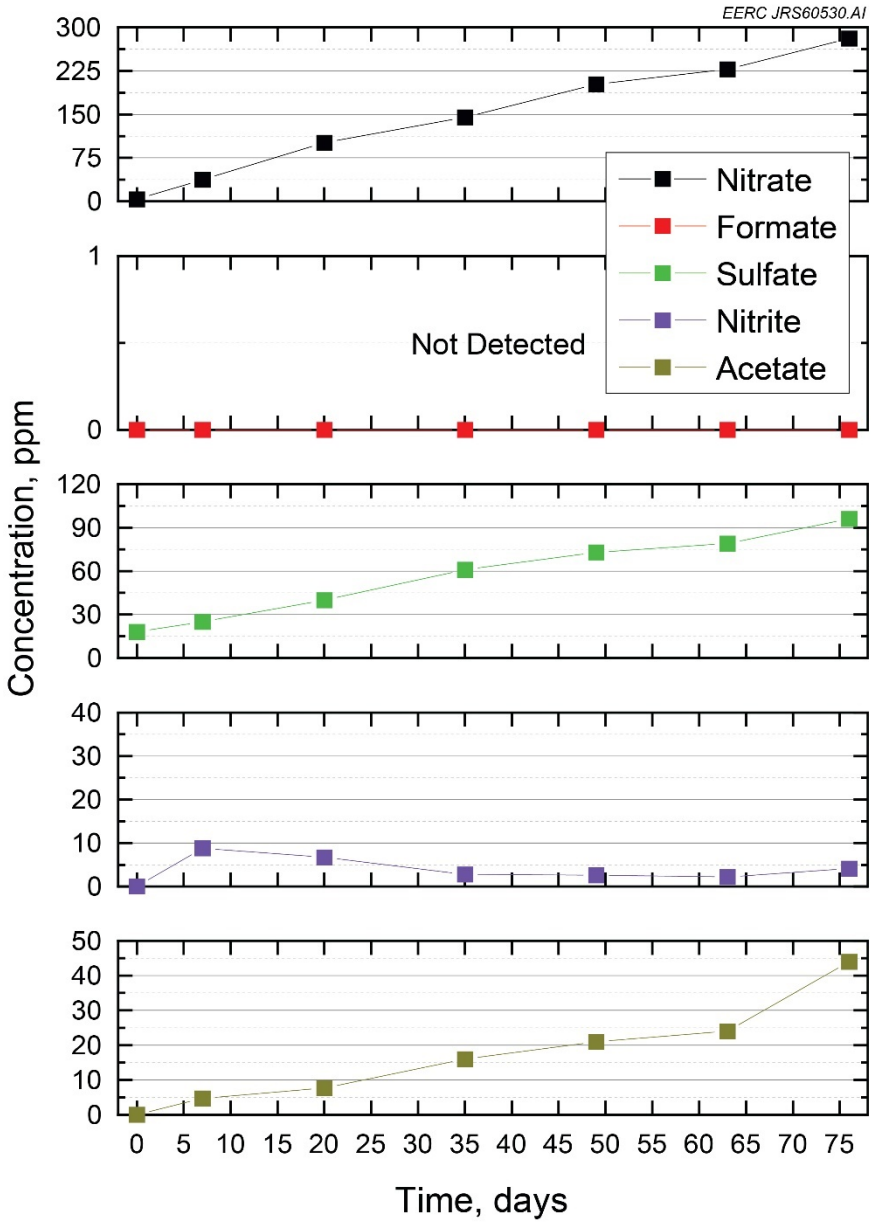

Figure 10. Concentrations of nitrate, formate, sulfate, nitrite, and acetate for KS-1. A concentration of zero means that the analyte was not detected.

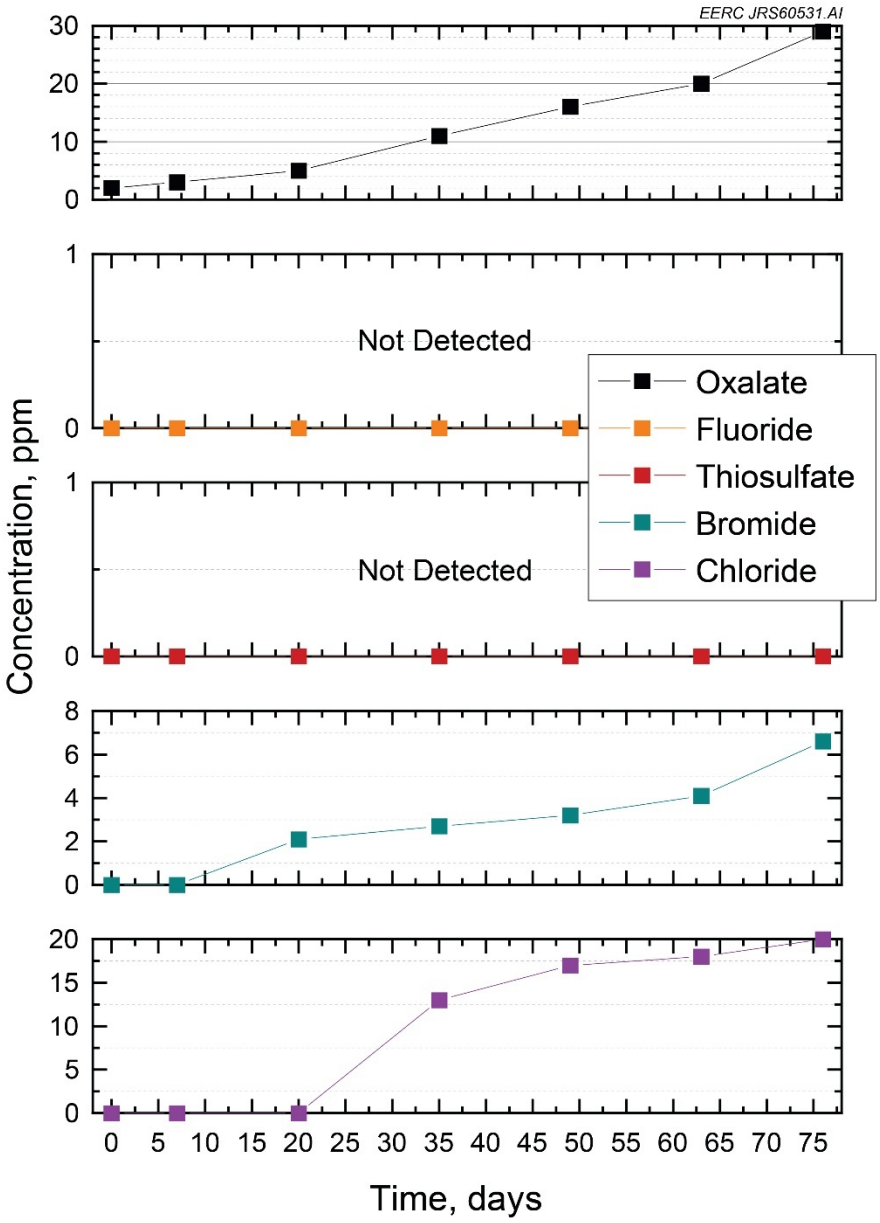

Figure 11. Concentrations of oxalate, fluoride, thiosulfate, bromide, and chloride for KS-1. A concentration of zero means that the analyte was not detected.

and magnesium. These analytes were not detected in any of the samples submitted for analysis. Aluminum and iron analytes are also associated with fly ash and were detected as indicated in Figure 8. Aluminum concentrations increased in the early part of testing and then dropped off quickly to a low concentration of 300 ppb by the end of testing. Iron concentrations rose steadily throughout the period of operation. The iron concentration is most likely a combined result of both fly ash accumulation and materials of construction used in the capture system, but it is impossible to differentiate between the two sources of iron buildup. Chromium and nickel (Figure 9) also

increased but remained at much lower concentrations. The similar changes in chromium, nickel, and iron would directly relate to the stainless-steel materials used in the capture system.

Manganese, selenium, and mercury concentrations were very low and are not at levels that would indicate concern. Mercury was detected in all samples but was below the LLQ (0.2 ppb) in all samples except the final one taken.

Nitrate, acetate, and sulfate concentrations rose throughout the test campaign but remained very low. Formate was not detected in any sample analyzed. Nitrite was present but remained at an extremely low and fairly steady concentration throughout the period of operation.

Like formate, fluoride and thiosulfate were not detected in any of the solvent samples. The lack of thiosulfate supports the low concentration of sulfur measured in the flue gas entering the absorber. Bromide and chloride remained below reporting limits early in the period of operation before slowly increasing in concentration.

Dekati Substrates – IC/ICP/ICP–MS Analyses

Dekati substrates collected during operation of the capture system were cut in half. Half of each substrate was dissolved and analyzed by IC/ICP/ICP–MS to estimate particulate composition, and the other half of each substrate was retained for morphological examination by field emission scanning electron microscope (FESEM).

The IC/ICP/ICP–MS results for particulate matter collected on Dekati substrates during operation with KS-1 are presented in Figure 12 for samples taken with the WESP off-line and in Figure 13 for samples taken with the WESP online. The fine particulate matter measured at the plant stack (without the capture system operating) was enriched in aluminum, alkali, alkaline earth, iron, and sulfur, with lesser amounts of chromium and nickel. (It should be noted that silica content was not analyzed.) These results indicate that the particulate matter was mostly fly ash. By point of contrast, samples taken in previous work at MRYS were enriched in sodium and potassium, indicating that much of the particulate matter at that plant was present as condensed alkali sulfate, with comparatively little fly ash. This difference in results is an expected effect of the different burner configurations: MRYS uses a higher-temperature slagging cyclone burner that removes much of the inorganic material as slag and also vaporizes more of the alkali material. The pulverized coal (pc)-fired burner at Coal Creek Station operates at a lower temperature, leaving much of the coal ash entrained in the flue gas stream.

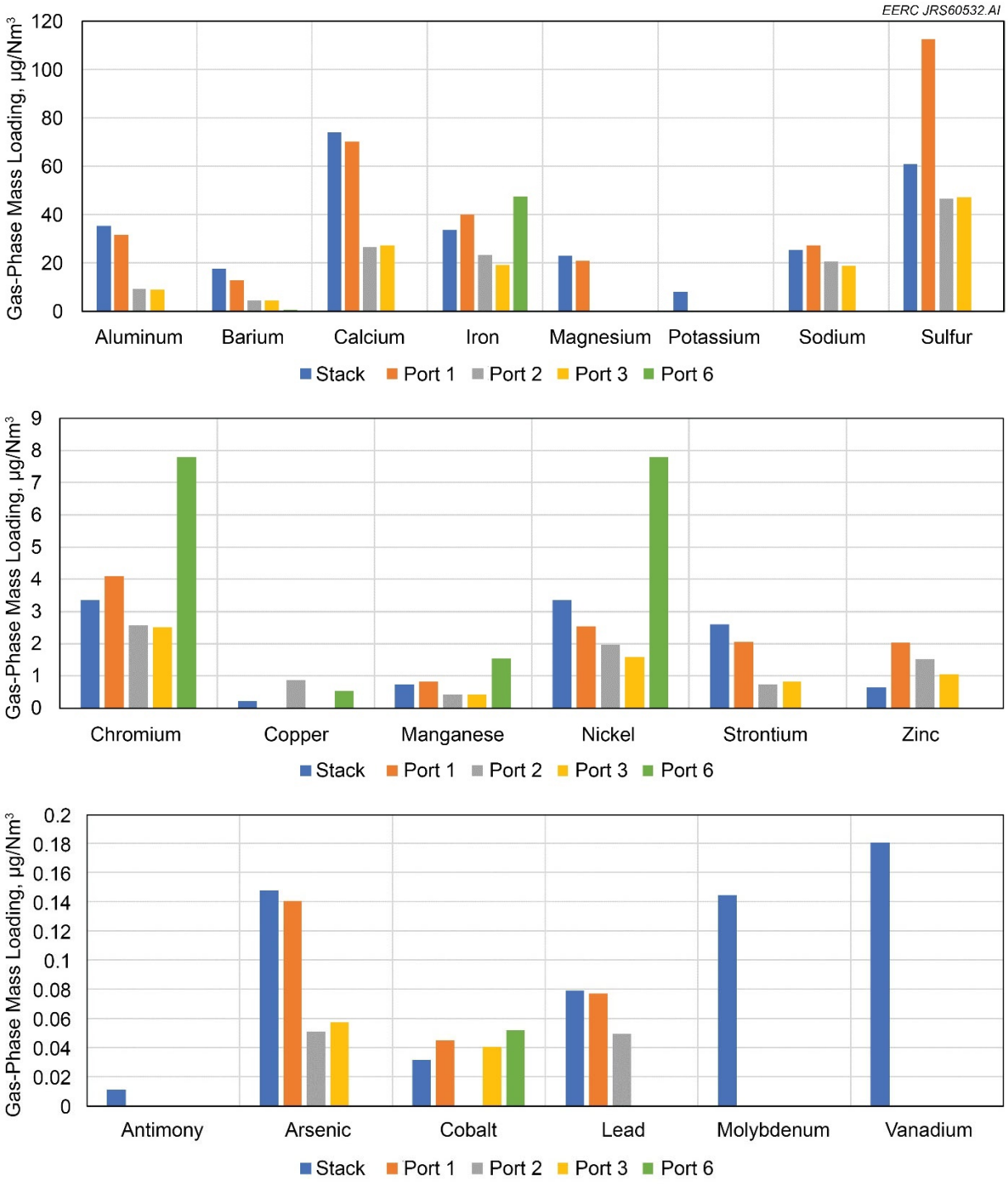

Figure 12. Concentrations of various analytes in particulate matter collected during KS-1 operation with the WESP off-line.

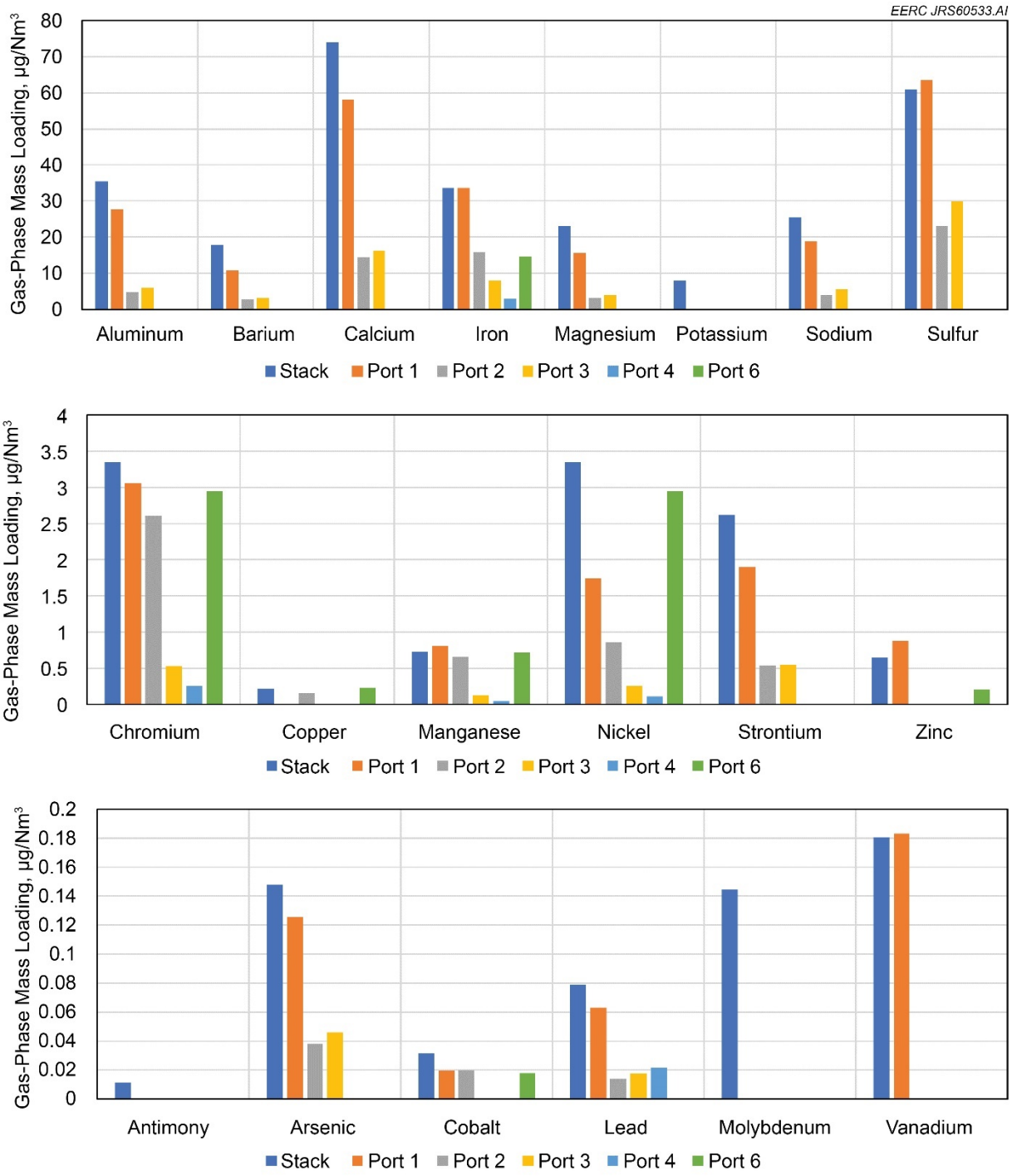

Figure 13. Concentrations of various analytes in particulate matter collected during KS-1 operation with the WESP online.

The composition at Port 1 was generally very close to what had been measured at the stack and indicates a relatively stable particulate loading and composition entering the system, with the exception that potassium and some of the trace elements were below calibrated reporting limits at Port 1 during testing with KS-1 solvent. Substrates collected at Port 1 were exposed to less flue gas and contained lower total mass of accumulated particulate, and it is likely that at least some of these species were present at similar flue gas concentrations to what had been observed at the stack but were below reporting limits in the dissolved substrate solution. Port 1 also saw high sulfur during operation without the WESP, which may be related to changes in coal or plant operating conditions during this sampling period.

The mass loading of different analytes decreased through the FGD and DCC, then largely disappeared through the WESP (Port 4) when it was operating. When the WESP was off-line, the mass loading of major ash components similarly disappeared at the system outlet (Port 6), indicating that the residual particulate matter was being largely removed in the absorber and/or AERU. As noted previously, sampling between the absorber and AERU was not possible.

Upstream of the absorber column, the relative balance of different analytes in the particulate captured on Dekati substrates did not appear to vary much through the various capture devices, indicating that each unit was removing the entrained particulate without chemical transformation or selective removal. However, the concentrations of chromium, iron, nickel, and manganese were elevated on the substrates collected at the system outlet when using KS-1 solvent, particularly when the WESP was off-line. Other analytes (with the exception of copper and cobalt) were below reporting limits, indicating that this material was not likely ash-derived. The high mass loading of these metals is likely derived from the stainless-steel materials of construction used in the absorber column being carried over with solvent escaping the system. Analysis of the solvent fabric filters (discussed later in this report) showed an early spike in copper content of micrometer-scale material that decreased in later samples, with a few larger pieces being especially concentrated in copper. Similarly, iron content was high in the filtered material but was especially concentrated in a few small bits of particulate. These results suggest that at least some of the metal content detected in the solvent and in the Dekati substrates from the absorber outlet was from discrete materials already present in the absorber being physically picked up by the solvent and slowly filtered out over time.

Dekati Substrates – FESEM Analyses

FESEM morphology, shown in Figure 14, supports the observation that the particulate matter at Coal Creek Station was mostly fly ash. All morphological images are of the substrate taken from Stage 10 of the Dekati particle impactor, which corresponds to a mean particle diameter of 0.949 μm, and are from the week of December 18–22, 2020, when the unit was run with the WESP on-line with KS-1 solvent. At the inlet to the system (Port 1), particles were numerous and well defined as would be expected from fly ash particles. Energy-dispersive x-ray (EDX) spectral analysis in Figure 15 suggests that this material is mostly calcium aluminosilicate. This agrees well with IC/ICP/ICP–MS analyses of the stack particulate.

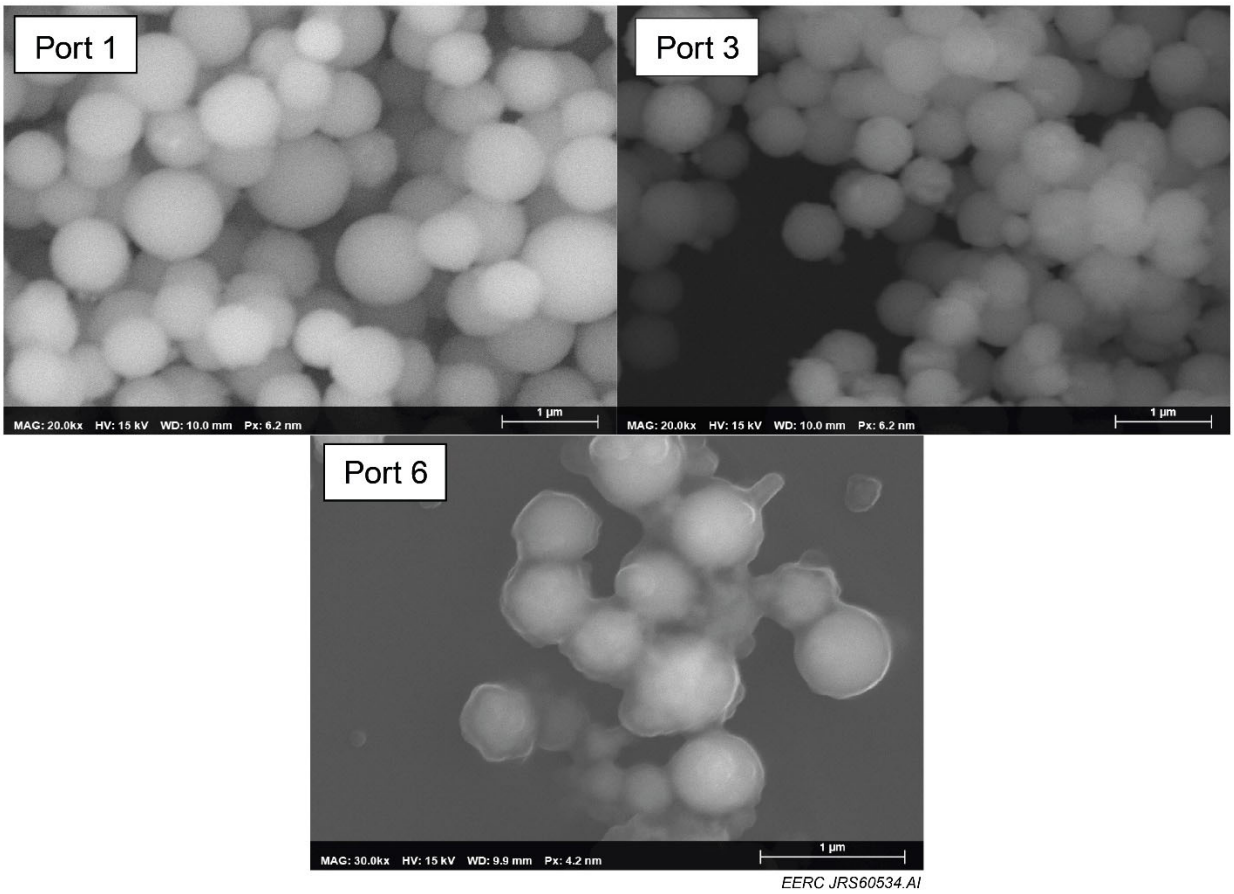

Figure 14. Dekati impactor Stage 10 particulate morphology.

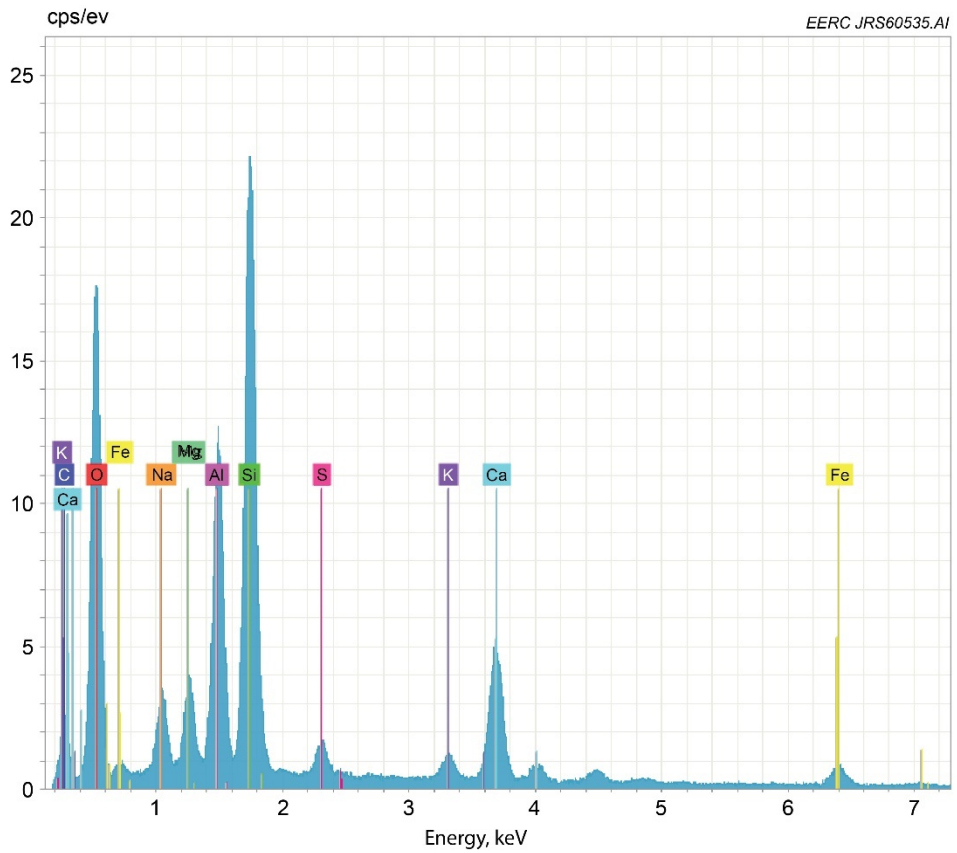

Figure 15. EDX spectrum of Dekati Stage 10 particulate collected at Port 1.

At the exit to the DCC (Port 3), particles are slightly less numerous and more of the smaller particles are adhering to the larger particles, which may indicate some condensation from the gas stream. EDX spectral analysis showed that the particulate chemistry at this port was indistinguishable from the material collected at Port 1. At the system exit (Port 6), particles are far less numerous and appear to have agglomerated inside of a bonding material. Although EDX spectrum of the Dekati Stage 10 substrate is not available, analysis of Stage 8, which showed similar agglomeration, revealed a prominent peak around carbon, as shown in Figure 16. In an EDX spectrum, the peak for nitrogen would fall almost on top of this peak and would likely be obscured by and add to this large spike. This is an indication that the binding agent is amine-derived from the KS-1 solvent that condensed onto the fly ash particles as they passed through the absorber column and that this amine is now leaving the system with the fly ash particles.

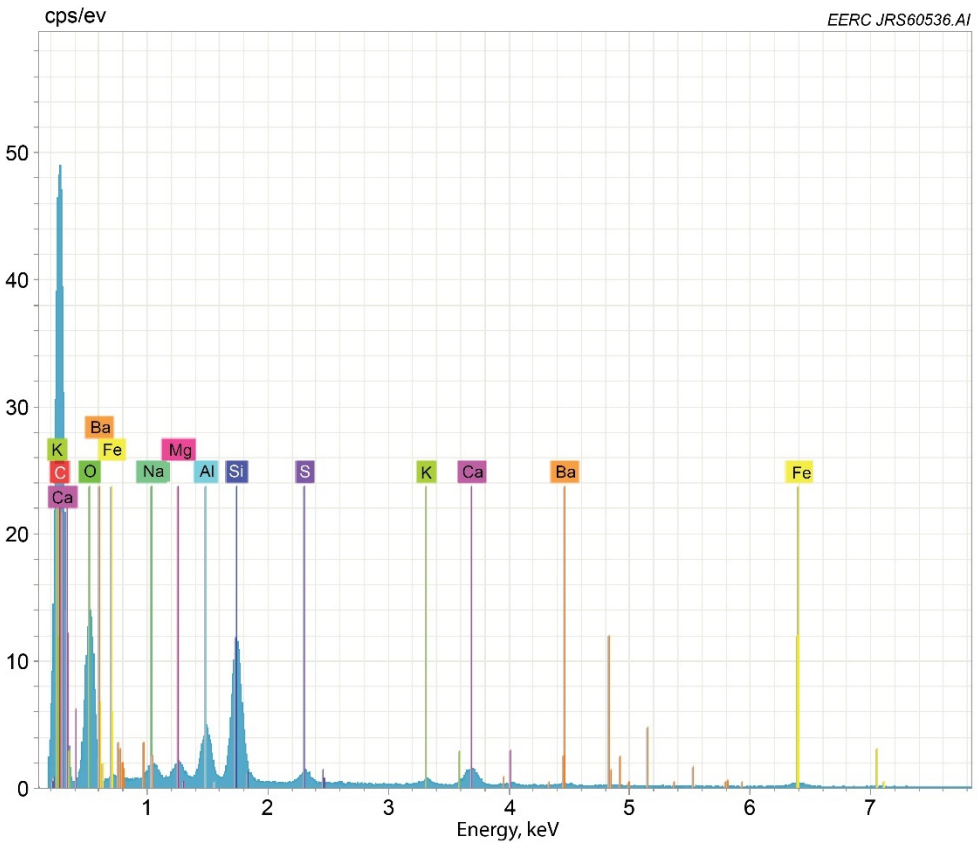

Figure 16. EDX spectrum of Dekati Stage 8 particulate collected at Port 6.

FESEM morphology of the particulate collected at the system outlet during the week of November 16–20, 2020, when the unit was run with the WESP off-line with KS-1 solvent, is shown in Figure 17. Compared to material collected at other sample ports and during all later test periods, this particulate was irregularly shaped and had a very different structure than the spherical particles collected at the system inlet. This material exhibited a strong peak of carbon and/or nitrogen when analyzed by EDX spectral analyses under the FESEM, and as previously discussed and indicated in Figure 12, the bulk material was mostly iron, chromium, and nickel, with lesser amounts of manganese, copper, zinc, and cobalt. Based on the anomalous structure and composition, this material is suspected to be fine metal residue left in the system during fabrication and carried out with the flue gas and entrained solvent.

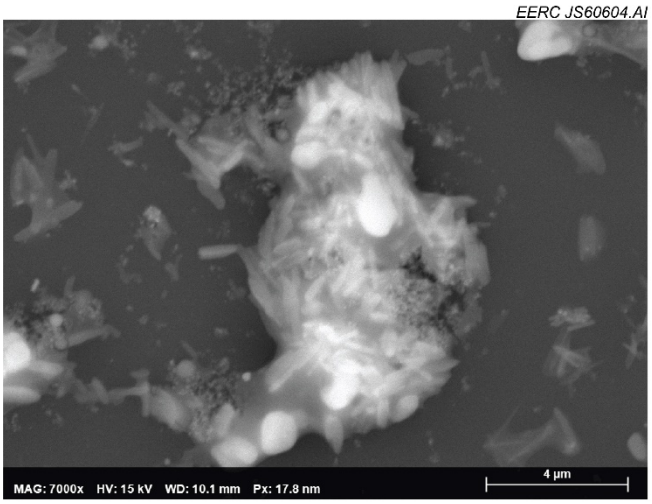

Figure 17. SEM (scanning electron microscopy) morphology of ELPI+ impactor substrate collected at Port 6 during operation with KS-1 and WESP offline. Image is of substrate collected at Stage 8 of the impactor, indicating a nominal mean particle diameter of 0.380 µm.

Dekati Substrate Particle-Size Distribution Assessment

A computer-based program was used to automatically identify and size spherical particles visible in the SEM morphology. An example output is shown in Figure 18 for Stage 12, which had a nominal diameter of 2.5 µm. Statistical analyses of the particulate collected on Dekati substrates showed that average particle size was smaller than the nominal size expected for each impactor stage. This was true for all samples collected throughout the capture system and when operating with either solvent. The relationship between expected and actual particle size was nearly linear for the early (small-diameter) stages, with average particle diameter slightly more than half of the expected diameter, but then flattened out at less than 700 nm with later (high-diameter) stages, as illustrated in Figure 19. Many individual particles were close to nominal size, as indicated by the long right tail in the distribution of Figure 18, but the average diameter was kept low by the presence of many smaller particles. Examining clusters of particles, it appears that some of the smaller particulate may have sintered together prior to entering the Dekati, with each cluster of small particles acting as a single particle with a larger effective diameter. This effect is illustrated in the second image in Figure 20, which superimposes a nominal circle (940 nm for Stage 10) over a cluster of three smaller-diameter particles that appear to be partially sintered. One implication of this is that a typical single particle as measured by Dekati or SMPS is likely to be an irregularly shaped cluster of smaller particles with higher surface area (and, thus, higher potential for aerosol condensation) than would be predicted by assuming each particle is a perfect sphere.

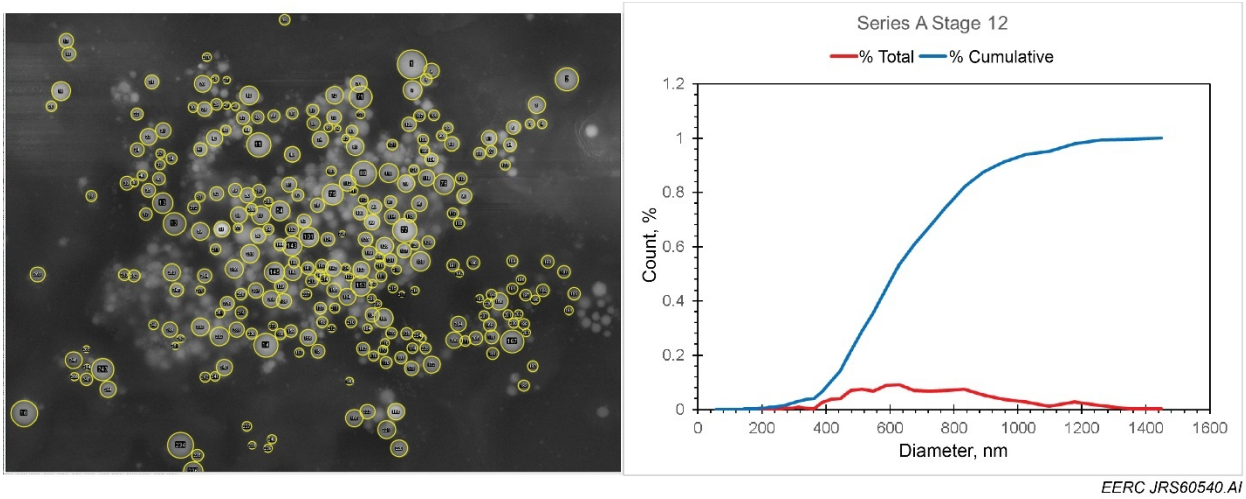

Figure 18. Example output of image analysis with cumulative distribution.

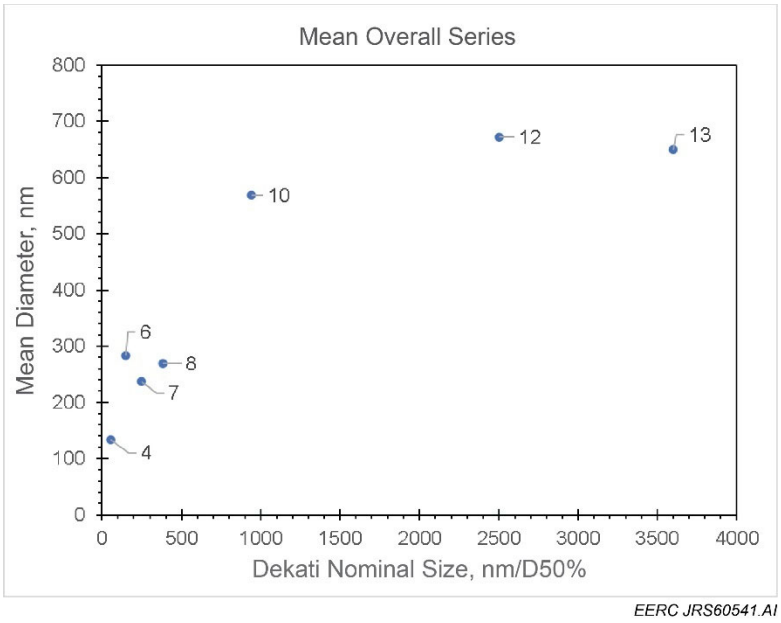

Figure 19. Average actual particle diameter versus nominal diameter for select Dekati stages.

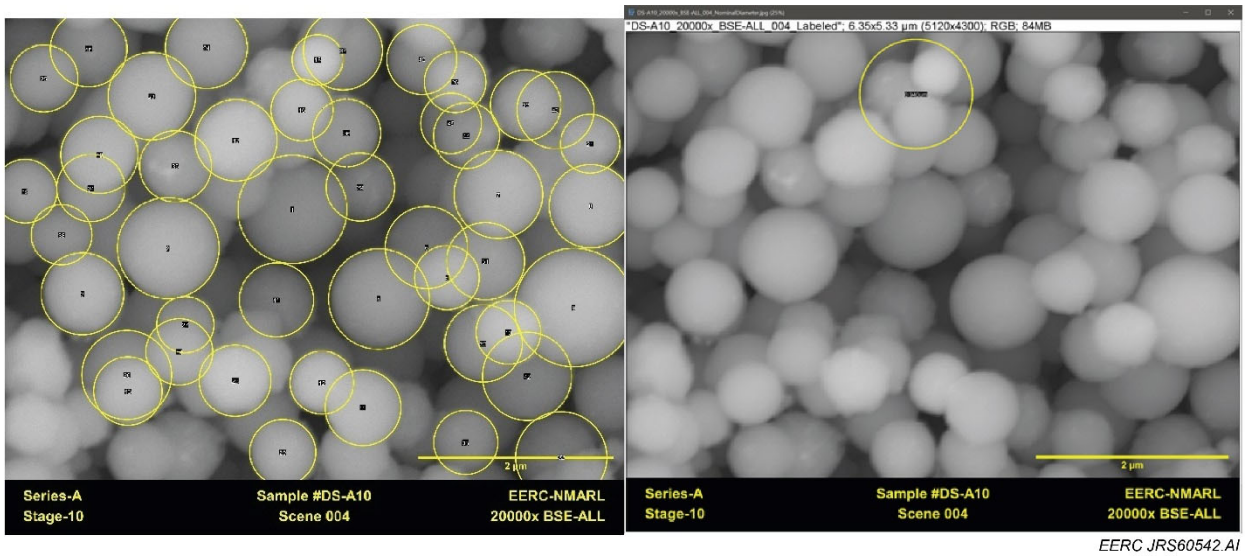

EERC JRS60542.AI

Figure 20. SEM image illustrating that clusters of particles match the nominal diameter. The image on the left is as-processed, and the image on the right shows a superimposed nominal-diameter circle over a cluster of small individual particles.

Activity 3 – Advanced Solvent Testing

Advanced KS-21 solvent was delivered to Coal Creek Station at the end of December. It was mixed and loaded on December 30, 2020, and capture ran through January 17, 2021.

Sampling During KS-21 Operation

Key FTIR results with KS-21 are shown in Figure 21. Results are similar to what was observed when running with KS-1 solvent. As can be seen, the FGD and DCC were effective at reducing moisture and SO_2 at the absorber inlet. The moisture and measured ammonia then spiked at the absorber outlet as the heated gas exiting the column carried through moisture and solvent. MHI's AERU system recovered some of this material again before the system outlet, but the moisture and ammonia levels in the final gas remained higher than they had been at the absorber inlet. The extremely high SO_2 at the absorber outlet is artificial. The presence of solvent has been observed to interfere with the signal for SO_2 in past testing using the EERC's FTIR configuration, and this artificially high SO_2 is believed to be the result of this interference. SO_2 readings returned close to inlet levels at the system outlet, indicating that the solvent in the gas had been effectively removed by the AERU.

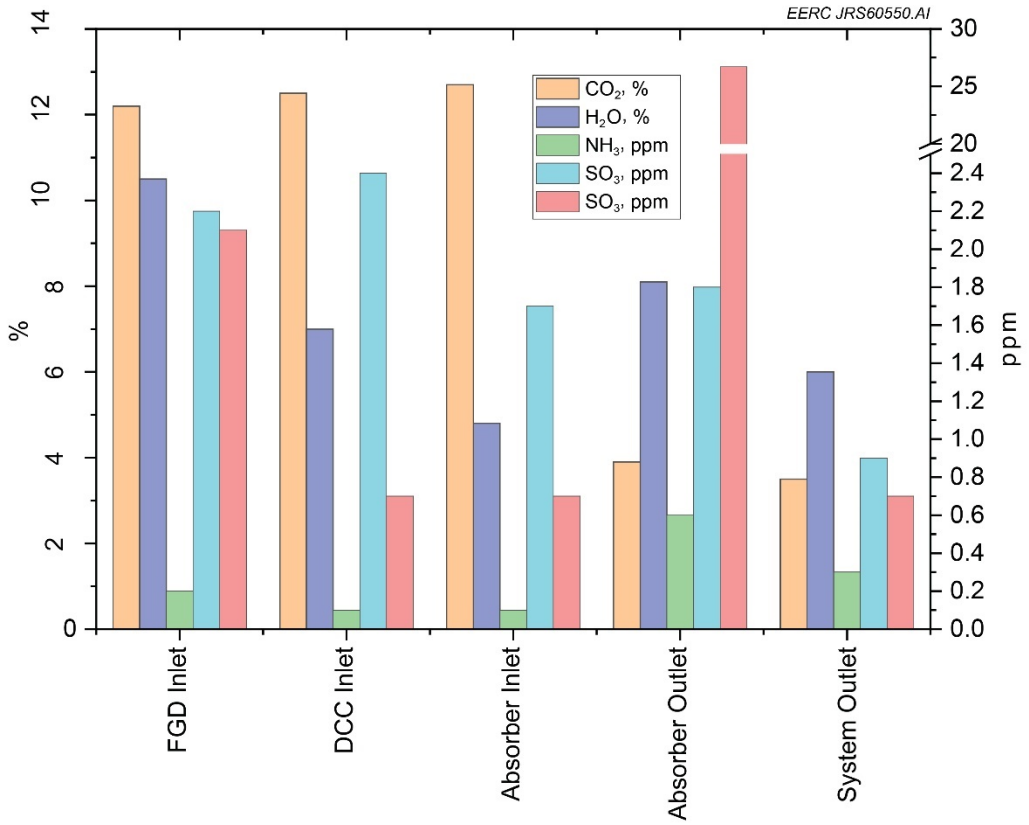

Figure 21. FTIR results from January 16 with KS-21 solvent and the WESP off-line. SO_2 values downstream of the absorber are not reliable and are included for informational purposes.

Figure 22 shows the particulate loading at the inlet and outlet to major unit operations when operating with KS-21. The FGD and DCC are combined into a single unit because of anomalous particulate loadings measured at the FGD outlet. The unusual aerosol measurements at the FGD outlet were repeatable through three different sampling periods and appear to be legitimate, but they do not reflect significant changes to the pilot plant FGD operation. The particulate loading returned to near-baseline conditions at the DCC outlet. The inlet PSD was shifted to a larger particle size during this sampling period. This shift was present in all samples taken over several days of sampling. The anomalous behavior through the FGD and the shift to larger particle sizes are believed to be related to changes in power plant operation and/or coal chemistry during this test period.

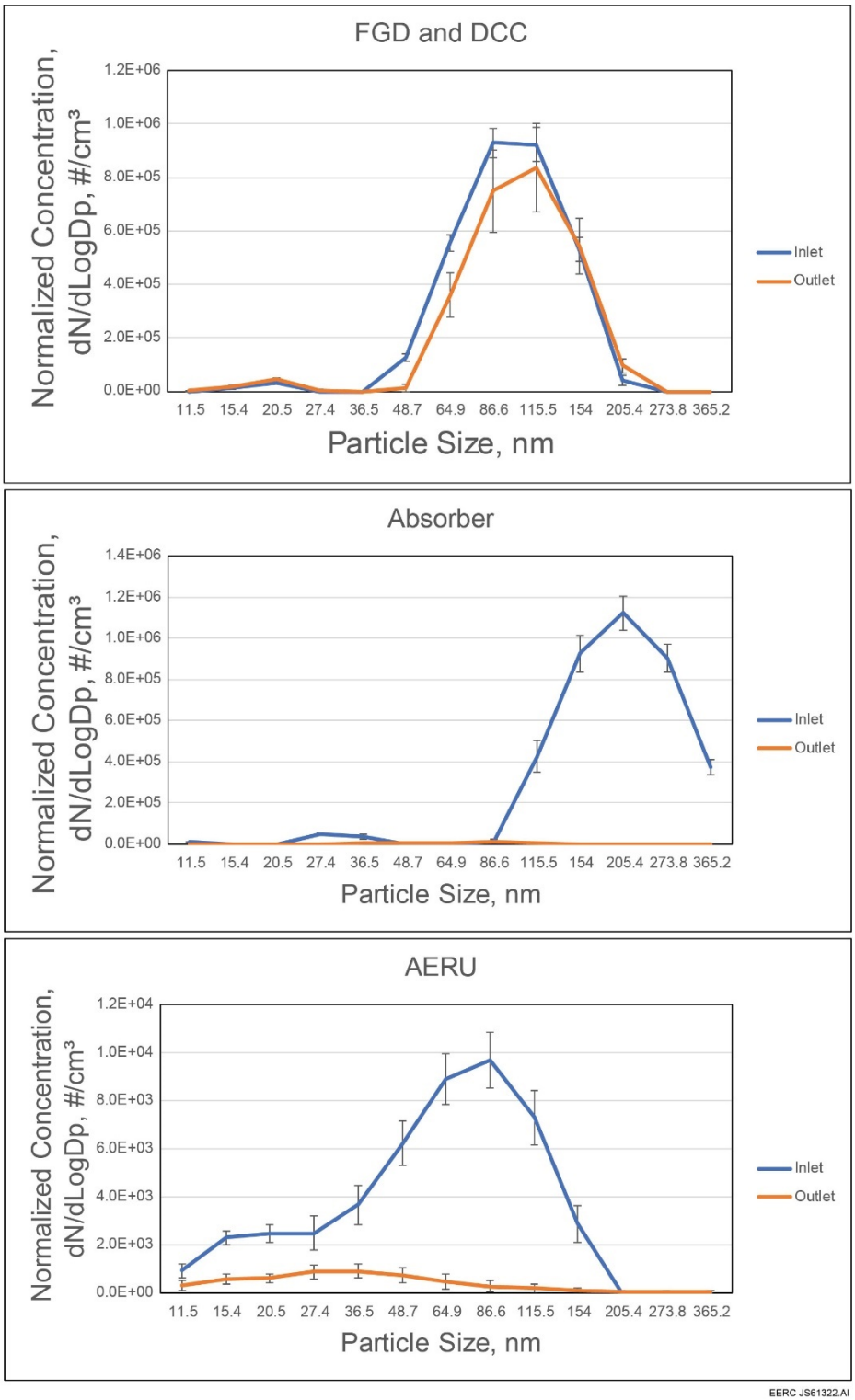

Figure 22. Normalized average particulate loading at the inlet and outlet to each major unit operation during January 14–17, 2021.

During the end of operation with KS-21, a single period of particulate sampling was conducted at the absorber outlet (Port 5 in Figure 2), which previously could not be sampled during operation with KS-1. The data from this port show that, during operation with KS-21, particulate loading decreased through the absorber columns and then continued to decrease through the AERU.

Solvent Analyses

For KS-21, steady-state operation spanned roughly 16 days, and only the starting and ending solvent samples were collected for analyses. Solvent samples were analyzed for a variety of analytes using IC, ICP, and ICP–MS.

Solvent analytical results for KS-21 are shown in Figures 23–26. Although trends cannot be reliably established with only two data points, it is notable that the concentrations of many of the analytes are higher than would be expected based on similar times of exposure from the KS-1 solvent analyses. The elevated levels for those analytes that increased may be due to residual traces of KS-1 solvent in the system from the previous run. Further discussion would require additional samples collected over a longer period of operation. Although some of these analyte concentrations were higher for KS-21 than for KS-1 after a similar time of exposure, the levels measured for the time frame of operation are not alarming.

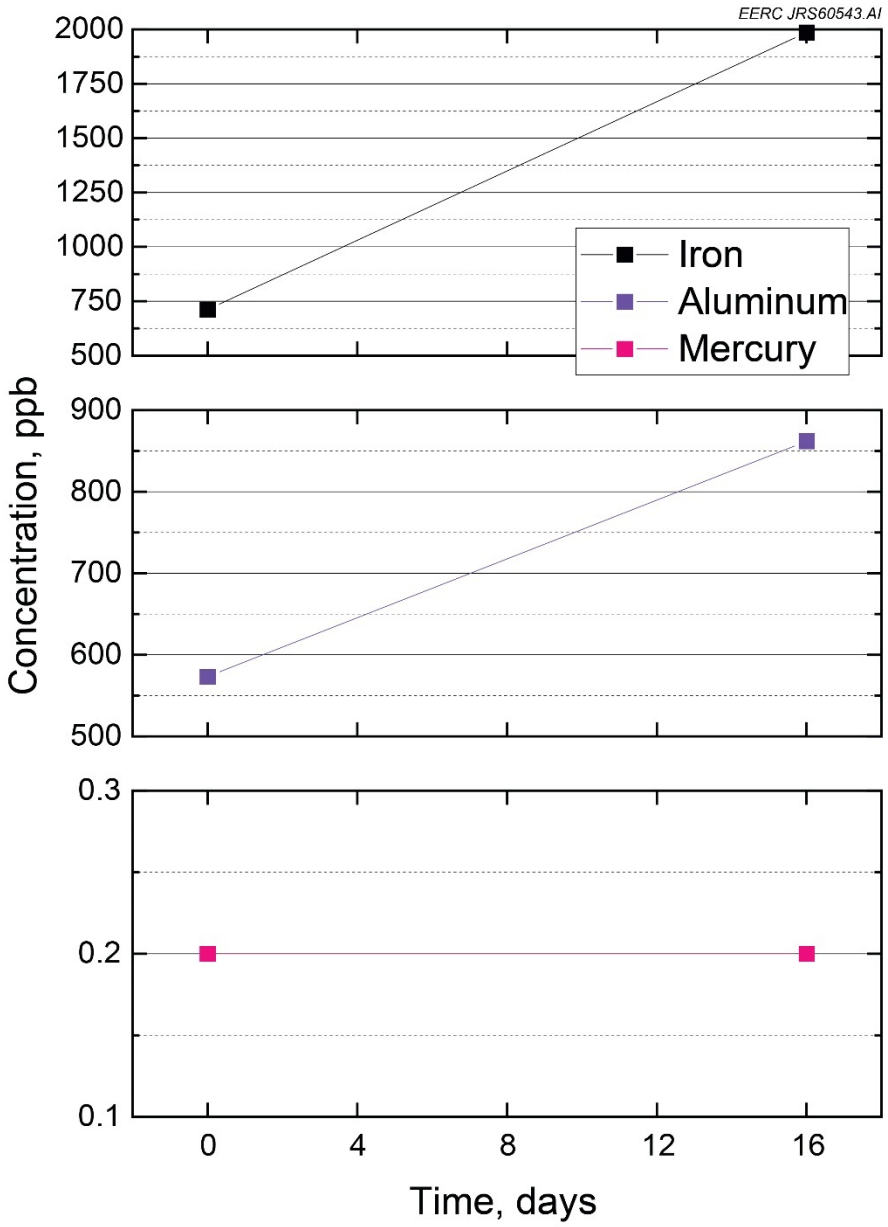

Figure 23. Concentrations of iron, aluminum, and mercury. The LLQ for mercury is 0.2 ppb.

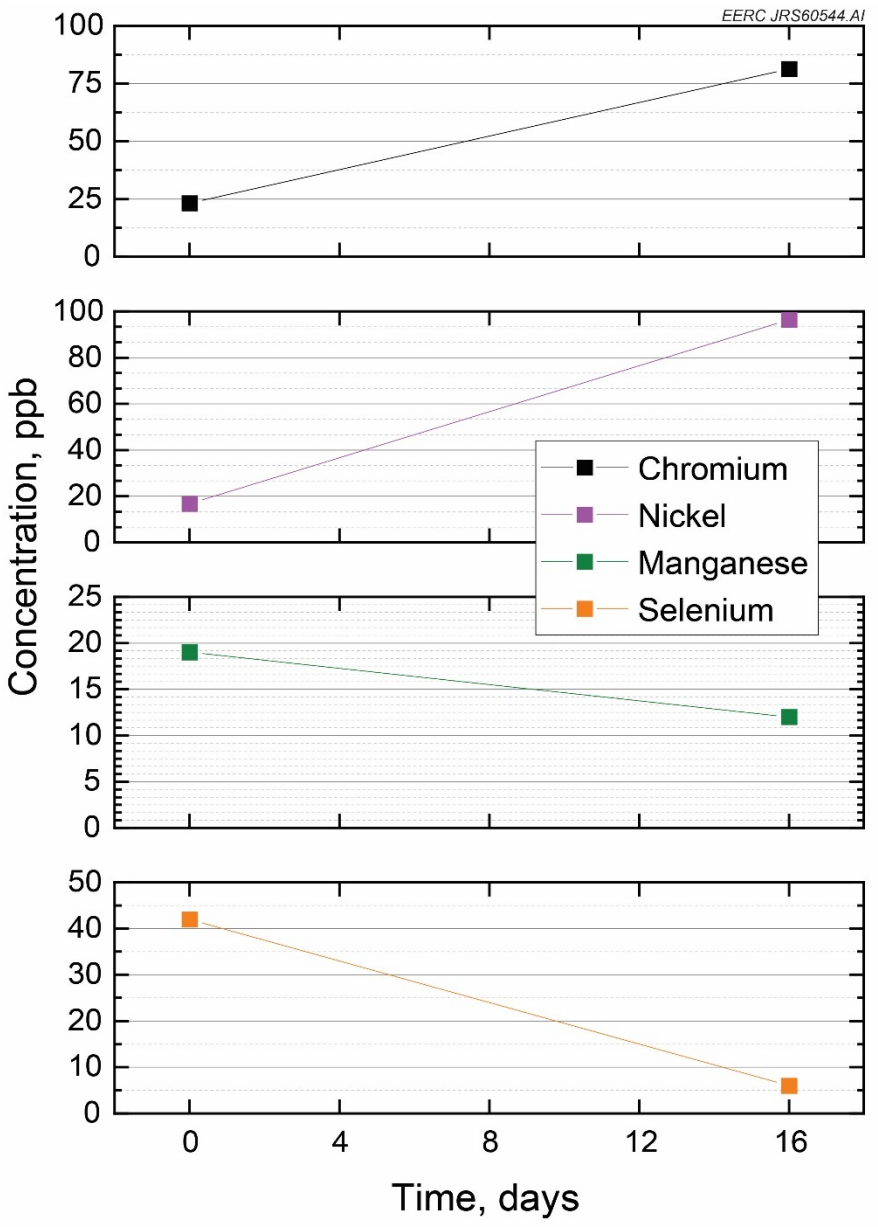

Figure 24. Concentrations of chromium, nickel, manganese, and selenium for KS-21.

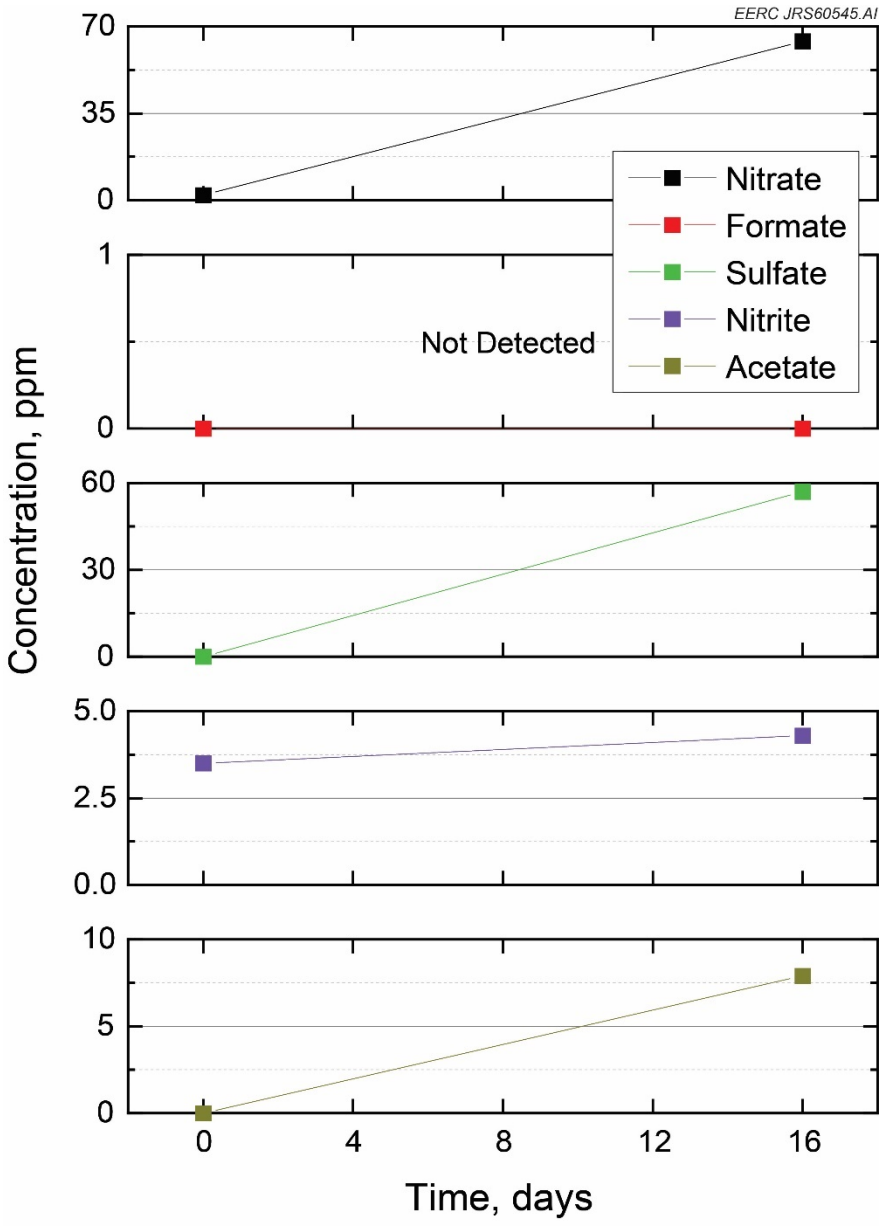

Figure 25. Concentrations of nitrate, formate, sulfate, nitrite, and acetate for KS-21. A concentration of zero means that the analyte was not detected.

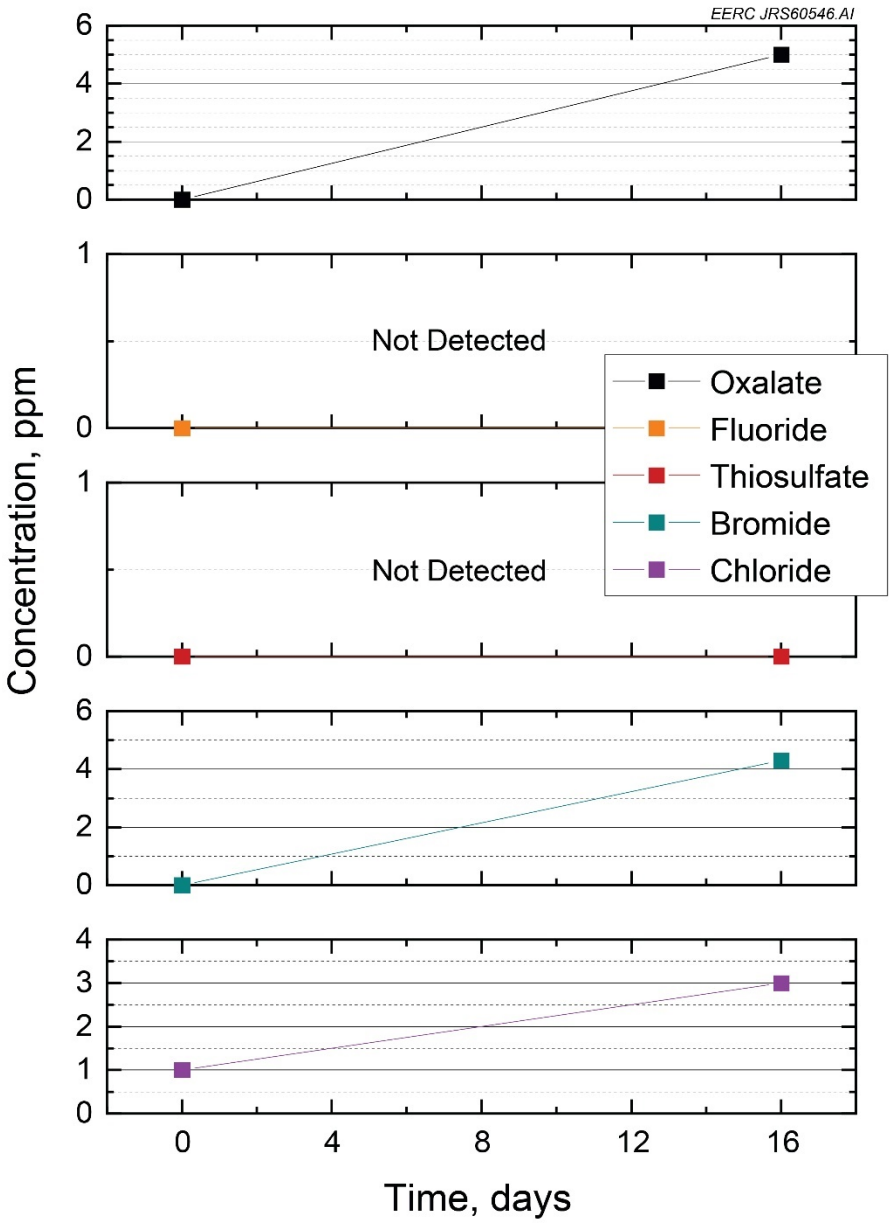

Figure 26. Concentrations of oxalate, fluoride, thiosulfate, bromide, and chloride for KS-21. A concentration of zero means that the analyte was not detected.

Dekati Substrates – IC/ICP/ICP–MS Analyses

Dekati substrates were only collected at Ports 1, 4, and 6 during testing with KS-21 solvent. The WESP was not run during sampling with KS-21 as one of the objectives of this sampling effort was to determine the potential differences in solvent carryover when using the advanced solvent. With the short sampling duration available for advanced solvent, it was decided that the higher particulate loading observed with the WESP off-line would provide greater insight into the effects of amine losses with particulate entrainment.

Figure 27 shows average analyte results at each port with the stack data from October 2020 included for reference. Particulate composition and loading at the system inlet (Port 1) was similar to that observed at the plant stack. Sampling was conducted over longer periods than had been done with KS-1 to allow for more total sample collection and better analyses.

Sampling after the FGD and DCC at Port 4 showed partial reduction in major analytes similar to that observed in earlier testing with the WESP off-line. In contrast to testing with KS-1 with the WESP off-line, very little material was detected at the system outlet (Port 6). There were minor traces of iron, chromium, and nickel, but these were over an order of magnitude lower than what had been observed when sampling downstream of the system operating with KS-1. The reduced metal loading at the system outlet is likely attributable to reduced solvent carryover with the advanced solvent. Reduced metal loading at the system outlet may also relate to the fact that much of the fine metal residue left from fabrication would have already been carried out of the system during the previous months of operation.

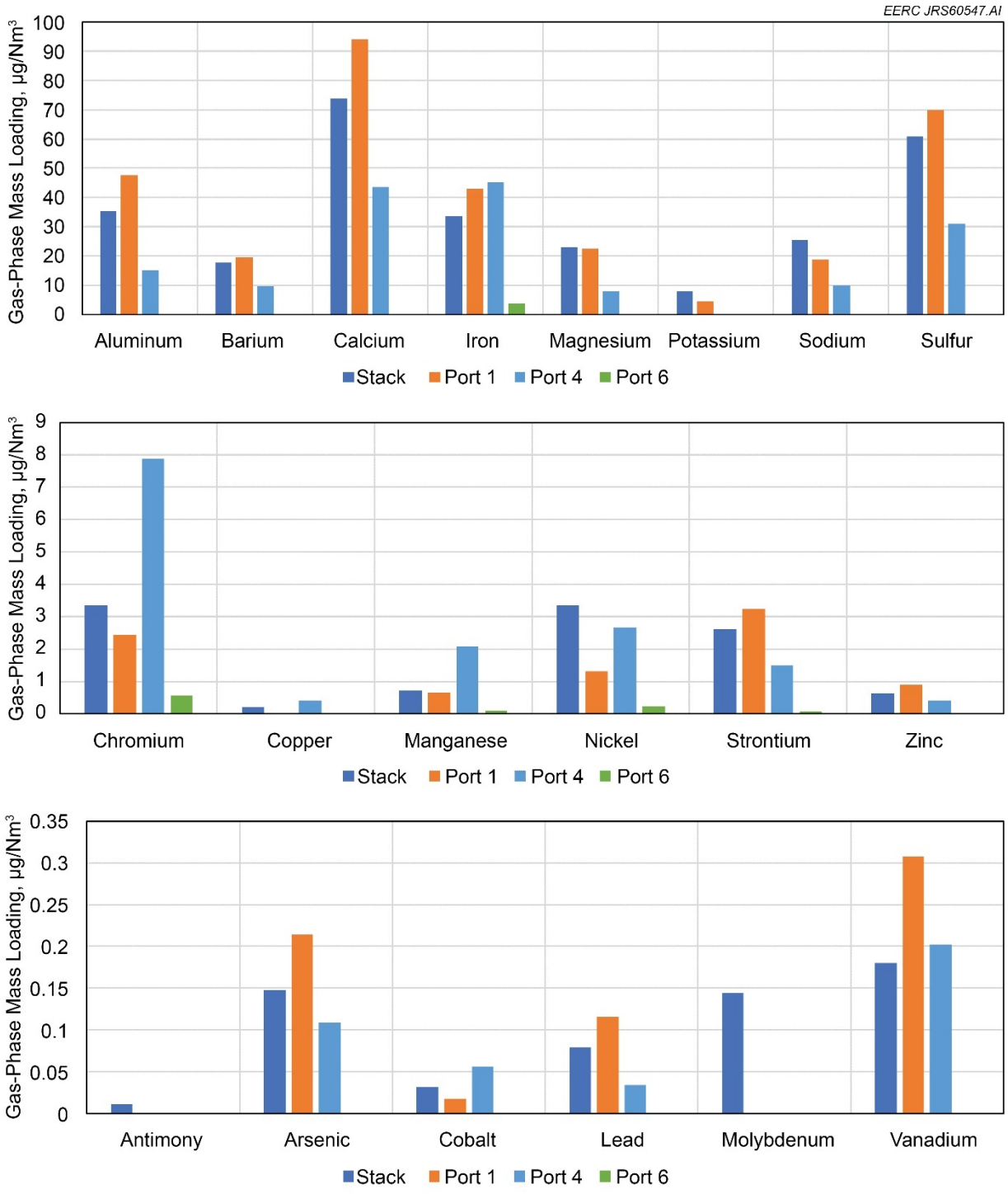

Figure 27. Substrate analytical results during KS-21 sampling.

Dekati Substrates – FESEM Analyses

FESEM morphology in Figure 28 shows particulate captured on the substrate taken from Stage 10 of the Dekati particle impactor, which corresponds to a mean particle diameter of 0.949 µm. The substrates are from January 16 and 17, near the end of operation, with KS-21 solvent. As compared to the particulate collected during operation with KS-1 solvent, the particulate in Figure 28 shows more agglomeration and deposition of small particles onto the larger fly ash particles at both the system inlet and outlet, possibly as a result of condensation of gas-phase species onto the fly ash. This change is likely due to changes in operation of the power plant and/or coal chemistry.

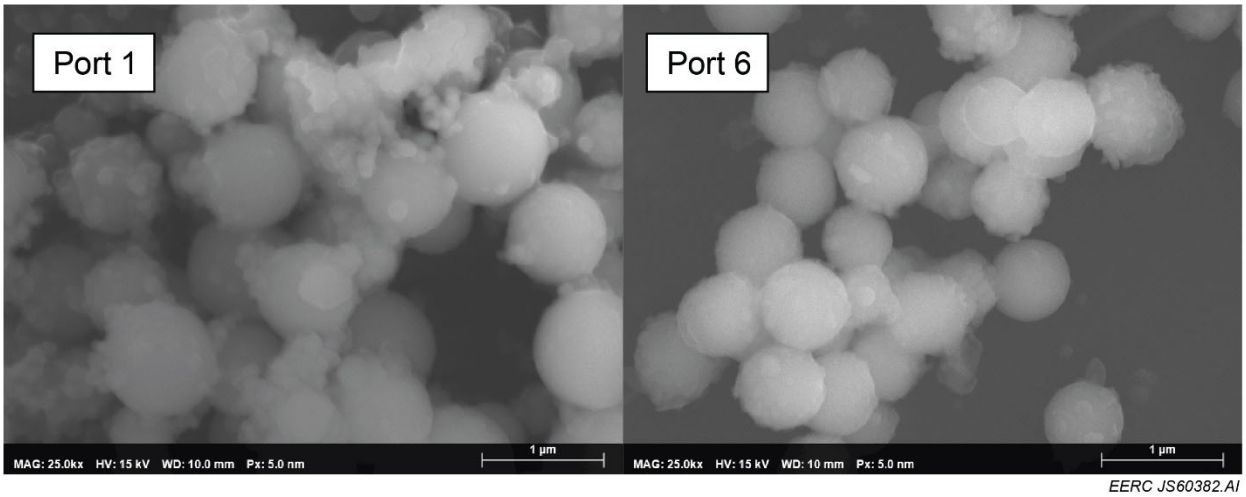

Figure 28. Dekati impactor Stage 10 particulate morphology during operation with KS-21.

During operation with KS-1, the particulate collected at Port 6 was observed to be coated in a thin layer of carbon- and/or nitrogen-rich material that was presumed to be derived from condensed solvent escaping as aerosol. No such layer was observed on the particulate collected during operation with KS-21 solvent. EDX spectral analysis in Figure 29 suggests that the particulate material is mostly calcium aluminosilicate, similar to the ash chemistry observed during operation with KS-1. This agrees well with IC/ICP/ICP–MS analyses. Comparing the carbon peak (which overlaps with the nitrogen peak) to that observed at Port 6 during KS-1 operation, there is much less indication of carbon and nitrogen on the particulate. Along with the visual absence of a coating layer in Figure 28, the EDX results further suggest that amine aerosol formation was less significant with KS-21 than had been observed with KS-1.

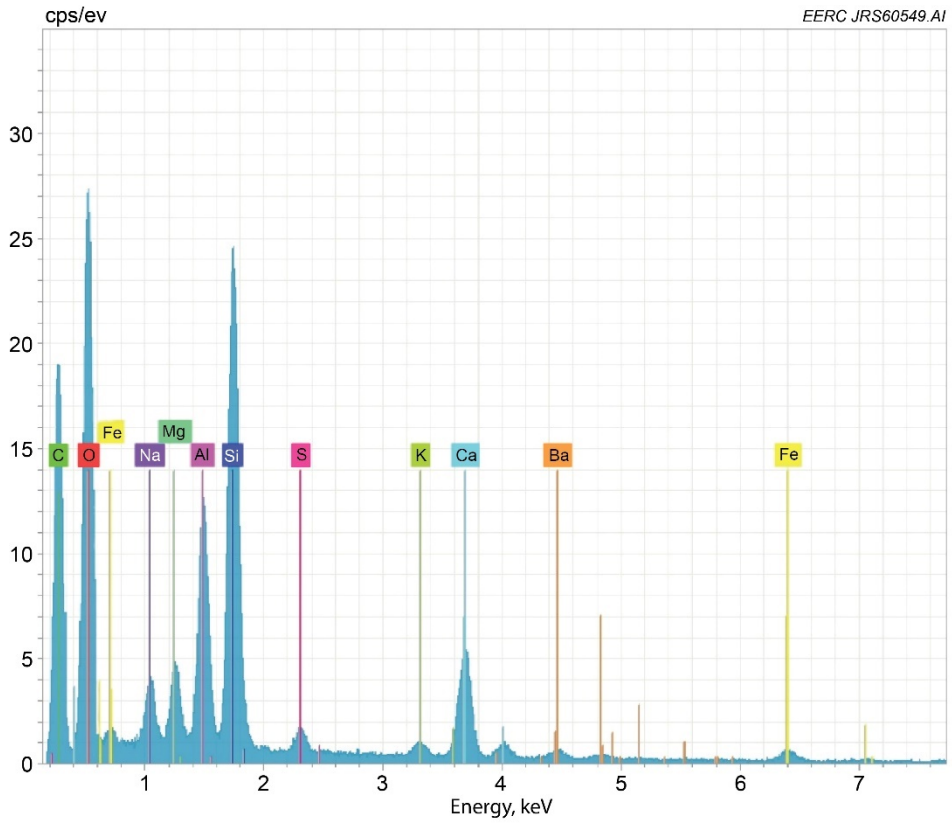

Figure 29. EDX spectrum of Dekati Stage 10 particulate collected at Port 6 during KS-21 operation.

Pilot-Scale MEA Testing

Following testing at Coal Creek Station, the pilot-scale capture system was disassembled and reinstalled at the EERC to support in-house pilot-scale combustion testing efforts under a separate project. A portion of these efforts were dedicated to combustion of North Dakota lignite from Falkirk Mine in a pilot-scale simulated boiler system. This system, known as the particulate test combustor (PTC), is a pc-fired system designed to generated fly ash representative of that produced in a full-scale utility boiler. The coal nozzle of the PTC fires axially upward from the bottom of the combustor, and secondary air is introduced concentrically to the primary air with turbulent mixing. Flue gas is treated with a selective catalytic reduction (SCR) unit, ESP, and wet FGD. This presents a different configuration and combustion environment than what is present at Coal Creek Station while using a similar fuel.

The pilot-scale capture system was loaded with MEA solvent during this combustion testing and was used to capture approximately 90% of the CO_2 from the flue gas. To better understand the impacts of boiler design on aerosol transformations and their effect on CO_2 capture performance when firing low-rank coals such as North Dakota lignite, the project team collected additional particulate data using an SMPS and Dekati ELPI+. When testing at Coal Creek Station, the Dekati was loaded with polycarbonate substrates that could be dissolved for chemical analyses. When

testing on the PTC, the Dekati was loaded with foil substrates that allowed for instantaneous online measurement of particulate loading and size distributions. Sample locations were similar to those shown in Figure 2, except that a water wash column was used in place of MHI's proprietary AERU, and the WESP was not installed.

Particle-size distribution (PSD) and total loading were not constant during on-site testing and shifted significantly throughout the day. As such, PSD results represent a snapshot in time and may not represent long-term average behavior. The SMPS results shown in Figure 30 indicate a typical drop in particulate through the absorber followed by a jump in particulate at the system outlet with a shift to smaller particle sizes. By comparison, the Dekati ELPI+ results in Figure 31 do not show a similar jump between the absorber outlet and the system outlet. However, the ESP was cleaned just before the Dekati outlet sample was taken, and it is likely that this reduced the overall particulate loading during Dekati sampling at the system outlet. Disregarding the sample taken at the system outlet, the online Dekati results generally agreed with the SMPS results as shown in Figure 32.

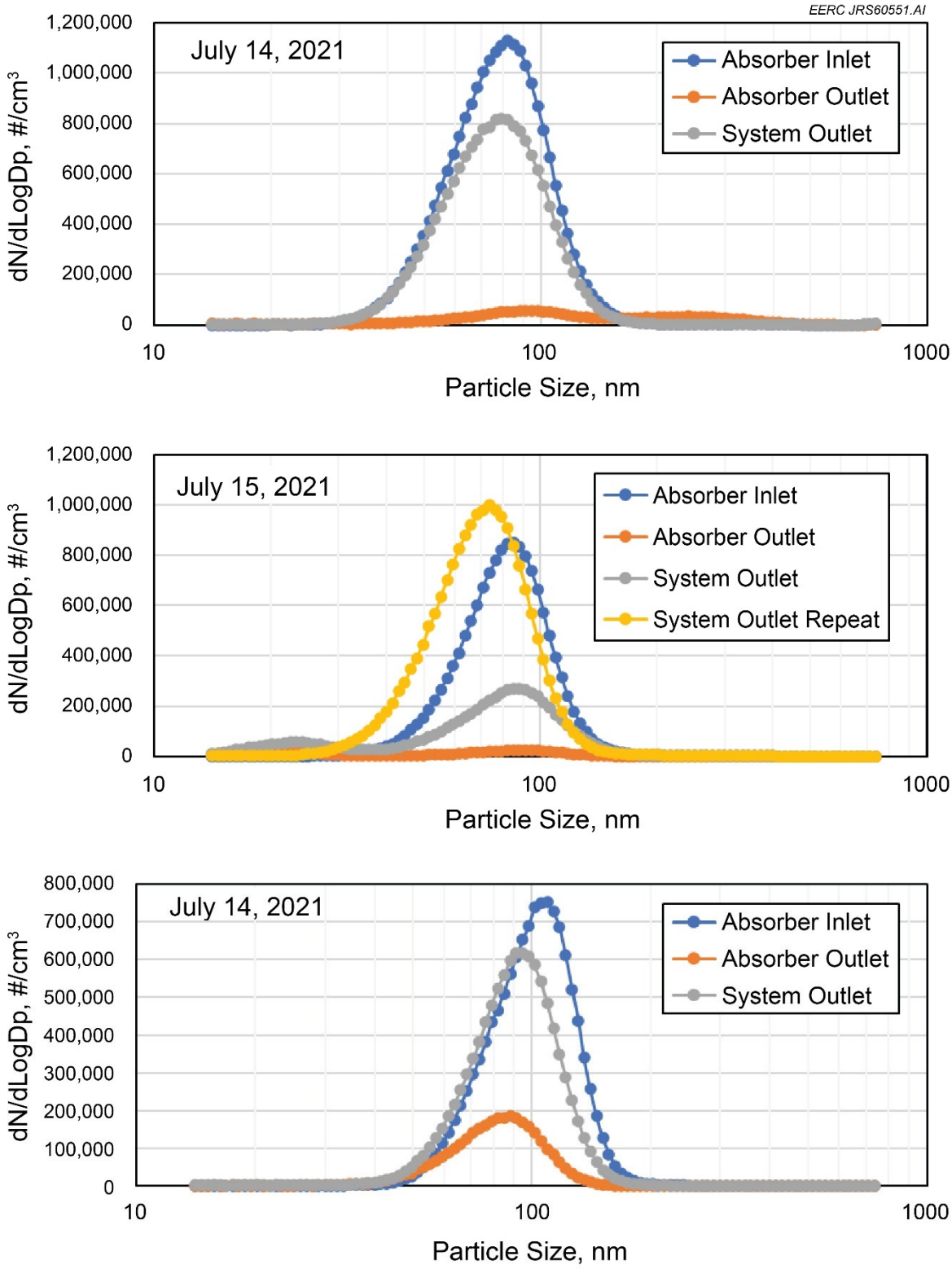

Figure 30. SMPS results collected during on-site testing.

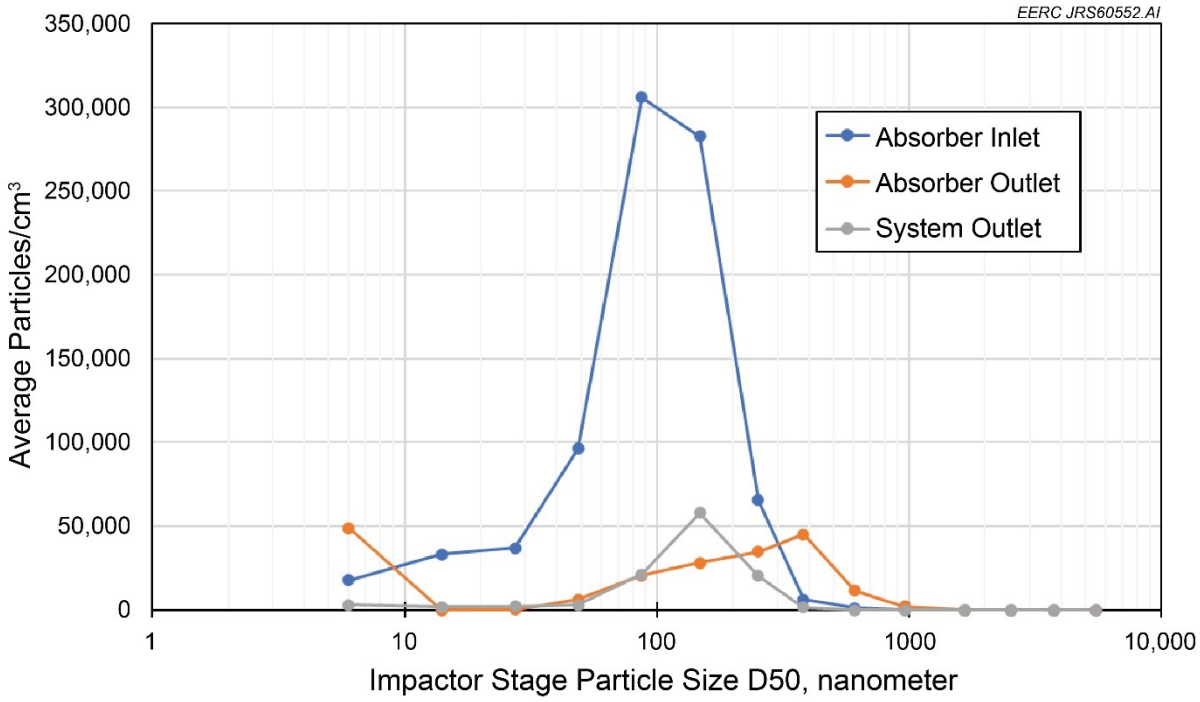

Figure 31. Dekati PSD measured during on-site testing.

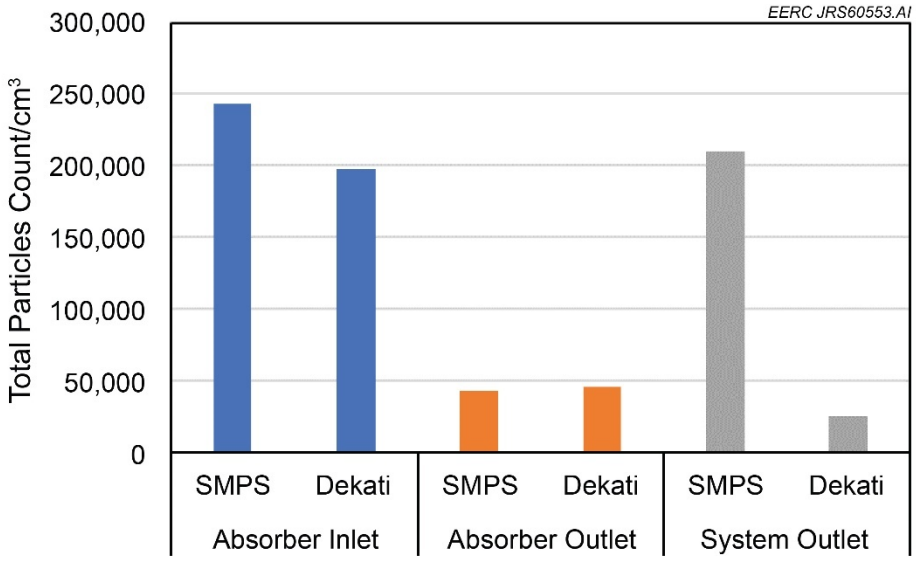

Figure 32. Comparison of SMPS and Dekati online particulate loading measurements.

The jump in particulate at the system outlet seen on each day of sampling with the SMPS suggests that the vapor entering the water wash column was supersaturated and continued to undergo aerosol formation during cooling. It should be noted that in Figure 31, the Dekati PSD indicates a jump in very fine (<10 μm) particulate at the absorber outlet at particle sizes below the range of the SMPS. This may indicate the onset of homogeneous aerosol condensation in the upper absorber column. These very fine mist particles might have continued to grow in size via condensation and coagulation during cooling in the water wash section, leading to a jump in SMPS-detectable aerosols at the system outlet. Because polycarbonate substrates were not collected during the on-site testing, it is impossible to examine the particulate under FESEM or to analyze for chemical composition. Such analyses would be necessary to verify that the jump in particulate measured at the system outlet resulted from aerosol growth in the water wash column.

It is worth noting that no such increase in particulate count was observed at the system outlet at Coal Creek Station, indicating that MHI's proprietary capture solvent and recovery processes were effective at reducing or eliminating this proposed mechanism of enhanced amine losses to aerosol formation from the EERC's pilot-scale absorber column.

Summary of Particulate Loading by Test

The chart in Figure 33 summarizes particulate loading relative to inlet conditions by sample location and test condition. During testing of MHI solvents with the AERU, the aerosol count measured at the system outlet was several orders of magnitude lower than at the inlet with the WESP online and when running with KS-21 advanced solvent. When running with commercial KS-1 solvent and no WESP, the outlet particulate loading was somewhat higher than in the other cases but still reduced. As discussed previously, much of the particulate collected during this first test is believed to have been derived from fine metal residue left in the system as its composition and structure were abnormal and not indicative of fly ash. Independent measurements by MHI showed amines below 0.1 ppm detection limits at the system outlet during all tests with the AERU running. This finding bolsters the assumption that much of the outlet particulate collected during operation with KS-1 and no WESP was derived from fine metal residue and not from aerosol mist formation. When running with MEA and a standard water wash column, the particulate dropped through the absorber column and then jumped through the water wash. Changes in the PSD suggest that very fine aerosol mist may have been starting to form at the absorber outlet and then coagulated through the water wash section into larger particles that were easier to detect by SMPS.

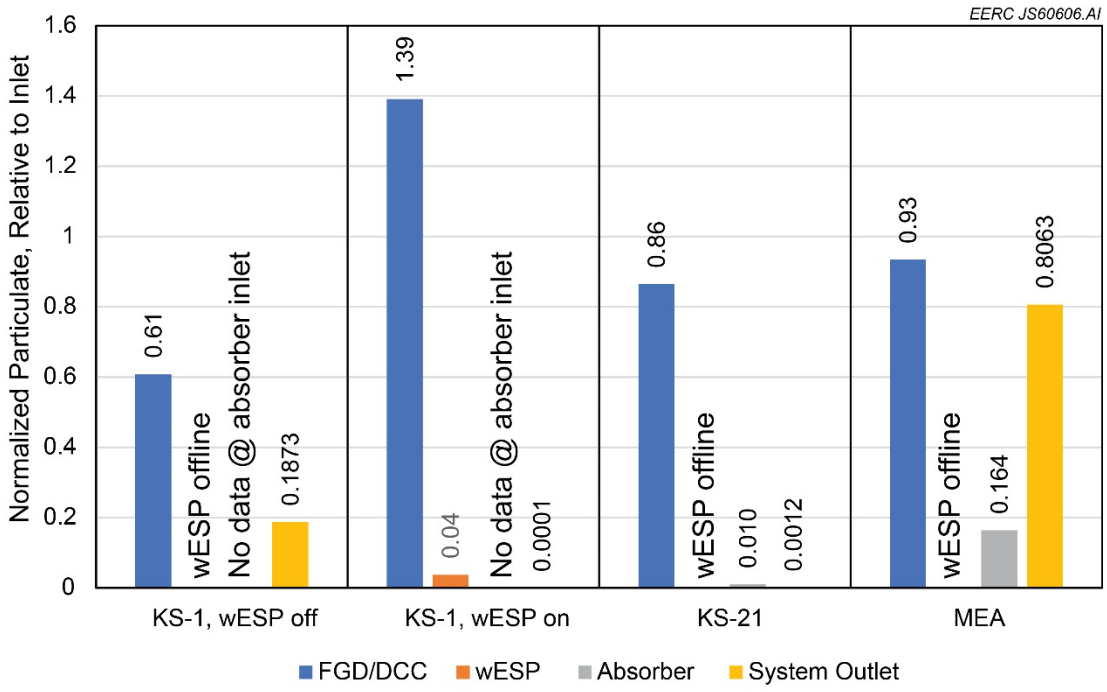

Figure 33. Particulate loading summary chart.

Filter Analysis

Select solvent filters were sectioned and examined by FESEM to identify and analyze material buildup. These filters were used to remove particulate from a slipstream of the lean solvent entering the absorber column and were changed periodically throughout the test campaign.

Especially in early filters, all of the regions analyzed by EDX contained high levels of copper despite there being little to no detectable copper in the solvent, particulate matter, or flue gas. Later filter samples contained progressively less copper. High copper has been observed in filter samples collected from this unit in the past and is believed to be the result of residual copper-rich material in the system. Except where otherwise noted, all trends in composition reported here are on a copper-free basis.

Figure 34 shows morphological images taken of a filter removed from the system on October 20, 2020, taken a few weeks after starting up with KS-1 solvent. This sample was anomalous compared to later filters. The micrometer-scale material shown in Figure 34a appears semiamorphous, with some regions rich in iron and titanium and few of the submicrometer spherical particles that were seen in later samples. The bulk matrix shown in Figure 34b appears to have a different structure, with more of the fabric fibers exposed near the surface as compared to later samples.

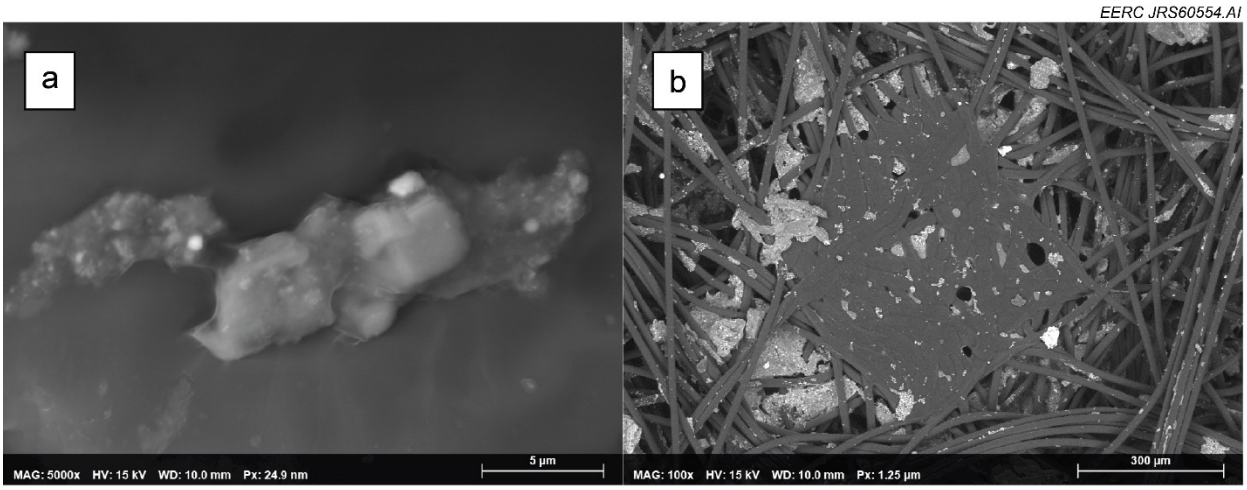

Figure 34. Morphology of solvent filter removed October 20, 2020. Image a is a close-up of individual micrometer-scale particles, and Image b is a wide-range image of material accumulated in the fibers of the fabric filter.

Figure 35 shows SEM morphology taken of a filter removed from the system on November 19, 2020, when running with KS-1 solvent. The spherical particles in Figure 35a were rich in silicon, aluminum, alkali, alkaline earth, and sulfur, with some iron and titanium also present. This suggests that these spherical particles were derived from fly ash and were rich in sulfate, with some metallic contamination possibly from the absorber system materials of construction. The more irregularly shaped particles in Figure 35b were rich in silicon, sulfur, titanium, and nickel. Comparing to Figure 34b, the mass of accumulated material in Figure 35c is coating and obscuring the surface of the fabric filters. This type of agglomerated structure was common to all later filters. The reason for the difference in the first sample collected is not clear but may be because of differences in the nature of the early particulate, in sample preparation, or in sample orientation.

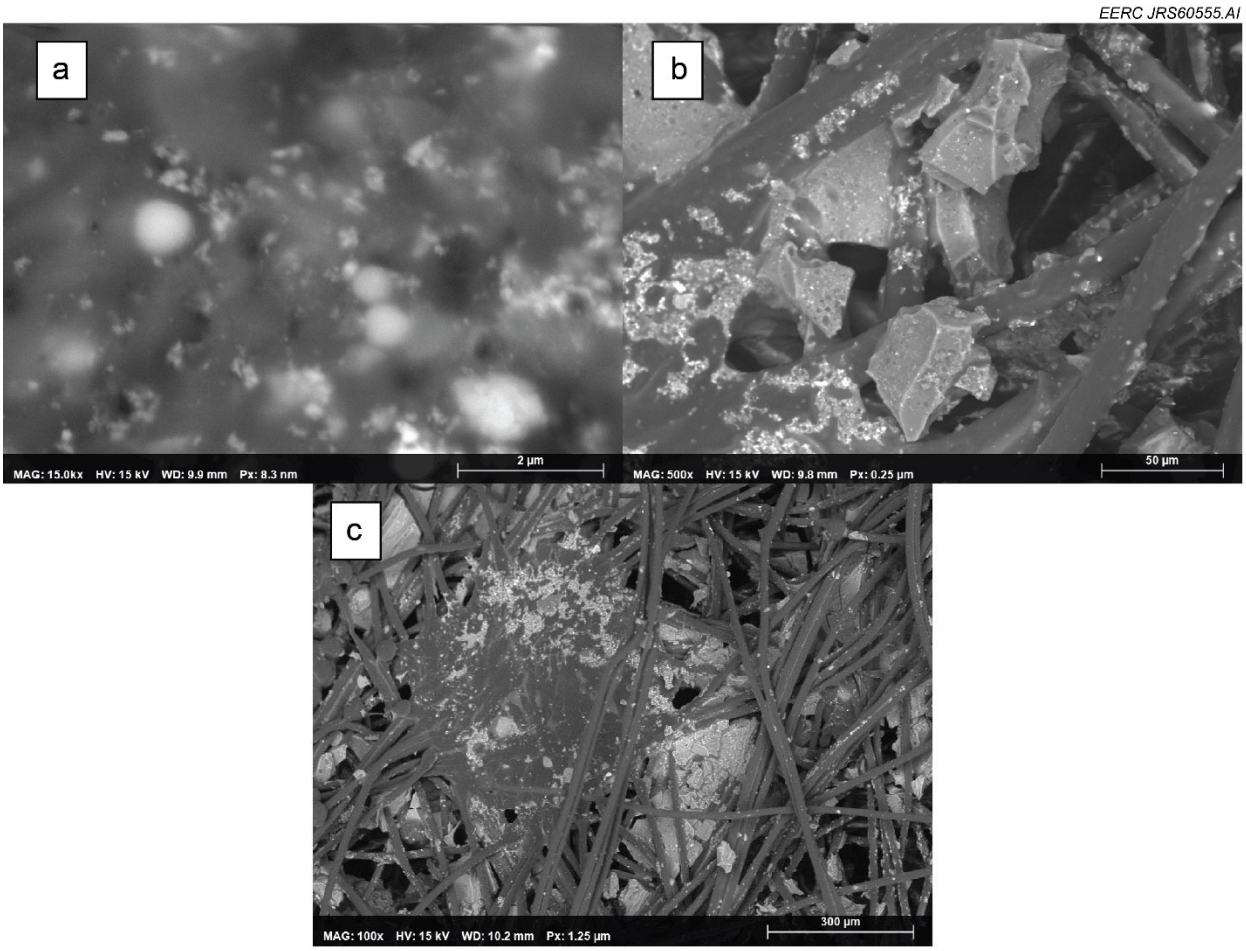

Figure 35. Morphology of solvent filter removed November 19, 2020. Image a shows individual submicrometer- to micrometer-scale particles, Image b shows irregular micrometer-scale particles, and Image c is a wide-range image of material accumulated in the fibers of the fabric filter.

Figure 36 shows SEM morphology for regions of a filter taken December 17, 2020. The spherical particles in Figure 36a were rich in silicon, aluminum, alkali, alkaline-earth, and sulfur as well as iron and titanium.

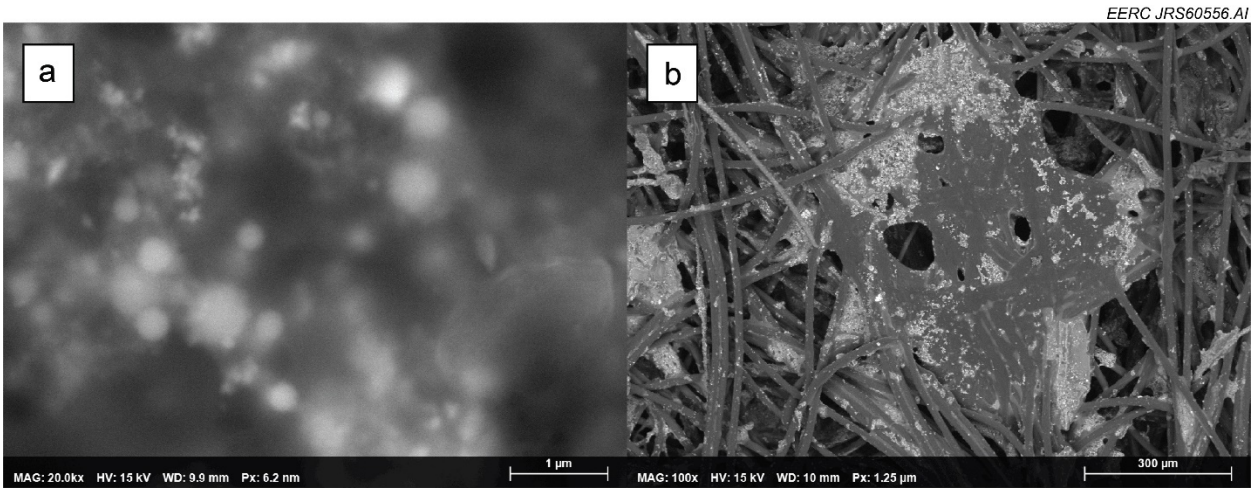

Figure 36. Morphology of solvent filter removed December 17, 2020. Image a shows individual submicrometer- to micrometer-scale particles, and Image b is a wide-range image of material accumulated in the fibers of the fabric filter.

Figure 37 shows morphology for regions of a filter taken December 20, 2020. This filter was online for only 3 days before the system was shut down to drain KS-1 and switch to KS-21 solvent, at which time a new solvent filter was installed. This filter was also operated while the WESP was online, which greatly reduced the amount of new fly ash particles entering the absorber system (although there was likely to be very fine particulate already recirculating in the system as this filter only treated a slipstream, not the entire lean solvent stream). As a result of the short sample duration and possibly also of having the WESP online, there was much less particulate matter accumulated than in other filters analyzed, as indicated by the small number of submicrometer particles in Figure 37a and by the prominence of exposed fabric filters showing through the matrix in Figure 37c. Unique to this sample, there were numerous crystals that appear as bright cubes or slivers in Figure 37c. The larger pieces of crystalline material were unusually rich in copper (up to 66% on a carbon- and oxygen-free basis), as were the brighter spots in the amorphous region shown in Figure 37b. The submicrometer spherical particles were rich in materials indicating a fly ash composition.

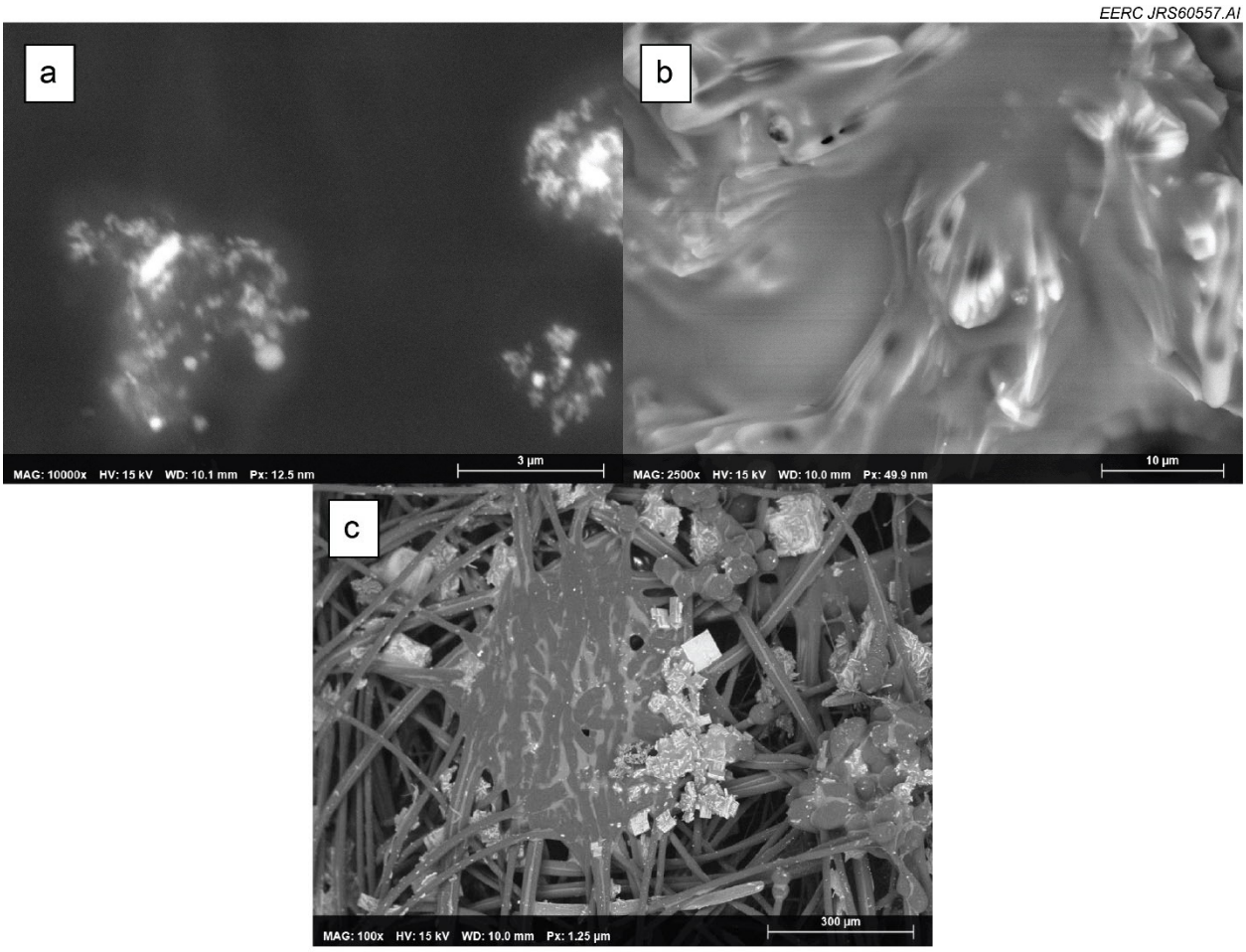

Figure 37. Morphology of solvent filter removed December 20, 2020. Image a shows submicrometer particles, Image b shows amorphous material accumulating in the matrix, and Image c is a wide-range image of material accumulated in the fibers of the fabric filter.

Figure 38 shows morphology for a filter taken on January 18, 2021, after completing operation with KS-21. Low levels of copper were still detected in the bulk matrix of this filter, but the individual particles analyzed from Figure 38a contained less than 1% copper. Many of the darker spherical particles contained high levels of elements suggesting that they were fly ash derived from the coal. The brighter and less spherical particles were very rich in iron, averaging roughly 80% on a carbon- and oxygen-free basis.

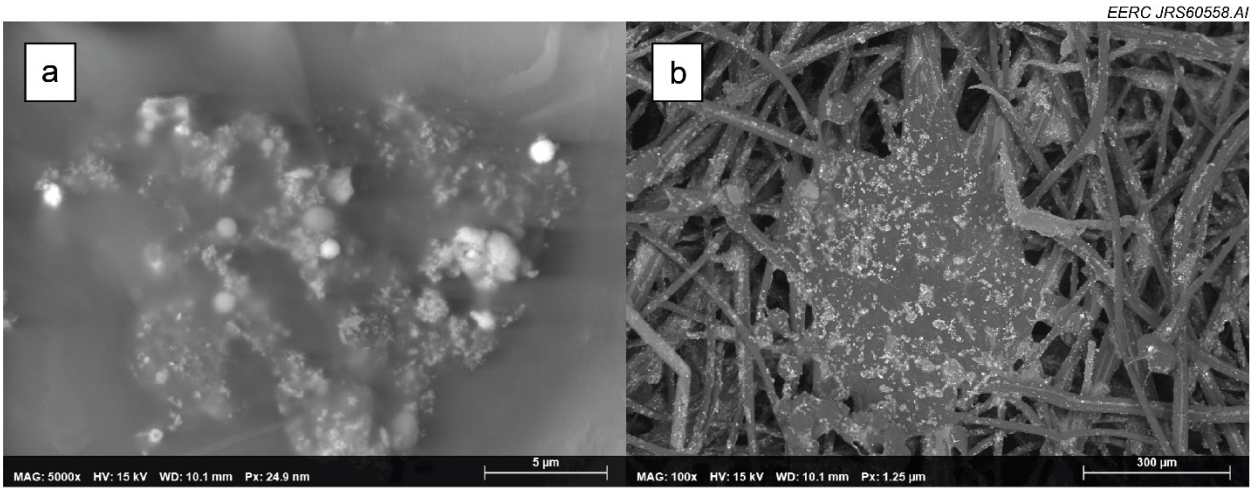

Figure 38. Morphology of solvent filter removed January 18, 2021. Image a shows submicrometer- to micrometer-scale particles, and Image b is a wide-range image of material accumulated in the fibers of the fabric filter.

Figure 39 charts the normalized elemental composition of submicrometer- to micrometer-scale particles on the filters that were measured by EDX, while Figure 40 shows the normalized average elemental composition of points and regions analyzed in the bulk matrix of the accumulated material. The filter removed on October 20, 2020, can be considered an outlier as the micrometer-scale material shown in Figure 34a was anomalous, and this filter may have picked up extra residual material already present in the absorber system. After this initial filter, the copper content spiked in the fine material, as discussed previously, then dropped off with each subsequent filter. Ignoring copper, the remaining particulate material was mostly silica, with lesser amounts of alumina, alkali, alkaline earth, and sulfur, with iron and titanium also reported in appreciable amounts. This suggests that the submicrometer- to micrometer-scale particles are mostly derived from fly ash with some metallic contamination, possibly from the absorber system materials of construction. The final filter collected (after operation with KS-21) contained micrometer-scale particles rich in iron, with individual measurement averaging ~80% for the very iron-rich particulate matter and a spike in the average iron content of the accumulated matrix. The cause for this spike in iron in the final filter is not immediately clear but may be simple sample bias, as only a few discrete points were analyzed. Alternatively, it is also possible that some very fine metal debris from the absorber system was stirred up and carried to the solvent filter when the system was drained of KS-1 and refilled with KS-21.

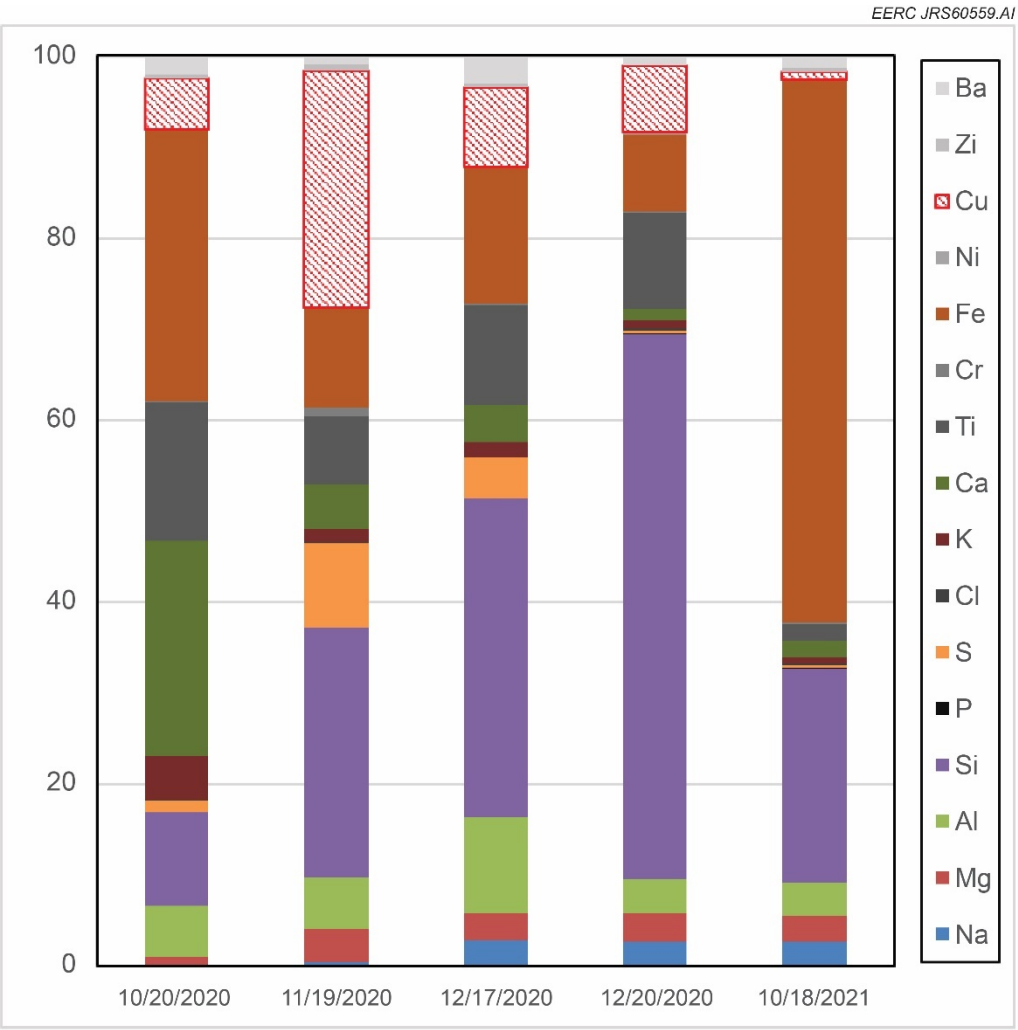

Figure 39. Normalized elemental composition of submicrometer particles on filters as measured by EDX.

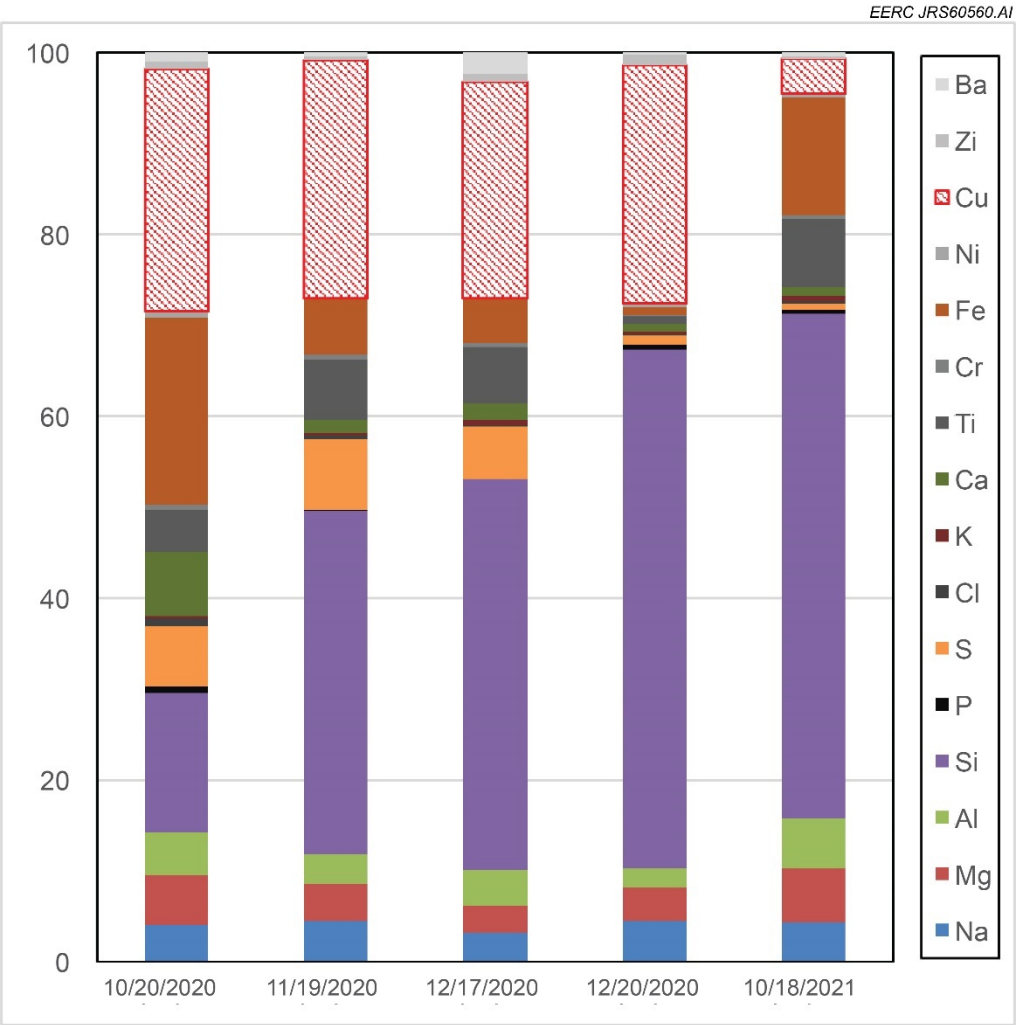

Figure 40. Normalized elemental composition of the bulk accumulated matrix on filters as measured by EDX.

GEOLOGIC STORAGE ASSESSMENT

Background of North Dakota Geology – Potential Storage Targets

To support techno-economic analysis of CCS specific to the Coal Creek Station site, a geologic storage assessment was conducted to estimate capture economics with different storage scenarios. While multiple geologic formations in western North Dakota show favorable characteristics for potential CO_2 storage, two formations, the Broom Creek and Deadwood/Black Island Formations, were selected for additional evaluation because of their prior identification as prime storage targets for CCS activities in the region. For these two formations, two different geographic locations were evaluated (Figure 41):

1) Directly below Coal Creek Station
2) Approximately 30 miles west, near Beulah, North Dakota.

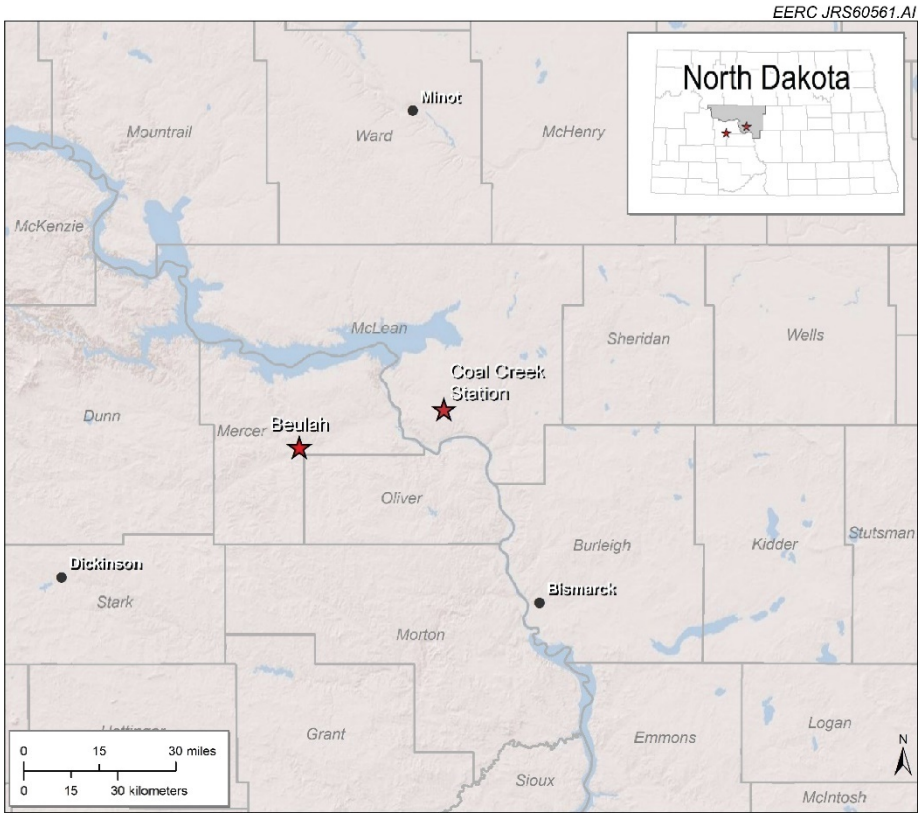

Figure 41. Location of Coal Creek Station and Beulah.

These two locations were selected because geologic properties (e.g., depth, thickness, density, etc.) will change enough to demonstrate the impacts of the variability in geology by location. Coal Creek Station is located on the edge of the Broom Creek Formation (Figure 42), and there is a significant difference in performance between injecting on the edge of that formation versus being some distance away from the edge. The locations were selected based solely on geologic properties and do not represent any preference or guidance for formally selecting a future project location.

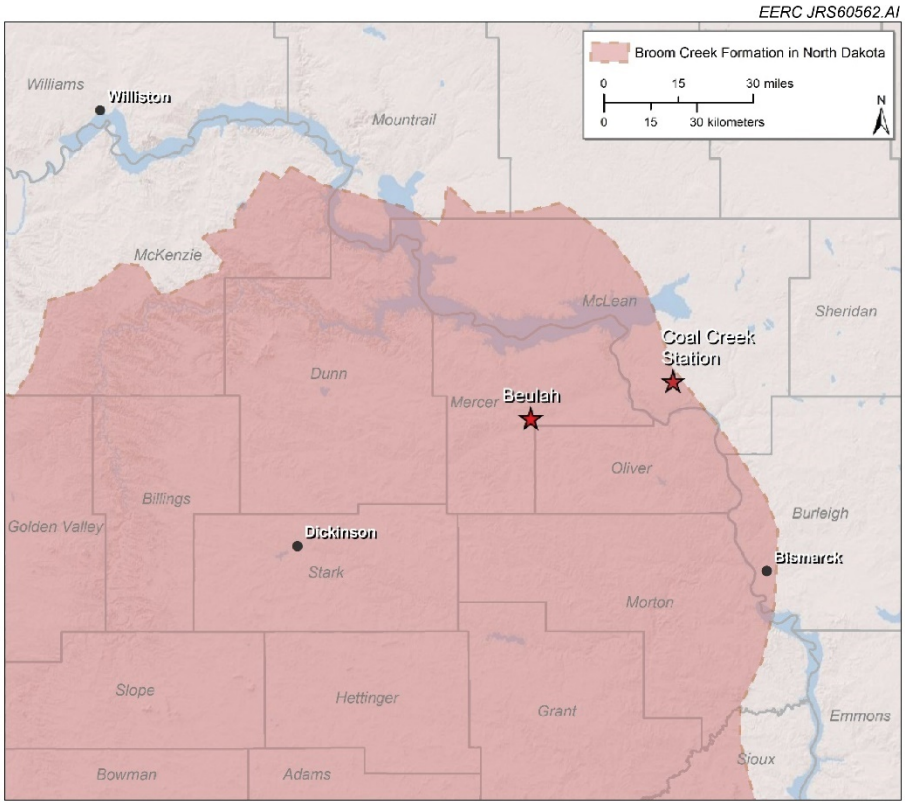

Figure 42. Location of Coal Creek Station and Beulah in relation to the Broom Creek Formation.

Geologic storage involves injecting captured CO_2 into deep underground geologic formations, typically in thick accumulations of sedimentary rock known as basins. Storage formations need to 1) have adequate capacity to store the expected volumes of CO_2, 2) be overlain with laterally continuous cap rock that prevents upward migration of CO_2, 3) be at depths greater than 800 meters (~2600 feet) to allow injected CO_2 to remain in the supercritical phase for efficient use of formation pore space, and 4) have formation fluid salinity values greater than 10,000 mg/L total dissolved solids (TDS) to meet U.S. Environmental Protection Agency (EPA) rules protecting underground sources of drinking water (USDWs).

Several sedimentary rock formations in the Williston Basin, which covers much of western North Dakota, have potential for CO_2 storage. For the purposes of this report, the focus is on the Broom Creek and Deadwood Formations. These two formations have been characterized in North Dakota and are potential storage targets that meet the above criteria.

Found in the Minnelusa Group of Permian age, the Broom Creek Formation (Figure 43) is an eolian and shallow-marine sandstone that both overlies and is overlain by low-permeability lithologies, thus preventing fluids from migrating out of the injection zone. The Broom Creek occupies the southwestern portion of the Williston Basin in western North Dakota (Figure 42) and ranges in formation thickness from zero to about 350 feet. The formation has areas that meet the general criteria for CO_2 storage (Figure 44) with depths near 5000 feet, salinity greater than

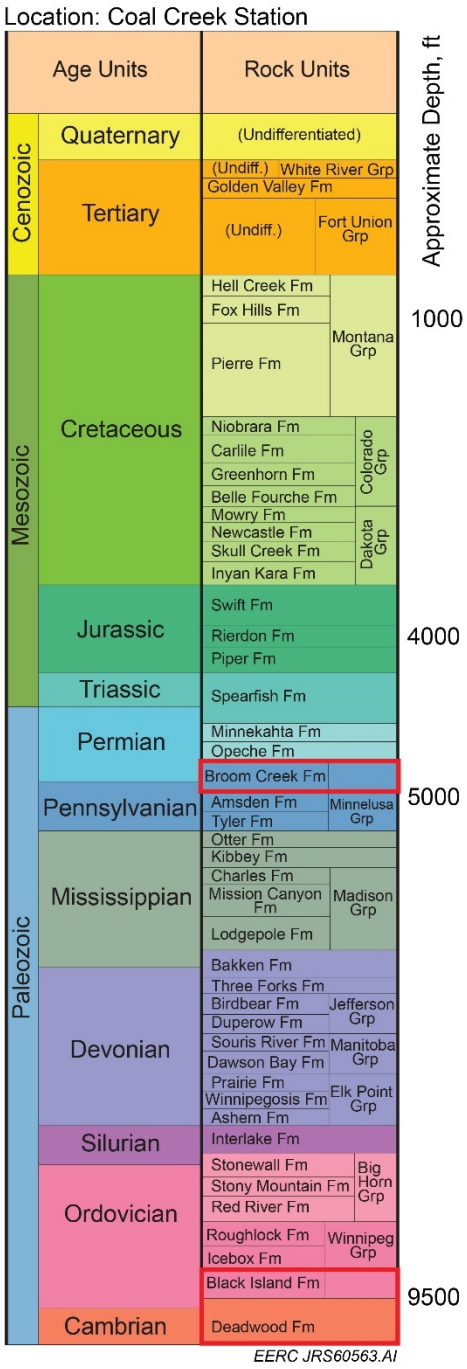

Figure 43. North Dakota stratigraphic column for the Coal Creek area.

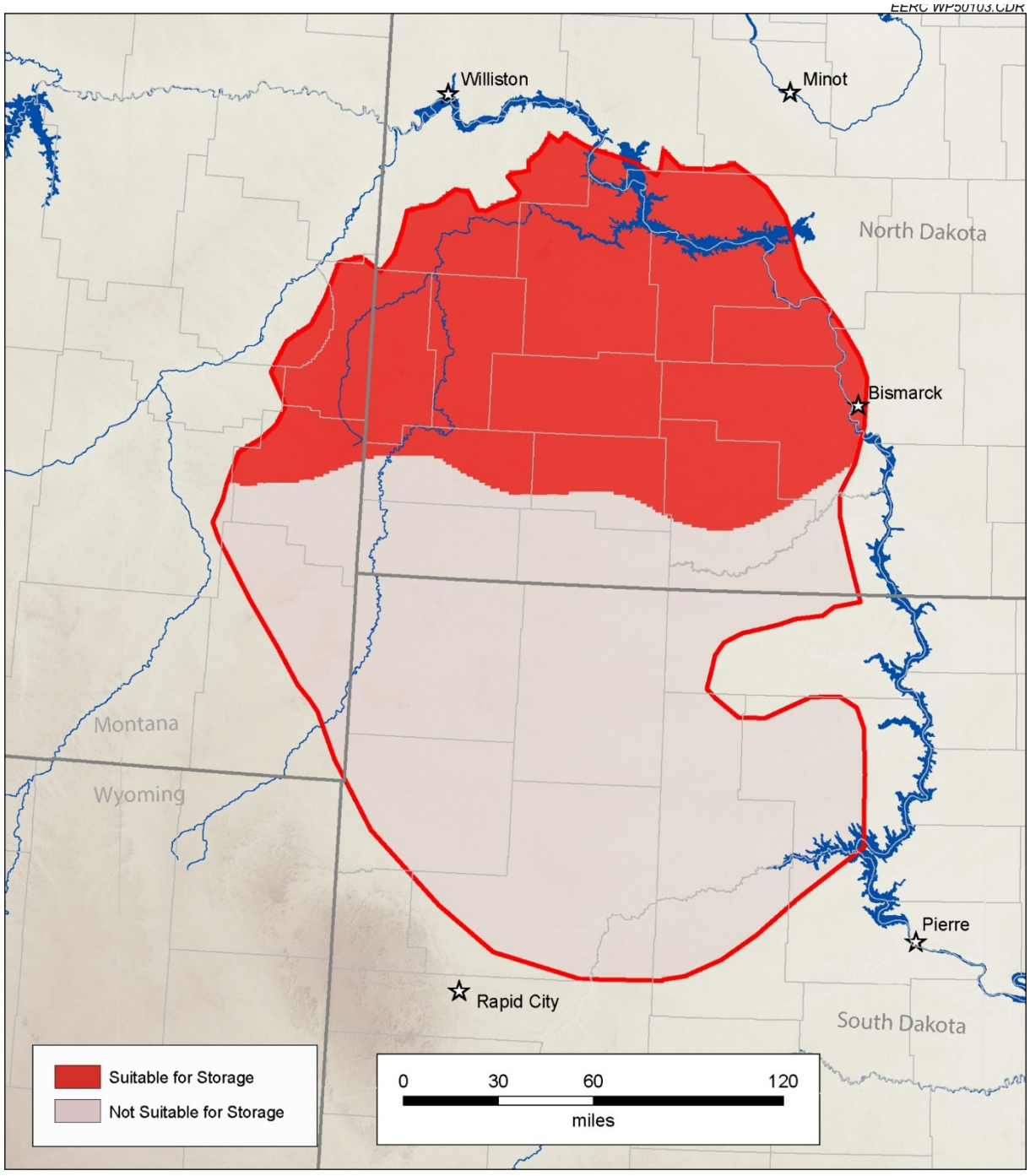

Figure 44. Area within the Broom Creek suitable for CO_2 injection. Suitability is based on formation depth greater than 800 meters (2600 feet) and salinity greater than 10,000 ppm. In this case, suitability is dictated by salinity cutoff (Peck et al., 2014a).

10,000 mg/L, while having adequate porosities (mean effective ~12%) and permeabilities (mean of 140 mD) (Peck et al., 2014a) that can support injection of fluids.

The Deadwood and overlying Black Island Formations of Cambrian–Ordovician age contain the basal sandstones of the Williston Basin located at depths of over 9500 feet (Figure 45). The overlying Icebox Formation acts as a seal against out-of-zone migration of fluids, and the minimal presence of hydrocarbons in these formations means that there are relatively few wellbore penetrations that could affect the integrity of this storage target. The Deadwood Formation has high salinity values approaching 350,000 mg/L TDS and porosity values ranging from 2% to 21%, with a mean of 8% in the United States (Peck et al., 2012). With the wide spatial distribution, favorable properties (salinity, porosity, etc.), and depth, the Deadwood can be a suitable storage target for CO_2.

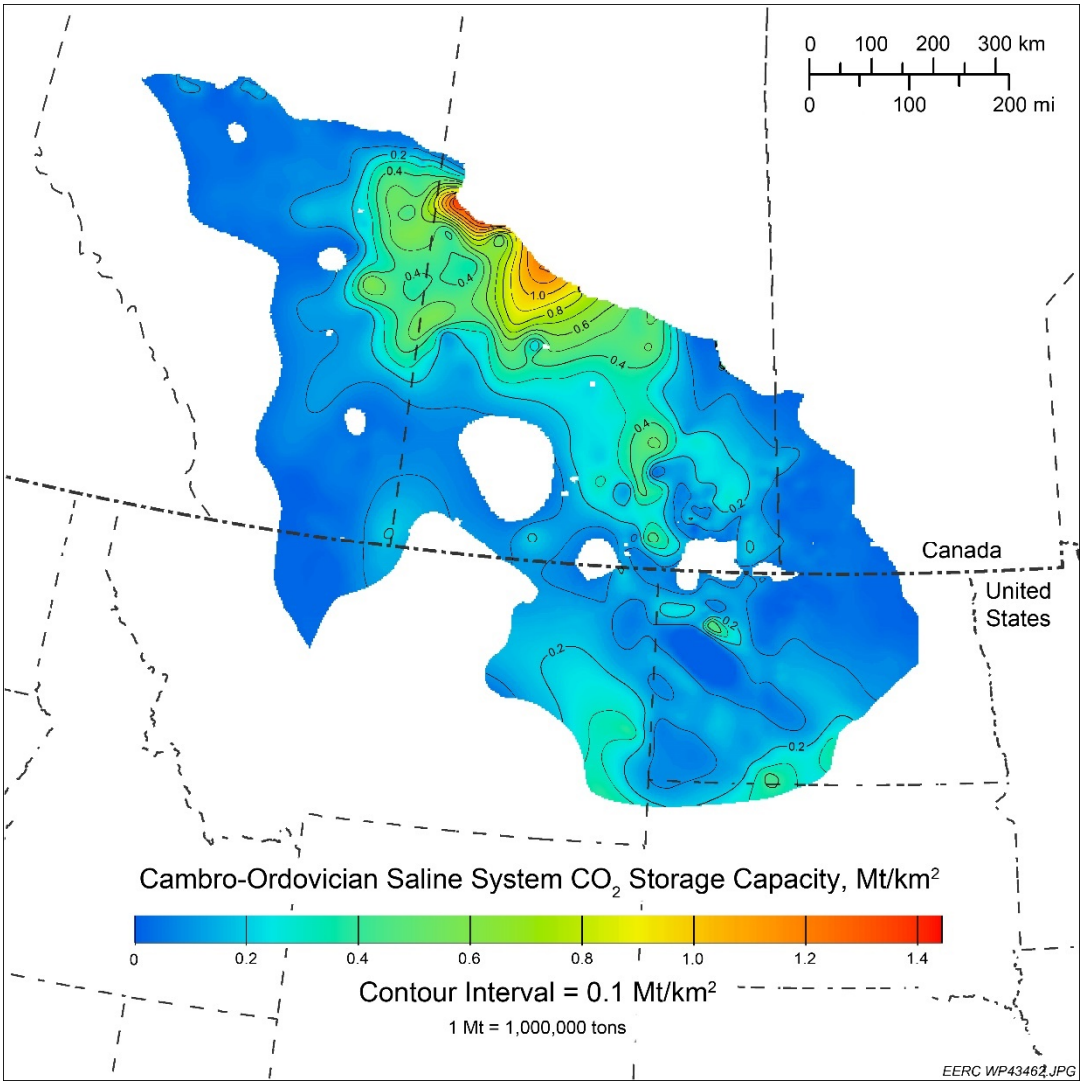

Figure 45. CO_2 storage distribution map for the Cambro–Ordovician saline aquifer system comprising the Deadwood and Black Island Formations (Peck et al., 2012).

Storage Potential in the Coal Creek Station Area

To support geologic storage of CO_2 captured at Coal Creek Station near Underwood, North Dakota, two deep saline formations were assessed to estimate 1) the number of wells needed to store approximately 8.6 million tonnes per year (MMtpy; a 90% capture rate based on 2018 facility emissions) of CO_2 in the Broom Creek and Deadwood/Black Island Formations and 2) the size of a generated CO_2 plume after 20 years of injection of each well into each formation. These two formations were assessed at two locations: directly below Coal Creek Station and approximately 30 miles west, near Beulah, North Dakota.

Number of Injection Wells

Per-well maximum CO_2 injection rates were estimated for the Broom Creek and Deadwood/Black Island Formations at both study sites based on regional knowledge and a survey of internal EERC simulation results (Table 1). Total number of wells needed was estimated by dividing the annual injection target (8.6 MMtpy) by the total estimated injection rate at each site for both formations together ("stacked storage") and individually (Table 2). The lowest values in Table 2 assume that wells perform somewhat better than the estimates shown in Table 1, while the highest values in Table 2 assume a somewhat worse performance.

Table 1. Estimated Maximum CO_2 Injection Rates and Cumulative Injection

	Beulah		Coal Creek Station	
	MMtpy/well	MMt/well over 20 years	MMtpy/well	MMt/well over 20 years
Broom Creek	1.9	38.0	0.754	15.08
Deadwood/Black Island	1.1	22.0	1.1	22.00
Total	3.0	60.0	1.854	37.08

Table 2. Estimated Range in Number of Injection Wells under Different Scenarios

	Beulah	Coal Creek Station
Broom Creek Only	4–6	11–13
Deadwood/Black Island Only	7–9	7–9
Broom Creek and Deadwood/Black Island Stacked	4–8	8–12

Field and simulation studies indicate greater injection efficiency when each injection well is open to a single reservoir; the stacked storage injection scenario presented here, therefore, assumes two wells to inject the "total" value in Table 1. Stacked storage is often considered if the goal is to minimize the area of the combined CO_2 plume, which requires optimization of well placement and combination of target reservoirs. In the case of stacked storage near Beulah, for example, three wells injecting into each of the two reservoirs is likely to result in a smaller storage facility area than six wells injecting into a single reservoir.

CO_2 Plume Dimensions

An Excel spreadsheet developed by the EERC was used to model CO_2 plume radius and area in an open system in which pressure barriers and other injection or extraction activity are not considered. The spreadsheet model uses average reservoir properties to estimate static CO_2 storage potential (Equation 1), diameter, and area of a CO_2 plume defined by a given injection rate and project duration:

$$M_{CO_2} = A \times h \times \varphi \times \rho_{CO_2} \times E_{saline} \quad \text{[Eq. 1]}$$

Where:

M_{CO_2} = CO_2 storage potential mass.
A = area covered by the potential storage reservoir.
h = thickness of the potential storage reservoir.
φ = porosity of the potential storage reservoir.
ρ_{CO_2} = CO_2 density under reservoir conditions.
E_{saline} = saline CO_2 storage efficiency factor.

Additional inputs (reservoir depth, surface temperature, reservoir temperature, and pressure gradients) were used to calculate CO_2 density for use in Equation 1 (Table 3). Density of

Table 3. Geologic Parameters Used to Estimate CO_2 Storage Potential

Site:	Beulah		Coal Creek Station	
Formation:	Broom Creek	Deadwood/ Black Island	Broom Creek	Deadwood/ Black Island
Reservoir Net Thickness, ft	160	306	62	150
Porosity, %	22.2	3.8	12.7	3.8
Depth, ft	6405	12,300	4780	9885
Pressure, psi	3142	5673	2357	4567
Temperature, °F	152	252	132	181
CO_2 Density, kg/m^3	712	679	686	748

supercritical CO_2 injected into the reservoir was calculated using reservoir temperature and pressure conditions at the beginning of injection; however, reservoir pressure will increase over the course of the injection period, resulting in the potential for higher CO_2 density and smaller plume sizes. Because this is a screening-level study, reservoir change in pressure during injection was not considered.

Efficiency factor (E_{saline}) refers to the proportion of available pore space that can be occupied by injected CO_2. Depending on the quantity of basic data used to evaluate a saline formation, differing storage efficiency factors and their associated confidence intervals need to be applied to ensure the most accurate prediction possible. Tenth (P10), 50th (P50, median), and 90th (P90) percentile E_{saline} factors were applied using the workflow described by Peck et al. (2014b). For the

current study, net area and net thickness are relatively well-known for each of the potential storage reservoirs. Net area represents the proportion of the potential storage reservoir that is amenable to CO_2 storage, and net thickness represents the proportion of the potential storage interval containing reservoir-quality rock (e.g., sandstone rather than shale). In clastic reservoirs with known net area and net thickness, the P10, P50, and P90 E_{saline} factors are 5.17%, 9.88%, and 17.24%, respectively.

To better quantify the effect of uncertainty in some of the input parameter values on the storage resource estimate, the storage resource estimate was developed using Monte Carlo sampling. Input parameters were modeled using a statistical distribution to create 500 probabilistic values. These 500 probabilistic values were then used to generate 500 separate storage resource estimates. Summary statistics were then calculated from the 500 separate storage resource estimates to provide interval estimates of the storage resource rather than a single value.

Uncertain parameters were modeled using a triangular distribution. The triangular distribution is a continuous probability distribution with lower limit a (minimum), upper limit b (maximum), and mode c (most likely estimate), where $a < b$ and $a \leq c \leq b$. The triangular distribution is commonly used when not much is known about the distribution of an outcome besides its smallest and largest values and the most likely outcome (Fenton and Neil, 2012).

Monte Carlo sampling of parameters and storage resource estimates resulted in a statistical distribution of possible CO_2 plume dimensions, summarized here with 10th (P10), 50th (P50), and 90th (P90) values. For each potential injection site (Coal Creek Station or Beulah) and storage reservoir (Broom Creek and Deadwood/Black Island), plume diameter and area were estimated using the injection rates and cumulative injection estimated in Table 1 over a 20-year injection period. These results were then translated into estimated CO_2 storage potential per unit area on the surface at the end of a 20-year injection period. CO_2 plume dimensions and storage potential are summarized in Table 4.

Table 4. Estimated CO_2 Plume Size and Storage Potential per Well

	Beulah		Coal Creek Station	
	Broom Creek	**Deadwood/ Black Island**	**Broom Creek**	**Deadwood/ Black Island**
Plume Diameter, mi				
P10	4.3	5.8	5.8	7.9
P50	4.9	6.6	6.6	9
P90	5.7	7.8	7.8	10.6
Plume Area, mi^2				
P10	14.2	26.2	26.3	48.7
P50	18.7	34.5	34.7	64.1
P90	25.7	47.5	47.6	88
CO_2 Storage Potential per Unit Area, MMt/mi^2				
P10	2.68	0.839	0.573	0.452
P50	2.03	0.637	0.435	0.343
P90	1.48	0.464	0.317	0.25

Estimated plume dimensions in Table 4 are greater and storage potentials lower for each formation at Coal Creek Station than near Beulah, largely because both reservoirs generally increase in thickness and depth to the west. Thicker portions of the reservoirs allow a longer section of a vertical well to be perforated, which can result in CO_2 remaining closer to the wellbore, and CO_2 density increases with depth, resulting in greater mass storage potential within the same volume.

Injection Well Spacing and Project Area

Injection well spacing depends on the number of injection wells, the injection rate of each, and the site-specific geology of the storage reservoir. Multiplying any of the number of potential injection wells in Table 2 by the estimated CO_2 plume areas in Table 4 can provide rough estimates of the total area needed for a CO_2 storage project. For example, five Broom Creek wells at Beulah are estimated to generate CO_2 plumes covering an area between 71 and 128.5 mi^2. Such a method does not consider interwell pressure effects beyond the edge of each CO_2 plume and should be considered as a minimum estimate of project area in the absence of site-specific geologic and simulation models.

Drilling and Completion Considerations: Cost and Timeline

Drilling and completion costs of an underground injection control (UIC) Class VI injection well are variable and typically range between $5 and $10 million. A Class VI well needs to meet specific requirements administered by EPA to ensure protection of USDWs for wells that are used to inject CO_2 for the sole purpose of geologic storage.

Many factors impact the cost of drilling and completing a UIC Class VI well. Two primary factors affecting the drilling and completion cost are the expected injection rate per well and the total depth of the well. Other factors impacting the cost are monitoring technology (i.e., tubing or casing-conveyed, fiber optic or downhole gauge), completion design (i.e., single completion or stacked storage), and properties of the geologic formation. Market availability and demand for materials and labor can also play a role in the cost variation of a new well. Besides cost, lead time for drilling and completion of a UIC Class VI well can impact the project timeline, especially for acquiring CO_2-resistant well materials. CO_2-resistant items such as cement, casing, tubing, and the wellhead may require between 3 and 12 months for delivery to the wellsite.

Geologic Comparison Discussion

This prefeasibility, or screening-level, effort provides an initial evaluation of the CO_2 storage capabilities of two geologic formations near Coal Creek Station. This effort illustrates that there are suitable geologic characteristics for storing CO_2 in both the Broom Creek and the Deadwood/Black Island Formations, and the storage potential is great enough to store the target capture rate of CO_2 coming from Coal Creek Station. The information regarding numbers of wells, CO_2 injection rates, and plume sizes were based on average formation characteristics information at the two sites, at Coal Creek Station and 30 miles west, near Beulah, North Dakota.

The location of Coal Creek Station along the eastern edge of the Broom Creek Formation (Figure 42) affects CO_2 injection performance, and moving CO_2 injection west will yield better performance for both formations. Some observations from this prefeasibility effort include the following:

- Maximum estimated injection rate on a per well basis for the Broom Creek is significantly improved if injection is moved west, away from the edge of the formation, and over a 20-year injection time frame, the amount of CO_2 injected can be more than doubled per well (Table 1).

- As a result of the reduced estimated injection rate at the Coal Creek Station site relative to the Beulah site, 2 to 3 times more wells would be needed to achieve the required injection volumes in the Broom Creek (Table 2). At $5 million to $10 million per well, the overall project cost could vary significantly depending on the site chosen.

- Estimated CO_2 plume diameters and areas on a per-well basis are larger at Coal Creek Station versus the Beulah location for both the Broom Creek and Deadwood/Black Island Formations (Table 4), mostly because of the difference in thickness between the two locations. The CO_2 plumes are nearly half the size at Beulah, which would significantly reduce the project area. These results do not provide an indication of the spacing required between wells due to pressure interactions. Even so, the project area size will vary based on location.

The proximity of the Coal Creek site to the edge of the Broom Creek Formation extent increases the likelihood of pressure interactions between injection wells into that formation because pressure would only be able to dissipate to the south and west. The relative lack of wells in the area that can be used to determine the extent of the Broom Creek makes it more difficult to estimate the continuity of the formation and rate at which it thins to the east, each of which are important to understand potential pressure interactions.

MODELING

Aerosol Formation Model

A spreadsheet-based model for predicting solvent losses to aerosols was developed from previous work done at the EERC (Benson et al., 2017). This model was meant to predict instantaneous solvent condensation rates on aerosol particles based on solvent properties and average particle size using output data from the absorber column model in Aspen Plus. This functionality was to be used to help estimate the impact that different particulate control options have on solvent losses during techno-economic modeling.

Where possible, key input for the model was provided using Aspen Plus model output, which includes the following:

- Surface tension of each pure species and of the mixed liquid phase

- Density of each component in the liquid phase
- Vapor pressure of each species in the bulk gas phase
- Vapor fraction of each species in the gas phase
- Bulk gas temperature and pressure

Other input not available in Aspen Plus, including diffusivity constants and saturated vapor pressure for each species, was estimated using literature values.

Initial model results were generated using output from Aspen Plus to compare against results from Khakharia et al. (2015). Constants not available through Aspen for this initial effort were assumed to be as reported in previous studies (Benson et al., 2017). The chart in Figure 46 shows initial model results for estimated cumulative MEA losses to aerosol and to vapor in each stage of the column, with Stage 1 being the top of the column and Stage 20 being the bottom. While cumulative vapor loss decreases near the top of the column as some of the vapor condenses back to liquid form, the aerosol remains entrained as the gas cools so that cumulative losses do not decrease. In terms of losses relative to gas flow, the model predicts 74 mg/Nm^3 of evaporative losses and 490 mg/Nm^3 in this simple column model. By comparison, Khakharia observed roughly 40 mg/Nm^3 of baseline losses and ~600 mg/Nm^3 of MEA losses at similar particulate loading to that assumed for this model.

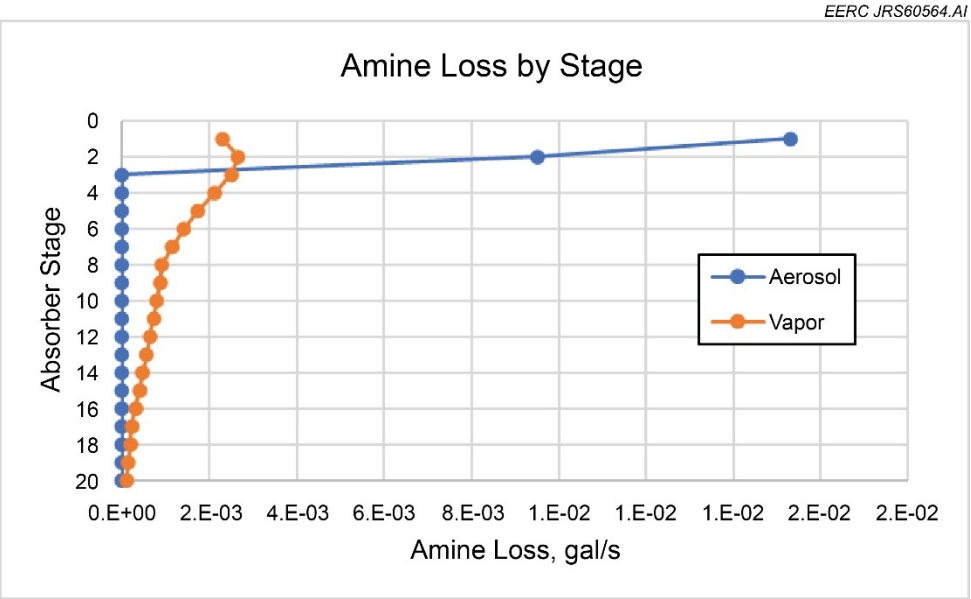

Figure 46. Amine loss estimates by absorber stage for the initial aerosol formation model.

Although initial results using data from smaller-scale systems were promising, when the model was further revised with improved data and applied to a full-scale Aspen Plus CO_2 capture model with a water wash section, MEA loss rate predictions were grossly high by several orders of magnitude. The simplified model does not include sufficient complexity to allow for adequate rates of aerosol reduction to evaporation and coagulation in a full-scale system such as that

required at Coal Creek Station. The model also does not account for aerosol reductions to deposition within column demisters. More robust models in the literature require numerical solution of multivariable differential equations over variable time increments as low as approximately 10^{-9} seconds (Dhanrag and Biswas, 2020; Majeed and Svendsen, 2018; Svendsen et al., 2021). Further model refinement would be required to incorporate similar changes into the current MEA aerosol formation model to more accurately predict aerosol-based losses from a full-scale power plant.

Aspen Plus Modeling

Baseline Case (no capture system)

An initial baseline lignite-fired power generation model was constructed using data provided by Coal Creek Station. The model layout was based on Case L12A from the DOE baseline study (Chou et al., 2011), with stream properties and flows adjusted to match steady-state operational data from Coal Creek Station Unit 1. The steady-state operational data provided by Coal Creek Station represent a specific time period close to when the capture work and aerosol sampling discussed previously were ongoing and may not be representative of operation during other periods. However, the data are self-consistent and allowed the EERC to construct a baseline model of power production at a plant of similar scale.

To reflect the layout of Coal Creek Station Unit 1 more closely, the model diverged from the DOE lignite base case, L12A, in the following ways:

- The model included operations to simulate the dry-fining process used at Coal Creek Station. This process reduces fuel moisture content and particle size, resulting in higher boiler efficiency.

- Lignite power plants in North Dakota do not employ SCR systems to control NO_x emissions, and SCR demands were not considered in this model.

- Coal Creek Station treats only a portion of its flue gas in the FGD. The model was adjusted to allow for slip around the FGD to better simulate solvent rates and sulfur content in the recovered gas.

- Coal Creek Station has an ESP for particulate removal. Case L12A assumes a baghouse.

As compared to the values reported in Case L12A of the DOE baseline study, boiler steam pressures and temperatures were lower during the period of steady-state operation, which resulted in lower overall plant efficiency. This means that the baseline Coal Creek case had higher coal feed and flue gas flows but a similar gross and net power output to Case L12A. Net power from the Aspen Plus model was 539 MW for Coal Creek Station Unit 1 based on average steady-state data available during the period of operation and the various assumptions that went into the model.

Carbon Capture Case

Using the flue gas output from the baseline Coal Creek case, a stand-alone Aspen Plus model was constructed to estimate equipment sizes and heat and material balances for a carbon capture facility suitable to capture 90% of the CO_2 from Unit 1 at Coal Creek Station. The property data for MHI's KS-1 and KS-21 solvents needed to construct predictive performance models in Aspen Plus are proprietary, so carbon capture models were constructed assuming MEA as a solvent. This provided similar column performance to Case L12B from the DOE baseline study (Chou et al., 2011). Similar to Case L12B from the DOE baseline study, this model included:

- An NaOH scrubber for cooling the incoming flue gas and removing residual sulfur.
- An additional induced-draft (ID) fan to overcome pressure drop through the absorber column.
- An absorber column with solvent removal, cooling, and reinjection at the middle stage.
- A water wash column for minimizing solvent losses.
- A heat exchanger to heat rich solvent from the absorber using hot, lean solvent from the stripper column.
- A stripper column to regenerate solvent using low-grade steam from the plant.
- An additional cooler to reduce lean solvent temperature entering the column.
- A six-stage CO_2 compressor with interstage cooling and water removal.
- Various pumps and makeup systems.

The heat and material balance data from the stand-alone CO_2 capture model were used to evaluate heat integration in the baseline power plant model. The baseline model was adjusted to remove a portion of the steam from an intermediate stage in the low-pressure turbine. The specific steam conditions and flow rate were selected to minimize excessively high local temperatures that might degrade MEA while still providing enough heat to regenerate the solvent with a reasonable temperature approach. The condensate leaving the stripper reboiler was returned to the condenser.

Table 5 summarizes the overall plant performance for the Coal Creek Station Aspen Plus model and compares against Cases L12A and L12B from the DOE baseline study. More detailed process layouts for the cases with and without CO_2 capture are provided in Appendix A. Key points to note are that although the baseline Coal Creek Station model has similar coal heating value and power generation to Case L12A, the steam turbine cycle pressure is lower, which results in lower baseline efficiency and more flue gas generated. As a result, the model predicts a flue gas flow rate closer to Case L12B than to Case L12A, and the auxiliary power needed for CO_2 capture and compression is likewise similar to that observed for Case L12B. It is worth stressing again that the Aspen Plus model results are based on conditions observed at Coal Creek Station during a single period of steady-state operation and include a number of assumptions, including use of MEA as a solvent. As such, the results shown here may not be representative of typical performance at Coal Creek Station, and they certainly would not be expected to represent performance with commercial or advanced solvents requiring less regeneration energy.

Table 5. Overall Plant Performance

	Case L12A	Case L12B	Coal Creek Baseline	Coal Creek with Capture
Steam Turbine Power	**584,700**	**683,900**	**585,794**	**486,242**
CO_2 Capture/Removal Auxiliaries	–	24,700	–	25,810
CO_2 Compression	–	52,930	–	55,770
Total Auxiliaries, kWe	**34,640**	**133,850**	**46,408**	**127,948**
Net Power	**550,060**	**550,050**	**539,386**	**358,294**
Coal Feed Rate, lb/hr	755,859	1,110,668	895,000	895,000
Coal Heating Value, Btu/lb	6617	6617	6782	6782
Heat Rate, 10^6 Btu/hr	5002	7349	6070	6070
HHV[a] Thermal Input, kWt	1,465,801	2,153,863	1,778,909	1,778,909
Net Plant Efficiency (HHV), %	**37.5**	**25.5**	**30.3**	**20.1**
HHV Net Plant Heat Rate, Btu/kWh	9093	13,361	11,253	13,799
Steam Turbine Cycle, psig	3500	3500	2868	2868
Flue Gas Flow Rate, lb/hr	5,215,347	7,656,679	7,320,381	7,320,381

[a] Higher heating value.

Techno-Economic Assessment

To estimate the impact that process improvements in CO_2 capture technology can have on the economics of a power plant, the Aspen Process Economic Analyzer (APEA) software package was used. APEA is a project-scoping tool that enables engineers to evaluate the economic impact of their process designs. APEA is most valuable in the early phases of conceptual design to compare competing technologies and evaluate alternative process configurations. Models constructed in Aspen Plus for calculating mass and energy balances were imported into APEA for economic analysis.

Key Economic Assumptions

Cost estimations in DOE studies are considered to be an Advancement of Cost Engineering International (AACE International) Class 5 "feasibility study" with an accuracy range of –25%/+50%. If an assessment is to be more specific, then it is conducted during the front-end engineering and design study. This assessment is intended to serve as proof-of-concept-level information.

APEA was used to estimate the capital and operating costs for the capture portion of the plant. Values for cost were adjusted from values given for DOE developed baseline cases for a lignite-fired supercritical pc boiler, with and without capture (Chou et al., 2011) by using information from Aspen modeling and DOE-derived adjustment factors (James, 2019). The methodology provides a system to modify costs from a base case using parameters that directly affect those costs.

To estimate cost of electricity (COE), a simplified equation that was a function of total overnight capital (TOC), fixed and variable operating and maintenance (O&M) costs, capacity factor, and net output was given in a DOE assessment of power plant performance (National Energy Technology Laboratory Office of Program Planning and Analysis, 2019):

$$COE = \frac{\substack{first-year \\ capital\ charge} + \substack{first-year \\ fixed\ operating \\ costs} + \substack{first-year \\ variable\ operating \\ costs}}{\substack{annual\ net\ megawatt\ hours \\ of\ power\ generated}} \quad \text{[Eq. 2]}$$

$$COE = \frac{(CCF)(TOC) + OC_{FIX} + (CF)(OC_{VAR})}{(CF)(MWh)} \quad \text{[Eq. 3]}$$

Where:

COE = Revenue received by the generator (US$/MWh) during the power plant's first year of operation (expressed in base-year dollars).
CCF = Capital charge factor.
TOC = Expressed in base-year dollars.
OC_{FIX} = The sum of all fixed annual operating costs.
OC_{VAR} = The sum of all variable annual operating costs, including fuel at 100% capacity factor.
CF = Plant capacity factor (85%).
MWh = Annual net megawatt-hours of power generated at 100% capacity factor.

Other details for the cost-estimating methodology can be found in the DOE assessment (Chou et al., 2011).

Project Cases

The project case was developed to reflect the layout of Coal Creek Station Unit 1 more closely. To achieve this, the DOE lignite base case, L12A, was adjusted in the following ways:

- The baseline power plant was adjusted to match gross power output and flue gas production with Coal Creek Station, which necessitated the adjustment of coal feed.

- Gross power remained fixed for the project case and net power was reduced to account for the auxiliary load on the plant.

- Coal Creek Station refines its coal in a process before firing. This process removes the need for mercury control equipment. Consumables costs associated with mercury removal were not used for the project case.

- Lignite power plants in North Dakota do not employ SCR systems to control NO_x emissions. Consumables costs associated with NO_x control were not used for the project case. Equipment costs directly related to SCR could not be separated from cost codes associated with Account 5, Flue Gas Cleanup; therefore, those costs were not modified.

- Transport and storage (T&S) costs were not modified.

Utilizing the methodology described in the DOE quality guidelines for capital cost scaling and Aspen modeling of Coal Creek Station, extrapolating for the changes in gross electrical output, flue gas flow, and fuel feed, a project baseline case without carbon capture was developed. Utilizing scaling factors as described by DOE (Chou et al., 2011), the project case was adjusted and a capture system added to develop the project case with capture. The comparison project costs between the project cases and the DOE L12A and L12B cases is given in Table 6. Costs are given in 2019 dollars for all cases. Dollar value was adjusted utilizing consumer price index values calculated for each year as given by the Federal Reserve Bank of Minneapolis (2021). Appendix B includes additional tables with details on total plant cost summary, owner's costs, and initial and annual O&M costs for the project case and for the project case with capture.

Table 6. Cost Results Comparing the Project Case with and Without Capture to the DOE Baseline Study. All values in 2019 dollars.

	DOE Case L12A, no Capture	DOE Case L12B, with Capture	Project Case, no Capture	Project Case, with Capture
Total Plant Cost, $/kW	2517	4392	2719	5126
Bare Erected Cost, $/kW	2052	3392	2217	3894
Home Office Expenses, $/kW	194	321	210	361
Project Contingency, $/kW	271	540	291	660
Process Contingency, $/kW	0	138	0	211
TOC, $/M	1669	2945	1790	2658
TOC, $/kW	3070	5355	3315	6224
Owner's Costs, $/kW	553	963	596	1098
Total As-Spent Cost, $/kW	3482	6104	3759	6897
COE, $/MWh (excluding T&S)	76.5	135.9	86.2	131.4
Capital Costs, $/kWh	47.8	89.4	55.2	91.1
Fixed Costs, $/kWh	11.9	19.4	13.7	17.4
Variable Costs, $/kWh	7.5	13.6	6.6	9.5
Fuel Costs, $/kWh	9.3	13.6	10.7	13.5
COE, $/MWh (including T&S)	76.5	142.2	86.2	138.4
CO_2 T&S Costs, $/kW	N/A	6.2	N/A	6.9
Cost of CO_2 Capture, $/tonne	N/A	49.6	N/A	41.2
Breakeven CO_2 Emissions Penalty (including T&S)	N/A	85.0	N/A	39.1

In the project case, the gross plant output remains fixed; therefore, the addition of a capture system reduces net power output and treats a flue gas flow that is not changed from the no capture case. The cost of CO_2 capture is, therefore, less than that of DOE Case L12B. Carbon capture and compression make up 30% of the total plant cost.

WESP Addition

A final iteration was conducted to determine the costs of adding a WESP upstream of the capture system to reduce solvent loss from the capture system absorber column. In this case, because gross power output of the plant remains fixed, the changes affect the cost of the additional equipment and loss of net power output due to the auxiliary needs of the WESP. Table 7 gives the summary results of this scenario as compared to the plant case with carbon capture. Appendix B includes additional tables with the summary information of the WESP case.

Table 7. Cost Results Comparing the Project Case with Capture to a Capture Case with the Addition of a WESP. All values in 2019 dollars.

	Project Case with Capture	Capture Case with WESP Added
Total Plant Cost, $/kW	5126	5372
Bare Erected Cost, $/kW	3894	4054
Home Office Expenses, $/kW	361	380
Project Contingency, $/kW	660	701
Process Contingency, $/kW	211	237
TOC, $/M	2658	2764
TOC, $/kW	6224	6520
Owner's Costs, $/kW	1098	1148
Total As-Spent Cost, $/kW	6897	7431
COE, $/MWh (excluding T&S)	131.4	136.1
Capital Costs, $/kWh	91.1	95.4
Fixed Costs, $/kWh	17.4	17.5
Variable Costs, $/kWh	9.5	9.5
Fuel Costs, $/kWh	13.5	13.6
COE, $/MWh (including T&S)	138.4	143.0
CO_2 T&S Costs, $/kW	6.9	7.0
Cost of CO_2 Capture, $/tonne	41.2	44.3
Breakeven CO_2 Emissions Penalty (including T&S)	39.1	42.6

A sensitivity analysis was conducted to determine original investment payback for the installation of a WESP to control MEA loss from the capture system. The plot is given in Figure 47. The orange line denotes the COE for the scenario of carbon capture with a WESP, utilizing the original rate of MEA use of 1.75 tons/day and is fixed at $143/MWh. For the project case with only carbon capture (no WESP), the change in the COE was plotted as the daily use of MEA increased. The intersection of the two lines, denoted with a red dot, corresponds with a daily use of 18.2 tons of MEA. This indicates that the use of a WESP is most applicable at MEA daily use rates above that value under the assumption that the use of a WESP would reduce MEA losses to those reported in the DOE baseline study.

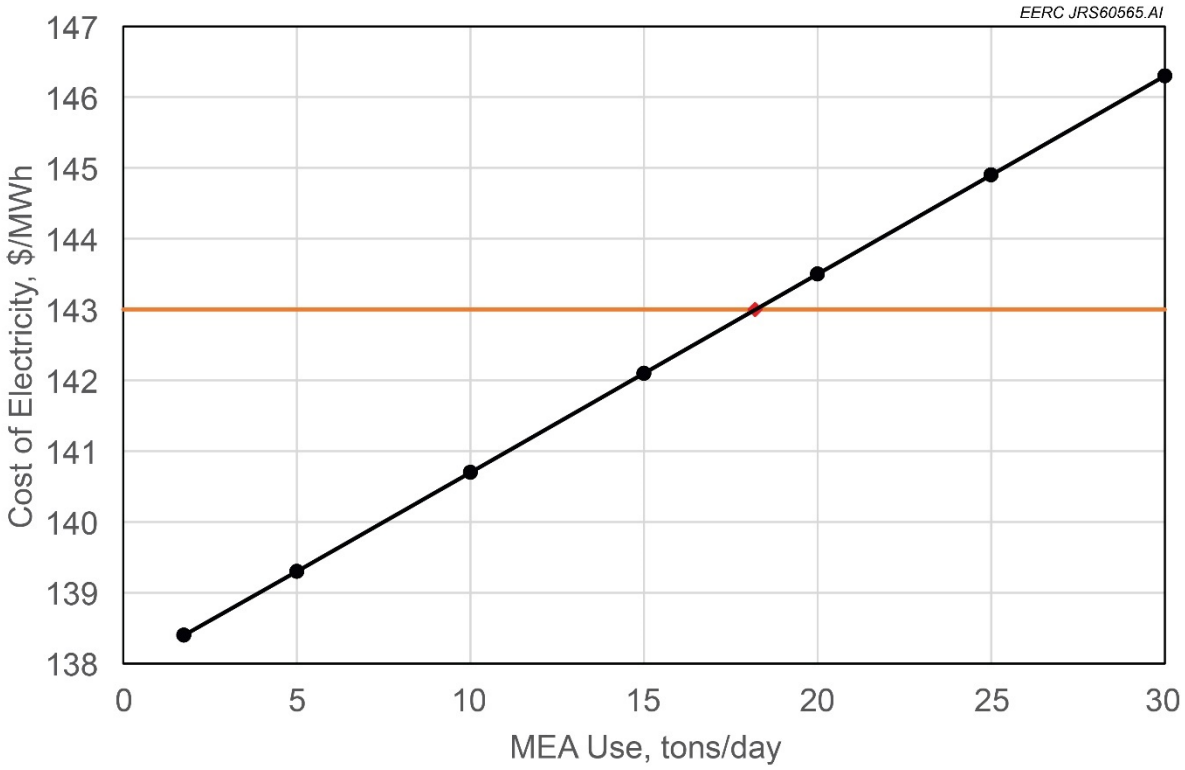

Figure 47. COE sensitivity to daily MEA use.

Wellsite Location

The baseline Coal Creek Station case used the same assumptions regarding CO_2 delivery costs as used by the DOE baseline study (Chou et al., 2011). To better assess the impact of local choices in storage formation on process economics, additional high-level case studies examined the impact of well count, pipeline distance, and wellhead pressure on process economics.

The geologic storage assessment showed that the most favorable options in terms of minimizing well count were injection into the Broom Creek Formation, if injecting off-site near Beulah, or injection into the Deadwood Formation, if injecting on-site at Coal Creek Station (Table 2), based on the flow rates reported in Table 1. Wellhead pressures were estimated at 2800 psi for the Deadwood Formation near Coal Creek or 1700 psi for the Broom Creek Formation near Beulah. Estimates for pressure and temperature drop through a 30-mi pipeline were made in Aspen HYSYS and validated against results from previous work done at the EERC. Total pressure drop through a 16-inch pipeline was estimated at roughly 200 psi, requiring a compressor delivery pressure of 1900 psi to achieve 1700 psi at the Broom Creek wellhead.

Simple Payback Period – Cost-per-Well Analysis

For the purposes of this simplistic high-level comparison, well staging was ignored, and it was assumed that all wells would come online at the same time and would operate at near-constant wellhead pressure. The Aspen capture model was then adjusted to estimate compressor capital

expenditure and operating expenses for each injection location, assuming constant CO_2 delivery conditions. The number of wells was fixed at the median values of five wells for the off-site Broom Creek and eight wells for the on-site Deadwood cases. The cost per well was varied from $7 to $10M for each Deadwood well and from $5 to $10M for each Broom Creek well, with the cost per Broom Creek wells not allowed to exceed the cost per Deadwood wells under the assumption that the deeper on-site wells would not cost less than the off-site, shallower wells. The total cost for the on-site Deadwood option was subtracted from the total cost for the off-site Broom Creek option (pipeline costs plus well completion costs) and the result divided by the net difference in estimated electrical costs for CO_2 compression to get a simple payback period.

Figure 48 charts the simple payback period by cost per well. For cases with a well completion cost of >$8.4M/well for the Deadwood and <$7.4M/well for the Broom Creek, there is a region of cases in the lower right of this chart in which the Broom Creek option has a lower up-front cost than the Deadwood option and has a negative payback period, indicating that it is inherently more cost-effective to inject into the Broom Creek, even without considering electrical penalties for the Deadwood. For Deadwood well completion costs of <$8.6M/well, when the Broom Creek well completion cost is close to the Deadwood well completion cost, the

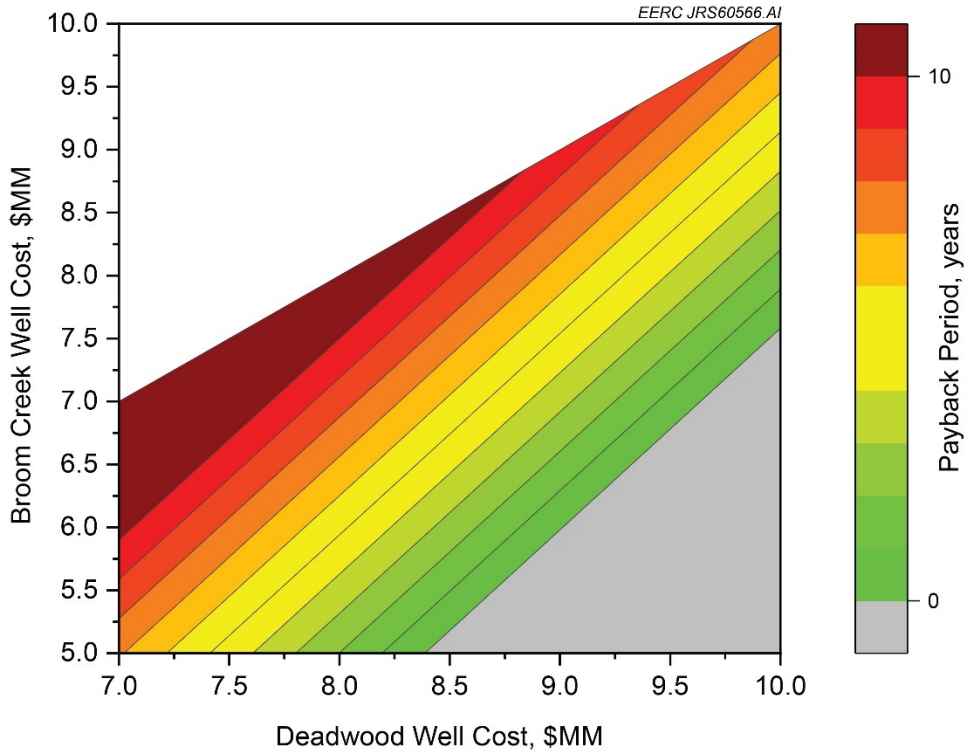

Figure 48. Simple payback period for the Broom Creek storage option versus well completion costs. The area in white was not considered, and the area in gray represents a negative payback period.

simple payback period for the Broom Creek option can exceed 10 years. It should be noted that there is an overlap in the ranges of Deadwood well costs between $8.4M and $8.6M/well where, depending on the cost per well for the Broom Creek option, the payback period may be less than 0 years or greater than 10 years. This uncertainty highlights the need for accurate well completion costs prior to selecting the most cost-effective injection scenario.

Breakeven Cost per Well for the Broom Creek Injection Scenario

This simple analysis considered only the capital costs associated with completing wells and constructing a 30-mi pipeline to find the cost per well at which the Broom Creek option has the same up-front cost as the Deadwood option. The breakeven cost per well for the Broom Creek injection scenario will depend on the number of wells required in each formation. Assuming that the well completion cost in the Deadwood Formation near Coal Creek Station is fixed at $10M/well (the high end of the range), Figure 49 displays the breakeven cost per well for injection into the Broom Creek Formation near Beulah. It should be noted that a higher breakeven well cost is more favorable, as it indicates that the Broom Creek option would be at cost parity with the Deadwood option, even at a very high well completion cost. With the choice of nine wells in the Deadwood at Coal Creek Station or four wells in the Broom Creek near Beulah, the breakeven cost is nearly $12M/well, indicating that the Broom Creek option would be preferred, even if the well completion cost were slightly higher than for the Deadwood option. For the worst-case scenario of six wells in the Broom Creek or seven wells in the Deadwood, the breakeven cost is only $4.66M/well, which is below the typical range of well completion costs of $5M–$10M/well. In this case, it is unlikely that the Broom Creek option would be at cost parity with the Deadwood option, although the payback period in this case might still be short if the actual cost per well is not much above $5M/well.

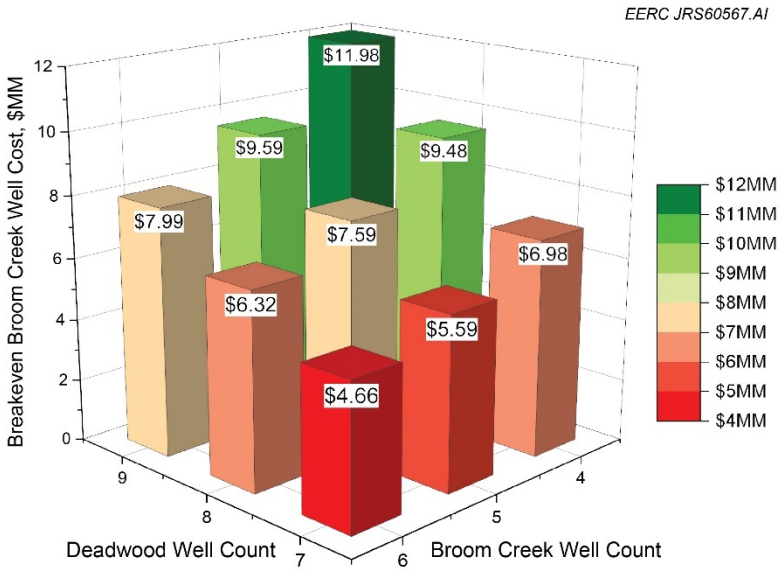

Figure 49. Breakeven completion cost per well for the Broom Creek option depending on the number of wells required at each location.

CONCLUSIONS

MHI's AERU was effective at reducing aerosol-based amine emissions when operating with both commercial KS-1 and advanced KS-21 solvent. When operating the AERU with MHI solvents at Coal Creek Station, the particulate count at the system outlet was much lower than at the inlet, indicating effective aerosol removal, whereas the particulate count actually increased at the capture system outlet when using a standard water wash column with MEA in the same absorber column. Total aerosol emissions at the system outlet were reduced when using KS-21 as compared to using KS-1. When operating with KS-1, the particulate collected at the system outlet was observed to be coated in a thin coating layer that was presumed to represent aerosol losses. The particulate collected when using KS-21 did not show any signs of a coating layer. Operation with the WESP eliminated nearly all particulate at the system outlet and also reduced the metal loading on substrates collected at the system outlet without affecting sulfur speciation through the column. Levels of analytes accumulated in the solvent were not of concern based on MHI experience, nor were the rates of amine losses or emissions measured at the system outlet.

The particulate matter exiting the absorber and accumulating in the solvent filter was enriched in metals that likely derived from the absorber materials of construction. SEM analyses of the particulate captured in the solvent filter suggest that at least some of this material was present as discrete submicrometer- to micrometer-scale particles that may have been left as fine residue in the absorber column following previous testing and on-site fabrication activities at Coal Creek Station. Corrosion of the materials used in this column has not been previously observed when using KS-1 or KS-21.

The unique geologic conditions near Coal Creek Station offered a case study in the costs of different storage options for captured CO_2. A high-level, prefeasibility study of CO_2 storage options suggests that pipeline transport for injection into the Broom Creek Formation near Beulah, North Dakota, would offer the potential for fewer wells, smaller plume sizes, and more CO_2 stored per unit land area than would be possible for on-site storage near Coal Creek Station. If on-site CO_2 injection is desirable, the most favorable formation geology in terms of minimizing well count in the area immediately below Coal Creek Station is likely to be found in the Deadwood Formation. The greater plume size for on-site injection into the Deadwood Formation could require additional landowner agreements/payments and a greater monitoring area. Combined with the higher number of wells required, these additional costs indicate that there is significant benefit to moving CO_2 away from Coal Creek Station to better geology in the west. Although the information provided in this prefeasibility effort is useful for initial conversations and provides some background and initial direction, a more comprehensive effort would be needed to understand the future project area with a greater degree of confidence. Factors not considered in this high-level study included financial wherewithal, relationship with landowners, geology in the region, and regulatory environment.

A techno-economic analysis of CO_2 capture at Coal Creek Station using an MEA solution estimates a 34% reduction in net power with simple steam integration at the low-pressure turbine, with net electrical production from Unit 1 dropping from 540 MW in the baseline model to 358 MW with capture. Roughly 100 MW of this loss is the result of steam use for solvent regeneration resulting in lower gross power production. The remaining 82 MW of this loss is

directly attributable to parasitic electric load, primarily for CO_2 compression, with added ID fan capacity also contributing significantly to the parasitic load. This energy penalty could be reduced by:

- Use of advanced solvents with lower regeneration energy and/or less pressure drop through the absorber column.
- Better steam integration strategies (e.g., with an additional turbine).
- Lower CO_2 delivery pressures to reduce compressor demands.

The cost for an MEA-based capture system was estimated at $671M, assuming a start date in 2019 and completion in 2021. A stand-alone WESP for inlet particulate control was estimated to cost $38M for equipment, which is in line with vendor quotes, with a total direct cost of $83.6M for the installed unit. The WESP addition would result in a nearly $5/MWh increase in electricity, but the reduced particulate loading offered by a WESP would be expected to result in lower amine losses to aerosol formation and to solvent degradation. If total MEA losses without the WESP were greater than 18.2 tons/day, or roughly 10 times the losses estimated in the DOE baseline study (Chou et al., 2011), operation with the WESP would result in a lower COE than operation without. This estimate ignores other potential costs of high particulate loading (such as water makeup, solvent treatment, and waste disposal) that may affect the breakeven point for a WESP.

MILESTONES

The completed milestone table can be found in Table 8.

Table 8. Milestones

Milestone Title/ Description	Planned Completion Date	Actual Completion Date	Verification Methods	Comments
M1 – Initiate Testing	10/15/20	10/07/20	Reported in subsequent quarterly report.	
M2 – Complete Wet ESP Installation	11/30/20	10/07/20	Reported in subsequent quarterly report.	
M3 – Complete Initial Testing of Advanced Solvent	2/28/21	1/18/21	Reported in subsequent quarterly report.	
M4 – Complete Substrate Analysis	4/30/21	6/09/21	Reported in subsequent quarterly report.	
M5 – Complete Techno-Economic Modeling	7/31/21	8/25/21	Reported in draft final report.	

REFERENCES

Benson, S.; Folkedahl, B.; Hurley, J. *Managing Aerosol Emissions from CO_2 Capture Systems*; Final Report for North Dakota Industrial Commission: July 2017.

Brachert, L.; Mertens, J.; Khakharia, P.; Schaber, K. The Challenge of Measuring Sulfuric Acid Aerosols: Number Concentration and Size Evaluation Using a Condensation Particle Counter (CPC) and an Electrical Low Pressure Impactor (ELPI+). *J. Aerosol Sci.* **2014**, *67*, 21–27.

Chou, V.; Haslbeck, J.; Kyle, A.; Kuehn, N.; Lewis, E.; Pinkerton, L.; Shah, V.; Varghese, E.; Woods, M.; Turner, B. *Cost and Performance Baseline for Fossil Energy Plants, Volume 3b*: *Low Rank Coal to Electricity: Combustion Cases*; DOE/NETL-2011/1463: March 2011.

Dhanrag, D.; Biswas, P. Influence of Particles on Amine Losses During CO_2 Capture: A Process Simulation Coupled Aerosol Dynamics Model. *Int. J. Greenh.* **2020**, *103*, 103179.

Dutcher, B.; Fan, M.; Russell, A.G. Amine-Based CO_2 Capture Technology Development from the Beginning of 2013 – A Review. *ACS Appl. Mater. Interfaces*. **2015**, *7*, 2137−2148.

Federal Reserve Bank of Minneapolis Consumer Price Index. www.minneapolisfed.org/ about-us/monetary-policy/inflation-calculator/consumer-price-index-1913- (accessed Aug 15, 2021).

Fenton, N.; Neil, M. *Risk Assessment and Decision Analysis with Bayesian Networks*; CRC Press: Boca Raton, 2012.

Fulk, S.M. Measuring and Modeling Aerosols in Carbon Dioxide Capture by Aqueous Amines. Ph.D. Dissertation, University of Texas at Austin, TX, 2016.

James, R. *Quality Guidelines for Energy Systems Studies, Capital Cost Scaling Methodology: Revision 4 Report*; NETL-PUB-22697: Oct 2019.

Kamijo, T.; Sorimachi, Y.; Shimada, D.; Miyamoto, D.; Endo, T.; Nagayasu, H.; Mangiaracina, A. Result of the 60 tpd CO_2 Capture Pilot Plant in European Coal Power Plant with KS-1™ Solvent. *Energy Procedia* [online]. **2013**, *37*, 813–816.

Khakharia, P. Aerosol-Based Emission, Solvent Degradation, and Corrosion in Post-Combustion CO_2 Capture. Ph.D. Dissertation, Technische Universiteit Delft, Netherlands, 2015.

Khakharia, P.; Brachert, L.; Mertens, J.; Anderlohr, C.; Huizinga, A.; Sanchez-Fernandez, E.; Schallert, B.; Schaber, K.; Vlugt, T.J.H.; Goetheer, E. Understanding Aerosol-Based Emissions in a Post-Combustion CO_2 Capture Process: Parameter Testing and Mechanisms. *Int. J. Greenh*. **2015**, *34*, 63–74.

Le Moullec, Y.; Neveux, T.; Al Azki, A.; Chikukwa, A.; Hoff, K.A. Process Modifications for Solvent-Based Post-Combustion CO_2 Capture. *Int. J. Greenh.* **2014**, *31*, 96–112.

Luis, P. Use of Monoethanolamine (MEA) for CO_2 Capture in a Global Scenario: Consequences and Alternatives. *Desalination*. **2016**, *380*, 93–99.

Majeed, H.; Svendsen, H.F. Characterization of Aerosol Emissions from CO_2 Capture Plants Treating Various Power Plant and Industrial Flue Gases. *Int. J. Greenh*. **2018**, *74*, 282–295.

Mertens, J.; Brachert, L.; Desagher, D.; Thielens, M.L.; Khakharia, P.; Goetheer, E.; Schaber, K. ELPI+ Measurements of Aerosol Growth in an Amine Absorption Column. *Int. J. Greenh.* **2014**, *23*, 44–50.

National Energy Technology Laboratory Office of Program Planning and Analysis. *Quality Guidelines for Energy System Studies: Cost Estimation Methodology for NETL Assessments of Power Plant Performance*; NETL-PUB-22580: Sept 2019.

Peck, W.D.; Crotty, C.M.; Knudsen, D.J.; Sorensen, J.A.; Gorecki, C.D.; Steadman, E.N. Geological Characterization of the Basal Cambrian System in the Williston Basin: Plains CO_2 Reduction (PCOR) Partnership Phase III Task 16 Deliverable D91 for U.S. Department of Energy National Energy Technology Laboratory Cooperative Agreement No. DE-FC26-05NT42592, EERC Publication 2012-EERC-04-19, Grand Forks, North Dakota, Energy & Environmental Research Center, Feb 2012.

Peck, W.D.; Glazewski, K.A.; Braunberger, J.R.; Grove, M.M.; Bailey, T.P.; Bremer, J.M.; Gorz, A.J.; Sorensen, J.A.; Gorecki, C.D.; Steadman, E.N. Broom Creek Formation outline: Plains CO_2 Reduction (PCOR) Partnership Phase III value-added report for U.S. Department of Energy National Energy Technology Laboratory Cooperative Agreement No. DE-FC26-05NT42592, EERC Publication 2014-EERC-09-09, Grand Forks, North Dakota, Energy & Environmental Research Center, Aug 2014a.

Peck, W.D.; Glazewski, K.A.; Klenner, R.C.L.; Gorecki, C.D.; Steadman, E.N.; Harju, J.A. A Workflow to Determine CO_2 Storage Potential in Deep Saline Formations. *Energy Procedia*. **2014b**, *63*, 5231–5238.

Svendsen, H.F.; Majeed, H.; Knuutila, H.K.; Hillestad, M.; Evjen, S.; Mejdell, T.; Einbu, A.; Hjarbo, K.W.; Haugen, G.; Hoff, K.A. Aerosol Growth in CO_2 Absorption with MEA, Modeling and Comparison with Experimental Results. *Int. J. Greenh.* **2021**, *109*, 103990.

Wu, X.; Yu, Y.; Qin, Z.; Shang, Z. The Advances of Post-Combustion CO_2 Capture with Chemical Solvents: Review and Guidelines. *Energy Procedia*. **2014**, *63*, 1339.

APPENDIX A

PROCESS FLOW DIAGRAMS

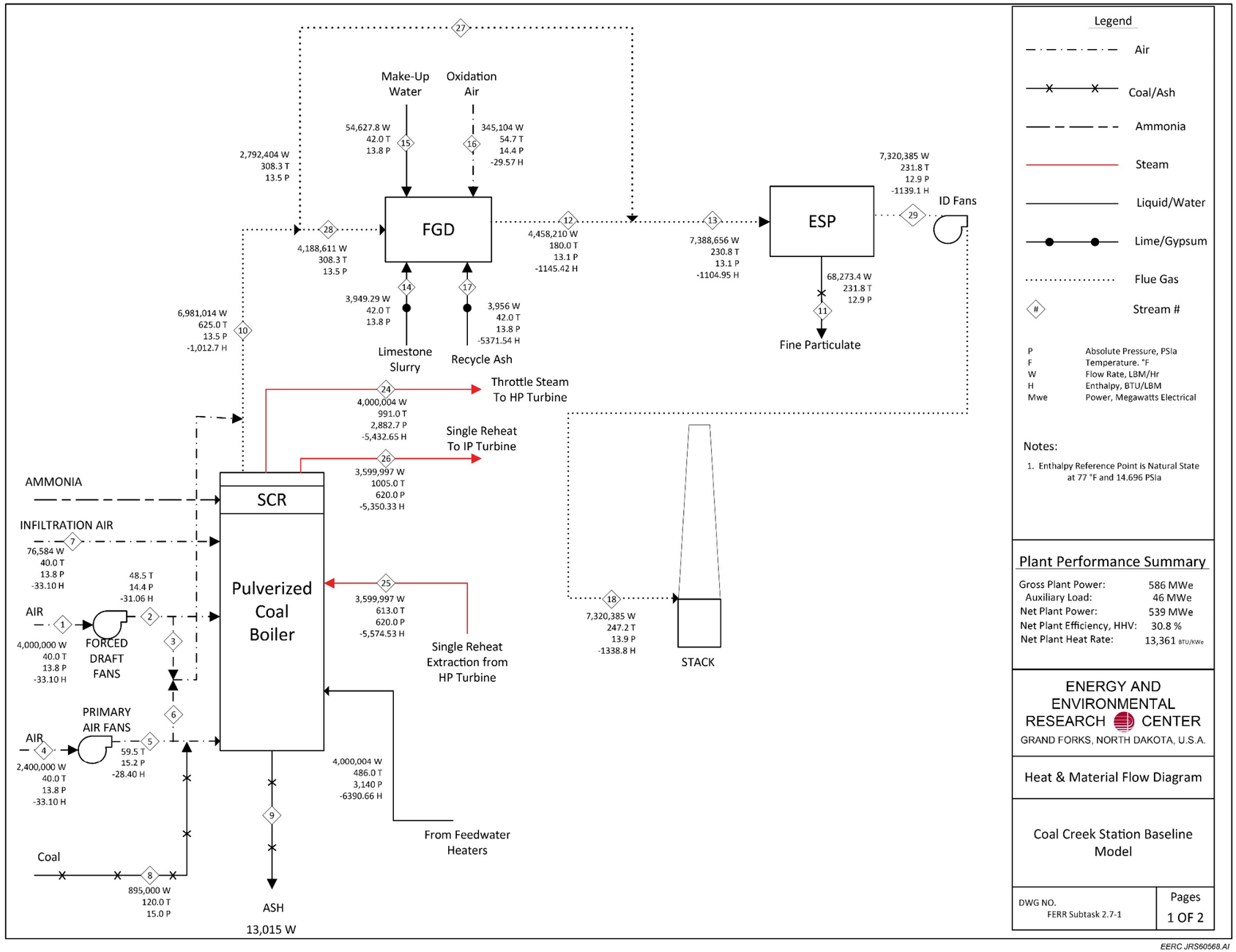

Figure A-1. Baseline Coal Creek Station power plant.

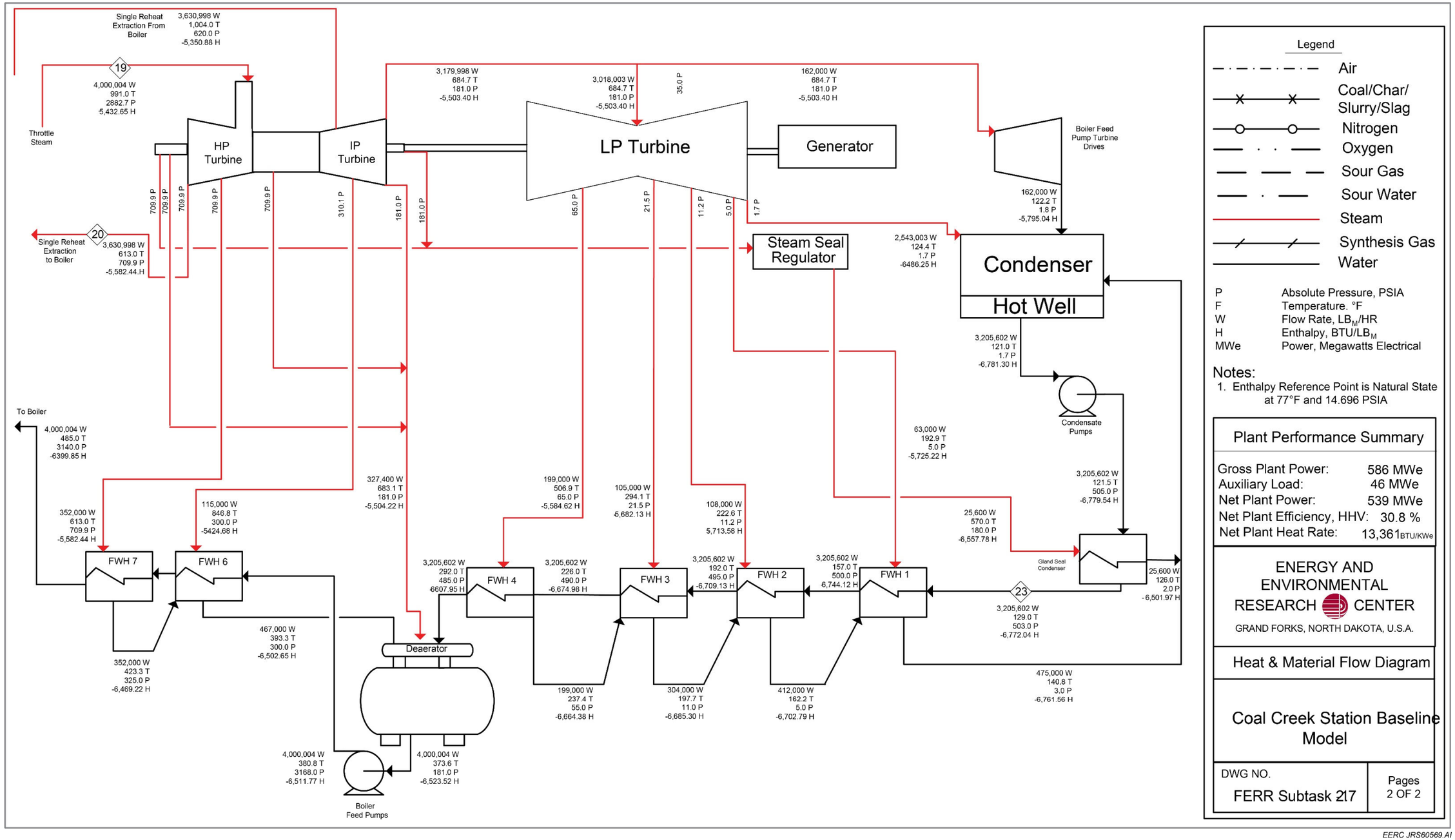

Figure A-2. Baseline Coal Creek Station steam cycle.

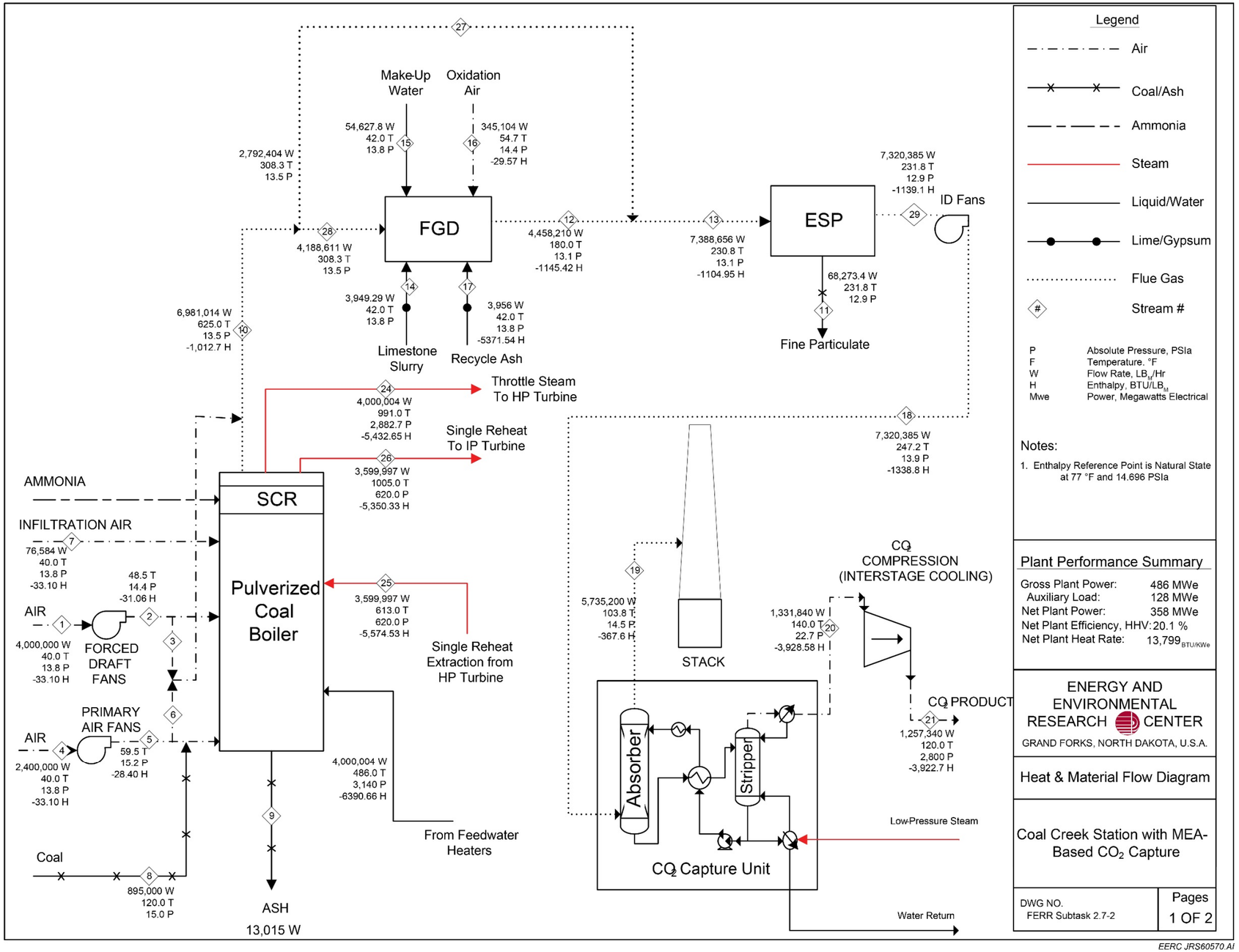

Figure A-3. Coal Creek Station power plant with MEA-based CO_2 capture.

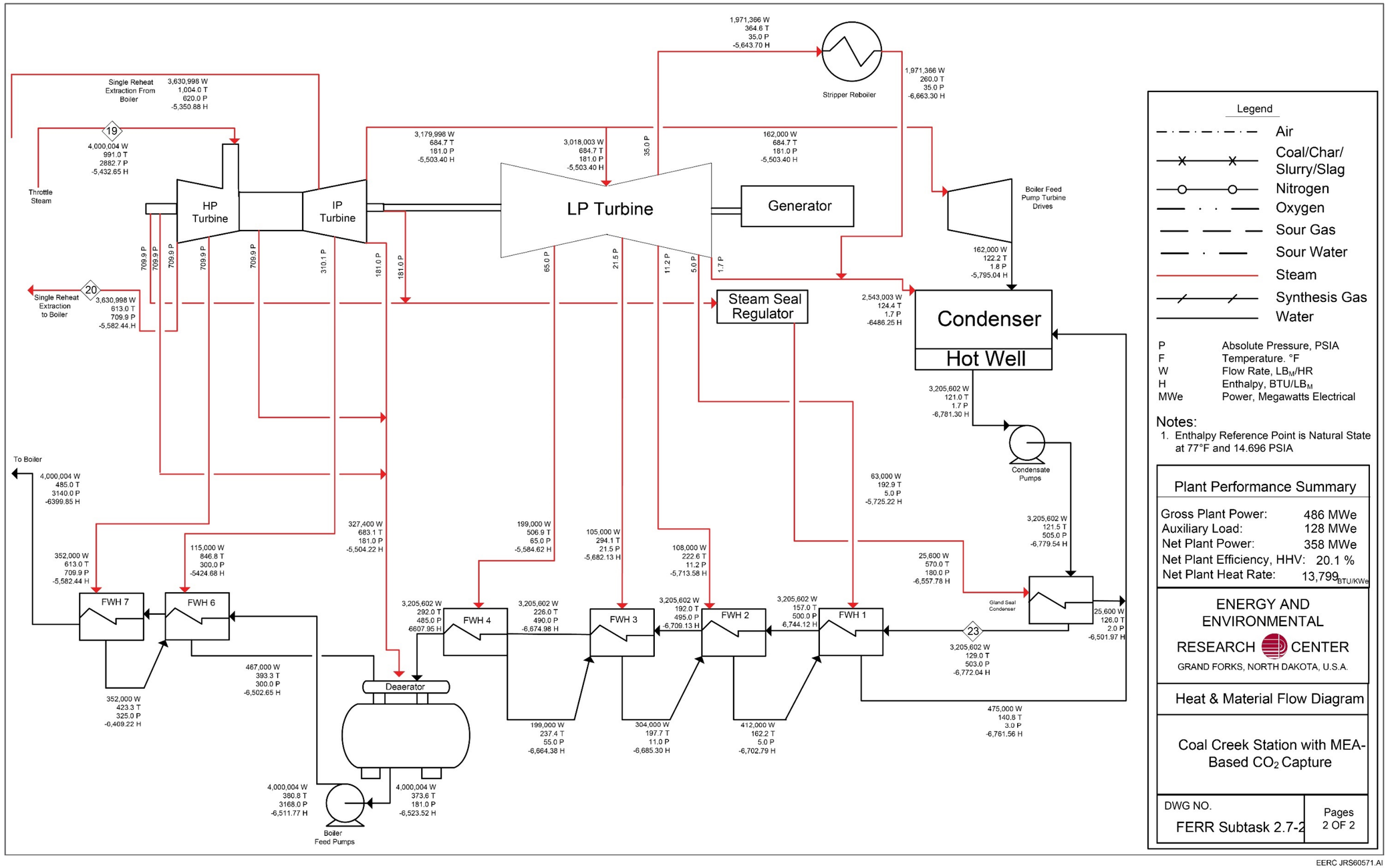

Figure A-4. Coal Creek Station steam cycle with MEA-based CO_2 capture.

APPENDIX B

PROJECT CASE COST TABLES

Table B-1. Total Plant Cost Summary, Project Case, no Capture

Case:		Supercritical Pulverized coal (pc) Without CO_2 Capture							Estimate Type:	Conceptual	
Plant Size (MW, net):		539.9							Cost Base:	2019	
										Total Cost	
Acct No.	Description	Equipment Cost, $/1000	Material Cost, $/1000	Direct, $/1000	Indirect, $/1000	Bare Erected Cost, $/1000	Eng'g CM, H.O., and Fee, /1000	Process, $/1000	Project, $/1000	$/1000	$/kW
1	Coal and Sorbent Handling	26,184	8114	17,668	0	51,965	4681	0	8500	65,145	121
2	Coal and Sorbent Preparation and Feed	13,767	1098	3836	0	18,702	1645	0	3052	23,398	43
3	Feedwater and Misc. Balance-of-Plant (BOP) Systems	54,333	0	26,600	0	80,933	7389	0	14,046	102,368	190
4	pc Boiler	304,355	0	137,794	0	442,149	42,963	0	48,511	533,622	988
5	Flue Gas Cleanup	143,909	0	51,017	0	194,926	18,665	0	21,357	234,948	435
5B	CO_2 Removal and Compression	0	0	0	0	0	0	0	0	0	0
6	Combustion Turbine/Accessories	0	0	0	0	0	0	0	0	0	0
7	Heat Recovery Steam Generator (HRSG), Ducting and Stack	25,748	1480	17,485	0	44,712	4105	0	6373	55,191	102
8	Steam Turbine Generator	136,380	1351	34,009	0	171,740	16,318	0	26,954	215,011	398
9	Cooling Water System	9547	5193	9276	0	24,016	2260	0	3604	29,880	55
10	Ash/Spent Sorbent-Handling Systems	8811	280	11,778	0	20,869	2006	0	2353	25,228	47
11	Accessory Electric Plant	22,280	8032	23,424	0	53,736	4739	0	7239	65,715	122
12	Instrumentation and Control	10,732	0	10,881	0	21,613	1960	0	2896	26,469	49
13	Improvements to Site	3676	2113	7407	0	13,196	1301	0	2899	17,396	32
14	Buildings and Structures	0	30,112	28,419	0	58,531	5278	0	9572	73,381	136
	Total Cost	**759,721**	**57,773**	**379,594**	**0**	**1,197,088**	**113,308**	**0**	**157,355**	**1,467,752**	**2719**

[1] Engineering construction management, home office, and fee.

Table B-2. Owner's Costs, Project Case, no Capture

Description	$/1000	$/kW
Preproduction Costs		
6-month All Labor	11,992	22
1-month Maintenance Materials	1690	3
1- month Nonfuel Consumables	214	1
1-month Waste Disposal	678	1
25% of 1-month Fuel Cost at 100% Capacity Factor	1050	2
2% of Total Plant Cost (TPC)	29,355	54
Total	**44,979**	**83**
Inventory Capital		
60-day Supply of Fuel and Consumables at 100% Capacity Factor	8705	16
0.5% of TPC (spare parts)	7339	14
Total	**16,044**	**30**
Other Costs		
Initial Cost for Catalyst and Chemicals	0	0
Land	1110	2
Other Owner Costs	220,163	408
Financing Costs	39,629	73
Total Overnight Cost (TOC)	**1,789,677**	**3315**
Total as Spent Cost (TASC) Multiplier	1.134	
TASC	**2,029,493**	**3759**

Table B-3. Initial and Annual Operating and Maintenance Costs, Project Case, No Capture

Case:	Supercritical pc Without CO_2				Cost Base:	2019
Plant Size, MW, net:	539.89	Coal Consumption, tons/day:		10,249	Capacity Factor, %:	85
Operating & Maintenance Labor						
Operating Labor				**Operating Labor Requirements per Shift**		
Operating Labor Rate (base):	42.74	$/hour		Skilled Operator:	2.0	
Operating Labor Burden:	37.00	% of base		Operator:	9.0	
Labor Overhead Charge Rate:	30.84	% of labor		Foreman:	1.0	
				Lab Techs, etc.:	2.0	
				Total:	**14.0**	
Fixed Operating Costs						
					Annual Cost	
					$	**$/kW-net**
Annual Operating Labor:					7,692,876	14.249
Maintenance Labor:					11,494,498	21.290
Administrative and Support Labor:					4,764,474	8.825
Property Taxes and Insurance:					31,260,970	57.902
Total:					**55,245,188**	**102.327**
Variable Operating Costs						
					$	**$/kWh-net**
Maintenance Material:					17,241,749	0.00429
Consumables						
	Consumption				**Cost**	
	Initial Fill	**Per Day**	**Per Unit**	**Initial Cost**		
Water, /1000 gallons:	0	2234	1.33	0	923,403	0.00023
Makeup and Wastewater Treatment Chemicals, lb:	0	10,812	0.21	0	703,396	0.00017
Limestone, ton:	0	66	27.14	0	555,661	0.00014
Hydrated Lime, ton:	0	0	0.00	0	0	0.00000
Activated Carbon ton:	0	0	0.00	0	0	0.00000
CO_2 Capture System Chemicals:	0	0	0.00	0	0	0.00000
Triethylene Glycol, gal:	0	0	0.00	0	0	0.00000
H_2SO_4, ton:	0	0	0.00	0	0	0.00000

Table B-3. Initial and Annual Operating and Maintenance Costs (continued)

Case:	Supercritical pc Without CO_2				Cost Base:	2019
Plant Size, MW, net:	539.89	Coal Consumption, tons/day:		10,249	Capacity Factor, %:	85
	Consumption				Cost	
	Initial Fill	Per Day	Per Unit	Initial Fill	$	$/kWh-net
Selective Catalytic Reduction (SCR) Catalyst, m^3:	0	0	0.00	0	0	0.00000
Subtotal:				**0**	**2,182,460**	**0.00054**
Waste Disposal						
Fly Ash, ton:	0	957	20.02	0	5,943,930	0.00148
Bottom Ash, ton:	0	156	20.02	0	968,916	0.00024
Amine Purification Unit Waste, ton:	0	0	0.00	0	0	0.00000
Thermal Reclaimer Unit Waste, ton:	0	0	0.00	0	0	0.00000
Prescrubber Blowdown Waste, ton:	0	0	0.00	0	0	0.00000
Subtotal:				**0**	**6,912,846**	**0.00172**
By-Products						
Gypsum, ton:	0	0	0.00	0	0	0.00000
Subtotal:				**0**	**0**	**0.00000**
Variable Operating Costs Total:				**0**	**26,337,055**	**0.00655**
Fuel Cost						
North Dakota Lignite, ton:	0	10,249	13.47	0	42,830,764	0.01065
Total:					**42,830,764**	**0.01065**

Table B-4. Total Plant Cost Summary, Project Case with Capture

Case:		Supercritical pc with CO_2 Capture					Estimate Type:			Conceptual	
Plant Size, MW, net:		427							Cost Base:	2019	
										Total Cost	
Acct No.	Description	Equipment Cost, $/1000	Mater. Cost, $/1000	Direct, $/1000	Indirect, $/1000	Bare Erected Cost, $/1000	Eng'g CM, H.O., and Fee, $/1000	Process, $/1000	Project, $/1000	$/1000	$/kW
1	Coal and Sorbent Handling	26,187	8118	17,674	0	51,978	4683	0	8500	65,162	153
2	Coal and Sorbent Preparation and Feed	13,773	1108	3845	0	18,725	1647	0	3057	23,429	55
3	Feedwater and Misc. BOP Systems	60,014	0	29,071	0	89,086	8103	0	15,833	113,022	265
4	pc Boiler	304,355	0	137,794	0	442,149	42,963	0	48,511	533,622	1250
5	Flue Gas Cleanup	143,909	0	51,017	0	194,926	18,665	0	21,357	234,948	550
5B	CO_2 Removal and Compression	305,939	0	102,505	0	408,444	35,881	89,030	115,355	648,709	1519
6	Combustion Turbine/Accessories	0	0	0	0	0	0	0	0	0	0
7	HRSG, Ducting and Stack	26,306	1491	17,850	0	45,646	4188	0	6519	56,353	132
8	Steam Turbine Generator	140,039	1358	35,752	0	177,149	16,774	0	27,823	221,745	519
9	Cooling Water System	21,031	10,512	19,286	0	50,829	4784	0	7534	63,148	148
10	Ash/Spent Sorbent-Handling Systems	8814	280	11,782	0	20,876	2006	0	2354	25,236	59
11	Accessory Electric Plant	25,657	9,079	26,232	0	60,967	5370	0	8211	74,549	175
12	Instrumentation and Control	11,133	0	11,286	0	22,419	1952	1077	3017	28,465	67
13	Improvements to Site	4060	2334	8182	0	14,576	1438	0	3203	19,217	45
14	Buildings and Structures	0	33,416	31,512	0	64,928	5855	0	10,618	81,401	191
	Total Cost	**1,091,216**	**67,695**	**503,789**	**0**	**1,662,699**	**154,309**	**90,107**	**281,891**	**2,189,005**	**5126**

Table B-5. Owner's Costs, Project Case with Capture

Description	$/1000	$/kW
Preproduction Costs		
6-month All Labor	11,992	28
1-month Maintenance Materials	1690	4
1-month Nonfuel Consumables	587	1
1-month Waste Disposal	678	2
25% of 1-month Fuel Cost at 100% Capacity Factor	1050	2
2% of TPC	43,780	103
Total	**59,777**	**140**
Inventory Capital		
60-day Supply of Fuel and Consumables at 100% Capacity Factor	9440	22
0.5% of TPC (spare parts)	10,945	26
Total	**20,385**	**48**
Other Costs		
Initial Cost for Catalyst and Chemicals	0	0
Land	1110	3
Other Owner Costs	328,351	769
Financing Costs	59,103	138
TOC	**2,657,731**	**6224**
TASC Multiplier	1.140	
TASC	**3,029,814**	**7,096**

Table B-6. Initial and Annual Operating and Maintenance Costs, Project Case with Capture

Case:	Supercritical pc with CO_2 Capture			Cost Base:	2019
Plant Size, MW, net:	427	Coal Consumption, tons/day:	10,249	Capacity Factor, %:	85

Operating and Maintenance Labor				
Operating Labor			**Operating Labor Requirements per Shift**	
Operating Labor Rate (base):	42.74	$/hour	Skilled Operator:	2.0
Operating Labor Burden:	37.00	% of base	Operator:	9.0
Labor Overhead Charge Rate:	30.84	% of labor	Foreman:	1.0
			Lab Techs, etc.:	2.0
			Total:	**14.0**

Fixed Operating Costs			
		Annual Cost	
		$	**$/kW-net**
Annual Operating Labor:		7,692,876	18.016
Maintenance Labor:		11,494,498	26.919
Administrative and Support Labor:		4,764,474	11.158
Property Taxes and Insurance:		31,260,970	73.211
Total:		**55,245,188**	**129.380**

Variable Operating Costs		
	$	**$/kWh-net**
Maintenance Material:	17,241,749	0.00542

Consumables						
	Consumption					
	Initial Fill	**Per Day**	**Per Unit**	**Initial Cost**	**Cost**	
Water, /1000 gallons:	0	2234	1.33	0	923,403	0.00029
Makeup and Wastewater Treatment Chemicals, lb:	0	10,812	0.21	0	703,396	0.00022
Limestone, ton:	0	66	27.14	0	555,661	0.00017
Hydrated Lime, ton:	0	0	0.00	0	0	0.00000
Activated Carbon, ton:	0	0	0.00	0	0	0.00000
CO_2 Capture System Chemicals:	1236	1.75	2775.19	3,430,127	1,506,755	0.00040
Triethylene Glycol, gal:	0	0	0.00	0	0	0.00000
H_2SO_4, ton:	83	13.82	534.93	44,399	2,293,616	0.00072

Table B-6. Initial and Annual Operating and Maintenance Costs (continued)

Case:	Supercritical pc with CO_2 Capture				Cost Base:	2019
Plant Size, MW, net:	427		Coal Consumption, tons/day:	10,249	Capacity Factor, %:	85
	Consumption				Cost	
	Initial Fill	Per Day	Per Unit	Initial Fill	$	$/kWh-net
SCR Catalyst, m^3:	0	0	0.00	0	0	0.00000
Subtotal:				**0**	**5,982,831**	**0.00188**
Waste Disposal						
Fly Ash, ton:	0	957	20.02	0	5,943,930	0.00187
Bottom Ash, ton:	0	156	20.02	0	968,916	0.00030
Amine Purification Unit Waste, ton:	0	0	0.00	0	0	0.00000
Thermal Reclaimer Unit Waste, ton:	0	0	0.00	0	0	0.00000
Prescrubber Blowdown Waste, ton:	0	0	0.00	0	0	0.00000
Subtotal:				**0**	**6,912,846**	**0.00217**
By-Products						
Gypsum, ton:	0	0	0.00	0	0	0.00000
Subtotal:				**0**	**0**	**0.00000**
Variable Operating Costs Total:				**0**	**26,337,055**	**0.00828**
Fuel Cost						
North Dakota Lignite, ton:	0	10,249	13.47	0	42,830,764	0.01347
Total:					**42,830,764**	**0.01347**

Table B-7. Total Plant Cost Summary, Project Case with Capture and WESP

Case:		Supercritical pc with CO_2 Capture and WESP							Estimate Type:	Conceptual	
Plant Size, MW, net:		424							Cost Base:	2019	
										Total Cost	
Acct No.	Description	Equipment Cost, $/1000	Material Cost, $/1000	Direct, $/1000	Indirect, $/1000	Bare Erected Cost, $/1000	Eng'g CM, H.O., and Fee, $/1000	Process, $/1000	Project, $/1000	$/1000	$/kW
1	Coal and Sorbent Handling	26,187	8118	17,674	0	51,978	4683	0	8500	65,162	154
2	Coal and Sorbent Preparation and Feed	13,773	1108	3845	0	18,725	1647	0	3057	23,429	55
3	Feedwater and Misc. BOP Systems	60,014	0	29,071	0	89,086	8103	0	15,833	113,022	267
4	pc Boiler	304,355	0	137,794	0	442,149	42,963	0	48,511	533,622	1259
5	Flue Gas Cleanup	183,712	0	58,278	0	241,990	24,585	10,406	34,840	311,821	735
5B	CO_2 Removal and Compression	305,939	0	102,505	0	408,444	35,881	89,030	115,355	648,709	1530
6	Combustion Turbine/Accessories	0	0	0	0	0	0	0	0	0	0
7	HRSG, Ducting and Stack	26,306	1491	17,850	0	45,646	4188	0	6519	56,353	133
8	Steam Turbine Generator	140,039	1358	35,752	0	177,149	16,774	0	27,823	221,745	523
9	Cooling Water System	21,031	10,512	19,286	0	50,829	4784	0	7534	63,148	149
10	Ash/Spent Sorbent-Handling Systems	8814	280	11,782	0	20,876	2006	0	2354	25,236	60
11	Accessory Electric Plant	25,657	9079	26,232	0	60,967	5370	0	8211	74,549	176
12	Instrumentation and Control	11,133	0	11,286	0	22,419	1952	1,077	3017	28,465	67
13	Improvements to Site	6570	3776	13,239	0	23,585	2326	0	5183	31,093	73
14	Buildings and Structures	0	33,416	31,512	0	64,928	5855	0	10,618	81,401	192
	Total Cost	**1,133,528**	**69,137**	**516,106**	**0**	**1,718,771**	**161,117**	**100,513**	**297,353**	**2,277,755**	**5372**

Table B-8. Owner's Costs, Project Case with Capture and WESP

Description	$/1000	$/kW
Preproduction Costs		
6-month All Labor	11,992	28
1-month Maintenance Materials	1690	4
1-month Nonfuel Consumables	587	1
1-month Waste Disposal	678	2
25% of 1-month Fuel Cost at 100% Capacity Factor	1050	2
2% of TPC	45,555	107
Total	**61,552**	**145**
Inventory Capital		
60-day Supply of Fuel and Consumables at 100% Capacity Factor	9440	22
0.5% of TPC (spare parts)	11,389	27
Total	**20,829**	**49**
Other Costs		
Initial Cost for Catalyst and Chemicals	0	0
Land	1110	3
Other Owner Costs	341,663	806
Financing Costs	61,499	145
TOC	**2,764,408**	**6520**
TASC Multiplier	1.140	
TASC	**3,151,425**	**7433**

Table B-9. Initial and Annual Operating and Maintenance Costs, Project Case with Capture and WESP

Case:	Supercritical pc with CO_2 Capture and WESP				Cost Base:	2019
Plant Size, MW, net:	424	Coal Consumption, tons/day:		10,249	Capacity Factor, %:	85
Operating & Maintenance Labor						
Operating Labor				**Operating Labor Requirements per Shift**		
Operating Labor Rate (base):	42.74	$/hour		Skilled Operator:	2.0	
Operating Labor Burden:	37.00	% of base		Operator:	9.0	
Labor Overhead Charge Rate:	30.84	% of labor		Foreman:	1.0	
				Lab Techs, etc.:	2.0	
				Total:	**14.0**	
Fixed Operating Costs						
					Annual Cost	
					$	**$/kW-net**
Annual Operating Labor:					7,692,876	18.144
Maintenance Labor:					11,494,498	27.110
Administrative & Support Labor:					4,764,474	11.237
Property Taxes and Insurance:					31,260,970	73.729
Total:					**55,245,188**	**130.295**
Variable Operating Costs						
					$	**$/kWh-net**
Maintenance Material:					17,241,749	0.00546
Consumables						
	Consumption				**Cost**	
	Initial Fill	**Per Day**	**Per Unit**	**Initial Cost**		
Water/1000 gallons:	0	2234	1.33	0	923,403	0.00029
Makeup and Wastewater Treatment Chemicals, lb:	0	10,812	0.21	0	703,396	0.00022
Limestone, ton:	0	66	27.14	0	555,661	0.00017
Hydrated Lime, ton:	0	0	0.00	0	0	0.00000
Activated Carbon, ton:	0	0	0.00	0	0	0.00000
CO_2 Capture System Chemicals:	1236	1.75	2775.19	3,430,127	1,506,755	0.00048
Triethylene Glycol, gal:	0	0	0.00	0	0	0.00000
H_2SO_4, ton:	83	13.82	534.93	44,399	2,293,616	0.00073

Continued . . .

Table B-9. Initial and Annual Operating and Maintenance Costs (continued)

Case:	Supercritical pc with CO_2 Capture and WESP			Cost Base:	2019	
Plant Size, MW, net:	424	Coal Consumption, tons/day:		10,249	Capacity Factor, %:	85
	Consumption				Cost	
	Initial Fill	Per Day	Per Unit	Initial Fill	$	$/kWh-net
SCR Catalyst, m^3:	0	0	0.00	0	0	0.00000
Subtotal:				**0**	**5,982,831**	**0.00190**
Waste Disposal						
Fly Ash, ton:	0	957	20.02	0	5,943,930	0.00188
Bottom Ash, ton:	0	156	20.02	0	968,916	0.00031
Amine Purification Unit Waste, ton:	0	0	0.00	0	0	0.00000
Thermal Reclaimer Unit Waste, ton:	0	0	0.00	0	0	0.00000
Prescrubber Blowdown Waste, ton:	0	0	0.00	0	0	0.00000
Subtotal:				**0**	**6,912,846**	**0.00219**
By-Products						
Gypsum, ton:	0	0	0.00	0	0	0.00000
Subtotal:				**0**	**0**	**0.00000**
Variable Operating Costs Total:				**0**	**26,337,055**	**0.00834**
Fuel Cost						
North Dakota Lignite, ton:	0	10,249	13.47	0	42,830,764	0.01357
Total:					**42,830,764**	**0.01357**